



Published in final edited form as:

J Med Chem. 2008 October 23; 51(20): 6512–6530. doi:10.1021/jm800698b.

Blocking Estrogen Signaling After the Hormone: Pyrimidine-Core Inhibitors of Estrogen Receptor-Coactivator Binding

Alexander A. Parent, Jillian R. Gunther, and John A. Katzenellenbogen*

Department of Chemistry, University of Illinois at Urbana-Champaign, Urbana, IL 61801

Abstract

As an alternative approach to blocking estrogen action, we have developed small molecules that directly disrupt the key estrogen receptor (ER)/coactivator interaction necessary for gene activation. The more direct, protein-protein nature of this disruption might be effective even in hormone-refractory breast cancer. We have synthesized a pyrimidine-core library of moderate size, members of which act as α -helix mimics to block ER α /coactivator interaction. Structure-activity relationships have been explored with various C, N, O and S-substituents on the pyrimidine core. Time-resolved fluorescence resonance energy transfer and cell-based reporter gene assays show that the most active members inhibit the ER α /steroid receptor coactivator interaction with K_i 's in the low micromolar range. Through these studies, we have obtained a refined pharmacophore model for activity in this pyrimidine series. Furthermore, the favorable activities of several of these compounds support the feasibility that this coactivator binding inhibition mechanism for blocking estrogen action might provide a potential alternative approach to endocrine therapy.

INTRODUCTION

Although historically considered female reproductive hormones, estrogens are now recognized to be major regulators of physiological functions in both reproductive and non-reproductive tissues in both men and women.^{1, 2} While estrogen activity is required or is beneficial in many cases, such as for fertility,^{3, 4} during pregnancy, and for bone health and metabolic function,^{5–9} the pro-proliferative effect of estrogens in many target tissues can be pathological.^{10, 11} Such is the case with breast cancer, where tumor growth is driven by estrogen in ca. one-third of tumors.¹² In such patients, good therapeutic responses can often be achieved by blocking estrogen action with antiestrogens (estrogen antagonists).¹³

Both estrogens and antiestrogens work through the estrogen receptors, of which there are two subtypes, ER α and ER β .^{2, 14} The ERs are ligand-modulated transcription factors that act through cis-regulatory gene sequences in chromatin to regulate patterns of gene expression in target cells. Estrogen agonists bind to the ERs and stabilize conformations that recruit key coregulatory proteins, in particular, members of the p160 steroid receptor coactivator family (SRCs) (Figure 1A).¹⁵ The ER-SRC interaction involves protein-protein contact between signature LXXLL sequences in the SRC and a hydrophobic groove on the surface of the ligand-binding domain of the ER-agonist complex with which the three leucine residues of the helix interact. The coactivators that are recruited by the ER-agonist complex are responsible for altering chromatin architecture, loosening nucleosome structure, and activating RNA

Address Correspondence to: John A. Katzenellenbogen, Department of Chemistry, University of Illinois, 600 South Mathews Avenue, Urbana, IL 61801, USA, Tel. 217-333-6310, Fax. 217-333-7325, E-mail: jkatzene@uiuc.edu.

Supporting Information Available: See for complete synthetic details, HPLC and CHN analyses, and more extensive biological data, including RBA values. This material is available free of charge via the Internet at <http://pubs.acs.org>.

polymerase II (polII), as required to up-regulate gene transcription.¹⁶ Estrogen antagonists occupy the same ligand binding site as agonists, but they stabilize different ER conformations, ones that preclude or reduce the binding of the SRC coactivators, thereby indirectly interrupting estrogen signaling (Figure 1B).¹⁷

While in many cases antiestrogen therapy in hormone-responsive breast cancer can stop or reverse tumor progression, resistance develops with time, so that typically after ca. 5 years, tumor growth resumes despite continued treatment with antiestrogens.^{18, 19} In fact, in laboratory models of breast cancer and even in the clinic, it has been shown that antiestrogens can even become stimulatory in hormone resistant breast cancer.²⁰ While a molecular-level understanding of the mechanism of resistance to endocrine therapy is still incomplete, it is clear that breast cancer cells can undergo adaptations such that antiestrogens can no longer block estrogen signaling. Nevertheless, tumor growth in this hormone-refractory state still appears to rely on the ER-SRC interaction.²¹

Such considerations motivated us to search for molecules that might inhibit this key ER-SRC interaction directly. Such small molecules, termed coactivator binding inhibitors (CBIs), would be designed to bind in the hydrophobic groove of the ER-agonist complex, thereby blocking the interaction between ER and SRC (Figure 1C).²² Because the CBIs would be blocking this key protein-protein interaction in a direct manner, rather than indirectly as do conventional estrogen antagonists, they might not be subject to the resistance mechanisms that compromise endocrine therapy with antiestrogens. The distinction between inhibition of estrogen signaling through ER by antiestrogens, which act in the ligand binding pocket, and CBIs, which act in the coactivator groove, is illustrated in Figure 1.

In designing CBIs, we have used a structure-guided approach, seeking to find simple cyclic systems that could be assembled in a modular fashion and would display three hydrophobic substituents that mimic the three key leucine residues in the LXXLL interaction sequence. In our earlier work, in which we explored a number of different approaches and core heterocyclic systems, we found that pyrimidine-core molecules appeared to be promising structures as based on their CBI activity and ease of preparation.²² Others have also reported on compounds with ER-CBI activity. Our initial publication was closely followed by a study from Shao et al. which identified 'guanyldrazone' ER CBIs,²³ and compounds based on bicyclo[2.2.2]octane²⁴ and pyridylpyridone²⁵ scaffolds have also been reported to have similar activity. Most recently, our laboratory has also published promising results utilizing the amphipathic nature of alternately substituted trialkyl/triamino benzenes as disruptors of the ER/SRC interaction.²⁶

In this study, we have explored a wide variety of trisubstituted pyrimidine-core systems as potential CBIs, and we have characterized their potency as inhibitors of the interaction of ER α and ER β with SRC-3 using a time-resolved fluorescence resonance energy transfer assay (TR-FRET), as well as in cell-based assays of estrogen transcriptional activity. Through this study, we have developed a refined pharmacophore model for CBIs of this pyrimidine class, and we have obtained a number of compounds that have low micromolar potency as CBIs in blocking the ER-coactivator interaction *in vitro*. These compounds are also effective in blocking estrogen-stimulated transcriptional activity in breast cancer cells in a manner that is insurmountable by increased estrogen, a hallmark that critically distinguishes CBIs from conventional estrogen antagonists. Nearly all of these CBIs also have high selectivity for ER α over ER β . The results of this study suggest that blocking estrogen action using CBIs might provide a viable alternative approach to endocrine therapies.

RESULTS AND DISCUSSION

Based on our initial success in developing ER-CBIs using 2,4-diamino-6-alkyl pyrimidines,²² we wanted to investigate this pharmacophore type further in hopes of increasing the affinity of the CBI. As shown in Figure 2, the design of the initial pyrimidine library was based on the roughly triangular orientation of the L690, L693, and L694 residues of an ER-bound LXXLL-containing peptide from SRC-2 (also known as glucocorticoid receptor interacting protein 1, GRIP-1).²⁷ Although we first reported that the 6-alkyl-2,4-diaminopyrimidines bound with K_i 's in the mid micromolar range (29–49 μM as measured by a fluorescence polarization assay), when they were tested in a more sensitive TR-FRET assay, the best of these, 2,4-diisobutylamino-6-isoamylpyrimidine (Figure 2b), was found to bind with a K_i approaching submicromolar concentrations.²⁴ The high affinity of these compounds, as well as the relative ease with which substituted pyrimidine heterocycles can be synthesized, provided a fruitful starting point for the preparation of an expanded ER-CBI library.

Library design and synthesis

In our initial attempts at expanding the pyrimidine library, we followed the synthetic route previously described.²² Although this path can be used to produce the desired substituted pyrimidines, it is laborious (due to sparsely soluble intermediates) and prohibitively low-yielding. Consequently, we quickly turned our attention to synthetic routes involving the preformed heterocycle, finally settling upon 2,4,6-trichloropyrimidine, which is a cheap, easily-modified starting material. As detailed below, we eventually applied a wide range of reactions, including aminations, alkylations, alkoxylation, and sulfide formation, on a variety of tri-, di-, and monochloropyrimidines, all of which proceeded in moderate to good yields. Additionally, alkylations and aminations could be applied to this precursor in a site-selective manner.^{28–31}

We designed our pyrimidine-based library to incorporate the leucine and phenylalanine-mimicking substituents of the previously synthesized compounds, as well as tryptophan-mimicking naphthyl groups. In addition to the N- and C-side-arms previously described, we also incorporated other heteroatom-containing substituents (O, S, and SO_2) into the pyrimidine core to probe, more deeply, the nature of the binding mode of the CBI in the coactivator groove. Triamino, trimercapto, and trialkoxy pyrimidines were also synthesized. The overall goal of this approach was to make a thorough exploration of the structure-activity relationships of the 2-, 4- and 6-positions of the pyrimidine ring with respect to substituent size, polarity, and hydrogen-bond donor/acceptor capability. In practice, the library design was an iterative activity, evolving with the project as progressive binding results were obtained.

Phenethyl and styryl pyrimidines

The first step toward formation of the CBI library involves the site-selective Suzuki-Miyaura cross-coupling reaction of *trans*-2-phenylvinylboronic acid with 2,4,6-trichloropyrimidine, which gives the 2,4-dichloro-6-styryl-pyrimidine **1** as the major isomer (73% yield), together with small amounts of the symmetric di-coupled 2-chloro-4,6-distyryl-pyrimidine as the only significant byproduct.²⁹ From this point, the synthesis splits into three routes. The first route (top pathway in Scheme 1) involves the double addition of an amine or alkoxy nucleophile to **1** to produce 'symmetrically' substituted pyrimidines **2a d**, followed by hydrogenation of the styryl double bond over 10% Pd on carbon at atmospheric pressure of H_2 to give the final pyrimidine products **3a c**. The second route (middle pathway in Scheme 1) involves the formation of intermediates that are labile under hydrogenation conditions (most notably thioethers). As such, it is necessary to first reduce the styryl double bond of **1** before addition of any nucleophile. The reduced 2,4-dichloro-6-phenethylpyrimidine (**4**) is subsequently reacted under $\text{S}_\text{N}\text{Ar}$ conditions with either an excess of alkoxide or thiolate to form the

'symmetrically' substituted pyrimidines **5a c**. The disulfanyl compounds **5b** and **5c** are then oxidized with mCPBA to form the disulfonyl pyrimidines **6a** and **6b** (for complete structural information see Tables 1 and 2 and Supporting Information).^{32, 33}

The third pathway of phenethylpyrimidine synthesis involves the formation of unsymmetrically substituted 2,4-diaminopyrimidines, as shown in the bottom pathway of Scheme 1. Starting from **1**, the chloride at the 4-pyrimidinyl position is selectively displaced using an NaH-deprotonated *tert*-butyl carbamate to form the 2-chloro-6-styryl-pyrimidin-4-yl carbamates **7a c**.³⁰ The pyrimidinyl carbamates then undergo addition of a second amine to form the S_NAr products **8a f**. At this point, either the double bond of the styryl group is reduced under mild hydrogenation conditions (10% Pd/C, 1 atm H₂) to give phenethyl derivatives **9a d**, or the Boc group is removed in TFA/CH₂Cl₂, followed by hydrogenation of the alkene, producing the unsymmetrical 2,4-diamino-6-phenethylpyrimidines **11a f**. This synthetic approach allowed for all four of the final unsymmetrical product types, stemming from and including the aminopyrimidinyl carbamates **8a f**, to be prepared and submitted for CBI assays.

Isoamyl and naphthethylpyrimidines

Because of the limited accessibility of the associated boronic acids or esters, we turned to the direct coupling of sp³-hybridized alkanes with the pyrimidinyl trichloride to form the 6-isoamyl and 6-naphthethylpyrimidine series. This was effectively accomplished through the use of a site-selective Fe(acac)₃-catalyzed Kumada-type coupling involving alkyl Grignard reagents, as developed by the Furstner laboratory.^{28, 34, 35} Following their procedure, we obtained the desired 6-alkyl pyrimidines **12a c** in moderate yields. The major byproduct is the 'symmetric', disubstituted 4,6-dialkylpyrimidine, with both the 2-naphthethylpyrimidine and the asymmetric, 2,6-dinaphthethylpyrimidine also isolated as minor products. The 2,4-dichloro-6-alkylpyrimidines **12a c** were then reacted with O-, N-, and S- nucleophiles to produce the 'symmetrically' substituted pyrimidines **13a k**. Additionally, the dithioethers **13g** and **13h** were oxidized with mCBPA in CHCl₃ to give the respective disulfonylpyrimidines **14a** and **14b** (top pathway in Scheme 2).

Unfortunately, it proved more difficult to create unsymmetrically-substituted diamines from the alkylpyrimidines **12b** and **12c** than from the styryl-substituted pyrimidine **1**. When **12b** was submitted to the same S_NAr conditions used to form **7a**, an unsymmetric dimer of the starting material was isolated as the major product instead of the desired carbamate. This reaction presumably proceeds through deprotonation of the isoamyl α -carbon of one pyrimidine, followed by displacement of the aromatic chloride on a second molecule. This problem is easily avoided by first introducing the carbamate site-selectively into 2,4,6-trichloropyrimidine at the 4-position (compounds **15a c**). This is followed by the Fe(acac)₃-catalyzed coupling of the alkyl Grignard to produce the 6-alkyl-pyrimidin-4-yl carbamates **16a g**. Amination under the same conditions used for the chlorostyrylpyrimidines leads to the aminoalkylpyrimidinyl carbamates **17a m**. The Boc group was subsequently removed with TFA in CH₂Cl₂ to produce the final 2,4-diamino-6-alkylpyrimidines **18a m** in modest overall yield (bottom pathway in Scheme 2a).

It should be noted that, for both of the site-selective steps described in the paragraph above, a small amount of the undesired isomer is also formed. To explore the effect of the exchange of the 6-alkyl and the 4-amino group on the pyrimidine CBIs, four of these minor isomers, **19a d**, were subjected to S_NAr conditions with isobutylamine, with subsequent removal of the Boc group to produce the 4,6-diamino-2-isoamylpyrimidines **21a d**, as shown in Scheme 2b.

To explore the SAR space of the pyrimidine library further, 4,6-dialkyl-2-aminopyrimidines were prepared from the 4,6-dialkyl-2-chloropyrimidines **22a** and **22b**, which were obtained by either Suzuki-Miyaura coupling of two equivalents of *trans*-2-phenylvinylboronic acid to

2,4,6-trichloropyrimidine or as the major byproduct from the reaction forming **12a**. The final monoamine products were obtained by amination of **22a** and **22b**, followed by reduction of the styryl groups of compounds **23d-f** to provide the 2-amino-4,6-diisopropylpyrimidines **23a-c** and 2-amino-4,6-diphenethylpyrimidines **24a-c** (Scheme 3).

In addition to the alkyldiaminopyrimidines and dialkylaminopyrimidines, we also wanted to probe the effect of three electronegative substituents on the binding of the pyrimidine core molecules. Thus, we formed the ‘symmetric’ trisubstituted pyrimidines **25a-f** with three heteroatom-containing substituents by the reaction of 2,4,6-trichloropyrimidine with O, N, and S nucleophiles (Scheme 4). In addition to the ‘symmetrically’ substituted triisobutylaminopyrimidine **25a**, at lower temperature and shorter reaction time, the unsymmetrical diamination byproduct, 2,4-diisobutylamino-6-chloropyrimidine, **26**, was also produced in modest yield from the reaction of isobutylamine with 2,4,6-trichloropyrimidine. Compound **26** was subsequently substituted with benzyl amine, isobutylalcohol, or isobutylmercaptan to form the unsymmetric tri-heteroatom substituted pyrimidines **27a-c**. Reductive dechlorination of **26** gave the 6-proteopyrimidine **27d**, and the isobutylsulfanyl pyrimidine **27c** was oxidized with mCPBA in CHCl₃ to form the diaminosulfone **28**.

Methylated aminopyrimidines

During the course of this study, it became clear that there was an important relationship between the activity of the CBI and the nature of the heteroatom substituents, suggesting that simple insertion of an electronegative atom was not sufficient to produce high-affinity compounds (see Table 2). The apparent requirement for a nitrogen-containing substituent at the 2- and/or 4-position of the pyrimidine suggested that H-bond donation might be playing a role in supporting the binding of the diaminopyrimidines. To probe this hypothesis, we synthesized *N*²-methyl, *N*⁴-methyl, and *N*²,*N*⁴-dimethyl diaminopyrimidines, as shown in Scheme 5. Methylation at these sites should obliterate the H-bond donor capability of the secondary amine, while retaining the polarity and planarity induced by the aryl nitrogen.

Both the *N*²-methylated and the ‘symmetrically’ substituted *N*²,*N*⁴-dimethylated pyrimidines were easily synthesized by the non-selective amination with *N*-methylisobutylamine and subsequent reduction of compounds **1** and **12b,c**; and **7a** and **16b,e** (see the middle and top pathways of Scheme 5, respectively). The *N*⁴-methylated compounds could be accessed through a K₂CO₃-catalyzed site-selective addition of *N*-methylisobutylamine to **12b,c** or as a byproduct from the formation of **29a**, followed by amination with isobutylamine and reduction of the styryl moieties when present (bottom pathway of Scheme 5).

The binding results for the *N*-methylated 6-isoamylpyrimidines **29a**, **31a**, and **34a** show that there is a strong preference for a free NH at the 4-position of the isoamyl-substituted pyrimidine ring (see Table 2). As H-bonding at the 2-position seemed less important to CBI binding, the O, S, and SO₂-containing 4-isobutylamino-6-isoamylpyrimidines **37a,b** and **39** were also synthesized according to the methods described above and as shown in Scheme 6. Based purely on polarity, these compounds should show CBI activity similar to the diaminopyrimidines **13b** and **31a**. On the other hand, if H-bond donation or overall planarity of the CBI is important, decreased affinity would be expected.

In vitro time-resolved FRET assay of the inhibition of coactivator binding to ER α and ER β by pyrimidine-core CBIs

The inhibitory activity of members of our pyrimidine CBI library for coactivator binding to both ER α and ER β systems was measured using a TR-FRET assay. This assay employs a site-specifically labeled terbium/streptavidin-biotin-ER-LBD construct and a fluorescein-labeled nuclear receptor domain of the steroid receptor coactivator 3 (SRC-3-NRD). In the presence

of agonist (17 β -estradiol) and the absence of a CBI, the SRC-3-NRD binds to the ER-LBD, allowing transfer of fluorescence resonance energy from the Tb donor (D) to the fluorescein acceptor (A). With increasing concentrations of CBI, the ER/SRC-3 complex is disrupted, and fluorescence resonance energy transfer decreases. This provides a dose-dependent inhibition curve, typically plotted on an A/D*1000 scale, from which K_i values for the various compounds can be calculated. An unlabeled peptide containing the NR Box II (LXXLL motif) of SRC-1, a natural coactivator of ER, is used as a positive control. The results from these binding studies are summarized in Tables 1 and 2 (additional binding data can be found in Supporting Information).

Initially, what is most striking about the data is the almost universal selectivity of the pyrimidine core CBIs for ER α over ER β coactivator binding inhibition. With the exception of three compounds that show only very modest affinity for ER β (**2a**, **8b**, and **25a**), all compounds assayed show binding only to ER α . (These results have been echoed in preliminary studies in cell-based reporter gene systems, which have also confirmed the ER α selectivity of pyrimidine compounds **3a**, **13b**, and **27a**, which show no mechanism-based inhibition of ER β .) Of these three, **2a** and **25a** are still over 30-fold ER α selective, while only the Boc-protected compound, **8b**, shows complete selectivity for ER β with no activity for ER α . Loss of ER β activity occurs readily, as observed in the relationship of compound **2a** to **3a** (converted by hydrogenation of the styryl double bond) and compound **8b** to **10c** (involving simple removal/addition of a Boc group from the 4-aminopyrimidinyl position). These two factors seem to be important in increasing ER β affinity, while also decreasing affinity for ER α (compare **3a** to **2a**, **11a** to **10a**, and **11c** to **10c**). It is likely that the combination of the styryl functionality and the Boc-protecting group gives **8b** its ER β selectivity, and this suggests that the ER β binding groove prefers compounds with greater rigidity coupled with increased hydrophobicity. Selectivity of small-molecules for ER α /ER β CBI activity has been mentioned only briefly before,²³ and seems surprising, since an examination of the coactivator groove of ER α and ER β bound to LXXLL-containing peptides shows very little dissimilarity. The homology of the binding groove is again supported by assay of the control SRC-1 BoxII peptide (LXXLL motif), which has approximately equivalent affinity for both receptors. Nonetheless, the preference of other peptide-based CBIs for ER α over ER β has been reported,^{36–38} and this selectivity is significant in that it may increase the ultimate therapeutic utility of these compounds.^{39–41}

Table 1 contains the binding data for the ‘symmetrically’ and ‘unsymmetrically’ substituted 2,4-diamino-6-alkylpyrimidines and 2,4-diamino-6-styrylpyrimidines. Because these compounds were the initial synthetic targets of this study, as well as the compounds most closely related to those reported in our first ER-CBI paper,²² we were hopeful that these alternative and ‘unsymmetrical’ additions would provide increased CBI activity. While somewhat disappointed by the lack of significant increase in affinity, we were nonetheless pleased that this approach produced many compounds with CBI activity having comparable or slightly higher affinity for ER α .

Included in Table 1 are compounds **3b**, **13a**, and **13b**, which represent the high affinity pyrimidine CBIs reported previously.²² Interestingly, while **13a** and **13b** show lower K_i values in our more sensitive TR-FRET assay than those we reported using our earlier fluorescence polarization assay, compound **3b** shows no measurable binding to either ER α or ER β by TR-FRET ($K_i = 49, 32,$ and $29 \mu\text{M}$ by FP vs. $>1000, 16,$ and $2.8 \mu\text{M}$ by TR-FRET, respectively, for **3b**, **13a**, and **13b**). We believe that the lower affinity value that we obtain for **3b** by the TR-FRET assay is the correct one, because it is consistent with a trend we have observed throughout this series of compounds, namely, the lack of affinity of the ER α coactivator groove for extremely bulky ligands. This is apparent in the general exclusion of pyrimidines that contain a naphthyl group, exceptions being those pyrimidines (**13i**, **18c**, and **18f**) that contain only two small isobutyl/isoamyl side-arms in addition to the larger aromatic group.

Additionally, while the coactivator groove readily tolerates CBIs with two phenyl groups and a single isoamyl/isobutyl group (**11a**, **11c**, and **13c**), addition of a third aromatic substituent (**3b**) results in complete loss of binding. In general, it appears that those compounds that bind best to the coactivator groove are those that fill it snugly, without exceeding certain steric limitations, as in compounds **11c**, **13i**, and **18f**.

Comparison of the pairs of compounds **11a** and **11c**, **18b** and **18d**, and **18c** and **18f** in Table 1 yields another general trend in CBI affinity. For each of these pairs, affinity is increased 1.5 to 3-fold when the amino substituents at the 2 and 4-positions are situated so that the larger moiety is in the 4-position. This effect becomes more dramatic as the size difference in the groups increases (**18c** and **18f** vs. **18b** and **18d**). Conversely, it appears that the size of the substituent on the alkyl group at the 6-position has little effect on binding, as both the 2,4-diisobutylaminopyrimidines with the large naphthethyl group (**13i**) and the isoamyl group (**13b**) bind with comparable affinity. Nevertheless, if the size of the group at the 6-position is reduced drastically, binding is negatively affected, as in the 6-ethylpyrimidine **18a** ($K_i = 10 \mu\text{M}$), and substitution with a chlorine or hydrogen atom at the same position results in complete loss of activity (**26** and **27d**). As mentioned above, introduction of a double bond at the 6-position decreases or, in extreme cases, obliterates ER α affinity, and, in all cases, pyrimidines with Boc-protection at the *N*⁴-amine fail to bind ER α (see Supporting Information for further examples of these compounds).

To better understand the effect of substituent type and placement on the pyrimidine ring, we next investigated the binding of 4,6-dialkyl-2-amino- and 2-alkyl-4,6-diaminopyrimidines, as shown in Table 2. Despite the overall hydrophobic nature of the coactivator groove and the distinct structural homology of the 4,6-dialkylpyrimidines **23a** **24c** to the high affinity 2,4-diamino compounds, we failed to observe binding with any members of this pyrimidine derivative class. Possibly more surprising is the complete lack of binding exhibited by the 2-alkyl-4,6-diaminopyrimidines **21a** **21d**. Although they are simple isomers of compounds **13b**, **13i**, **18b**, **18c**, **18d**, and **18f**, which all have K_i values below 10 μM , the compounds with a methylene group replacing the amino group at the 2-position suffer complete loss of CBI binding activity. Together, these results suggest that at least two electronegative substituents on the pyrimidine ring are required for CBI activity. Moreover, it is not sufficient for these substituents to have a general 1,3-relationship; rather, binding requires specific substitution at the 2 and 4 positions. Along with the two nitrogens of the pyrimidine core, these two substituent nitrogen atoms form a tetrad of electronegative atoms which appears to provide a unique and essential binding motif.

In contrast to the importance of the presence of the amino substituents at the 2 and 4 positions of the pyrimidine ring, the nature of the C-6 substituent seems to be of minimal importance, as the alkyl group can be replaced with a third amino substituent with minimal loss in binding affinity. Examples of this are the triamino CBIs **25a** and **27a** (Table 2), which have potencies similar to that of their alkyl-diamino analogs **13b** and **18d** (Table 1), with K_i values of 5.7 and 7.3, and 2.8 and 5.8, respectively. Nonetheless, there is some selectivity for atom type at the 6-position as is evidenced by the lack of activity of the 2,4-diisobutylaminopyrimidines **27b,c**, and **28** which contain O, S, and SO₂-linked substituents at that site (Table 2).

In addition to the amino pyrimidines already described, a number of other heteroatom-containing pyrimidines were also analyzed for CBI activity. Incorporation of the alkoxy, sulfanyl, and sulfonyl pyrimidines into the library (Table 2 and Supporting Information) allowed for further evaluation of the role of the amino substituents in CBI binding. Although we had anticipated that any electronegative atom or group would provide affinity similar to the previously assayed aminopyrimidines, we found that none of the pyrimidines incorporating two or three O or S substituents exhibited any inhibition of coactivator binding. (The lone

exception to this is the triisobutylsulfanylpyrimidine **25e**, which bound ER α with the relatively high K_i of 120 μM .) Even oxidation of the thioether function to the highly polar sulfone failed to elicit activity.

At this point, it became evident that there is a necessary relationship between the presence of nitrogen-bearing substituents at a specific position on the pyrimidine and the potency of the CBI. We rationalized that the importance of the N heteroatom was most likely based on either its ability to act as a hydrogen-bond donor or its planarity due to resonance interaction between the nitrogen lone pair and the aryl π -system. If H-bond donation was required for CBI binding, it was likely that it would be position specific. To probe these possibilities, we synthesized and assayed the N^2 -methyl, N^4 -methyl, and N^2 , N^4 -dimethyl diaminopyrimidine compounds, **29a** **35**.

As shown in Table 2, when both the N^2 - and N^4 -nitrogens are methylated, affinity for ER α is completely lost (**29a d**). Interestingly, some activity is regained in the selectively monomethylated compounds: When the N^4 of the 6-isoamylpyrimidine is methylated, no binding is observed (**34a**), but activity is nearly fully restored when the methyl group is switched to N^2 (**31a**). In the phenethyl and naphthethyl compounds, the opposite is observed, and the compounds with a free NH at the N^2 -position bind (**34c** and **35**), whereas the N^4 isomers are inactive (**31c** and **32**).

This restoration of activity associated with monomethylation suggests that N H H-bond donation is indeed important to binding. That this binding is specific to either the 2- or 4-position of the aromatic ring, depending on the nature and/or size of the C-6 substituent, implies that more subtle electronic effects are also playing a role in orientation of the CBI in the coactivator groove: sterically, the 2- and 4-positions of the pyrimidine should be practically equivalent, but the dipole moment of the heterocycle relative to the methyl-substituted amine is position-dependent, and the differential ability of the aromatic nitrogen atoms to act as hydrogen bond acceptors must also be considered. The preference for the free N H to switch from the 4- to 2-position as the steric bulk of the alkyl group increases from isoamyl to phenethyl may indicate that a different binding mode (i.e., 120° rotation) is involved in inhibition with these larger molecules. The manner in which these two somewhat contradictory observations might be understood has been analyzed using computation docking experiments and is discussed below.

After showing the selective importance of at least one free amine N H at either the 2- or 4-position of the pyrimidine, we wanted to probe the ability of other electronegative atoms to offer the same binding properties as the non-H-bonding N-methyl amine. To accomplish this, we prepared the 6-isoamyl-4-isobutylpyrimidines **37a,b** and **39**. None of these O- or S-containing pyrimidines showed any inhibition of the receptor/coactivator complex. Although not conclusive, this gives strong support for the need of two amino substituents at both the N^2 - and N^4 -positions of the pyrimidine ring. Although it is possible that subtle electronic changes are the basis of this marked affinity differential, it is more likely that the planarity and associated rigidity of the N aryl bond creates an overall CBI core structure that is more conducive to binding. A summary of the structure-activity relationships of the pyrimidine-core CBIs is shown in Figure 3.

***In vitro* radiometric assay of CBI binding affinity for the ligand binding pocket of ER α and ER β**

To further ensure that the inhibition we observe with these compounds in the TR-FRET CBI assay is not due to the compound binding as an antagonist at the ligand binding pocket, we conducted a competitive radiometric ligand binding assay using tritium-labeled estradiol as a tracer and full-length purified human ER α and ER β . The binding affinities of the CBIs relative

to the tracer and standard, estradiol, are expressed as relative binding affinity (RBA) values. The pyrimidine CBIs generally have RBAs for ER α of less than 0.005% (estradiol = 100%), and while there are a few significant exceptions, even the CBI with the highest affinity for the ligand binding pocket (**11a**) binds with only 0.051% the affinity of estradiol.

To properly interpret these results, it must be remembered that estradiol has a K_d for ER α of 0.2 nM; therefore, at the concentration of estradiol used for the TR-FRET CBI assay (1 μ M), a compound with an RBA of even 0.1% would show an IC₅₀ value of minimally 1 mM in the assay if it were acting as a conventional antagonist (i.e., competing with estradiol), rather than as a CBI (i.e., competing with SRC). Thus, we conclude that the inhibitions we are observing in our TR-FRET assay could not be due to the competition of these pyrimidines for the natural ligand estradiol with concomitant induction of an antagonist, non-coactivator binding conformation of the ER. Rather, the active pyrimidine CBIs reported in this library are disrupting the ER/SRC interaction by direct binding to the protein surface at the coactivator binding groove, not to the traditional, internal ligand binding site. (See Supporting Information for specific RBAs.)

Cell-based assay of the inhibition of estrogen-induced reporter gene transcriptional activity by the CBIs

To investigate the cellular activity of our pyrimidine core CBIs, we utilized a estrogen-responsive luciferase reporter gene assay performed in human endometrial cancer (HEC-1) cells lacking endogenous estrogen receptor, but transfected with a full-length ER α expression vector, an estrogen-responsive luciferase reporter gene plasmid (2ERE Luc), and pCMV β -galactosidase (β -gal; internal control). The cells were incubated with two concentrations of estradiol (1 nM and 100 nM) and titrated concentrations of CBI. After incubation for 24 hours, cells were lysed and assayed for luciferase reporter gene and β -galactosidase activity.

Those CBIs that were active showed not only a concentration-dependent reduction in reporter gene activity, but they also gave IC₅₀ values that were unaffected by changing the estradiol concentration. This inhibition, insurmountable by 100-fold excess estradiol, indicates that the CBIs are not competing against the ligand estradiol, as a conventional antagonist would; rather, they are acting through the CBI mechanism to block coactivator binding. Examples of the estrogen insurmountable reporter gene inhibitory activity of two representative CBIs (**3a** and **13b**) are shown in Figure 5a (TR-FRET curves for the same compounds are shown in Figure 3).

ERI-5, a previously published CBI inhibitor of the ER α -SRC interaction reported to have an IC₅₀ of 5.5 μ M in a COS-7 cell mammalian 2 hybrid assay,²³ was used as a positive control in these reporter gene assays; in our hands, it showed an IC₅₀ value of 1.4 μ M. Because of its cellular impermeability, the SRC-1 Box II control peptide used for the *in vitro* TR-FRET work could not be used in the cell-based assay. Measurement of β -galactosidase activity simultaneously with CBI testing serves as an internal control to confirm that decreased luciferase activity corresponds to a CBI blockade of ER α -coactivator binding, rather than to a generalized mechanism of cellular toxicity. The activity of the internal β -galactosidase control was affected by only the highest concentration of CBI used in the assay, 20 μ M, which decreased the activity of the control to approximately 70% of the expected maximal value for only the most potent pyrimidine compounds. A functionally different type of viability assay, probing cellular mitochondrial function, was also employed to confirm that the decrease in luciferase activity we observed was truly due to compound activity. This assay (CellTiter 96R Aqueous One Solution *Cell Proliferation Assay*, Promega) was run using compounds that showed the greatest discrepancy in IC₅₀ values between *in vitro* and cellular assays (i.e. **3a**, **10a**, **18b**, **25a**, and **37a**) and provided results in agreement with the β -galactosidase reporter gene assay controls, also showing that viable cell counts decreased significantly only at the

highest doses of compound (20 μM). Because the IC_{50} values we see for these compounds are significantly lower than 20 μM where cell toxicity first becomes apparent, we have concluded that the inhibition of estrogen-stimulated reporter gene activity by the CBIs was a transcription-based response rather than the result of general cell death.

In all instances where activity was observed in the TR-FRET protein-binding assay, comparable potencies or, in a number of cases, increased potencies were observed in the luciferase reporter gene assay (Tables 1 and 2). A comparison of potencies in the cell-based activity assay vs. the *in vitro* binding assay is illustrated in Figure 5b. The points below the dotted line represent cases where higher potency was evident in cell-based assay. While we can only speculate at this point, enhanced potency in the cell-based assays could be the result of decreased available concentrations of CBI compound *in vitro* because of sequestration by the small amount of detergent that needs to be present in the buffer of the TR-FRET assay. It could also be due to cell-based mechanisms that increase the local concentrations of the CBI by increased cellular uptake. In either case, we are encouraged by the increased potencies of these compounds when tested in a more physiologically relevant cell-based assay: not only do these results confirm the CBI activity of the library compounds observed in the TR-FRET assays, but they also provide evidence that these compounds are soluble and cell-permeable at concentrations necessary for inhibition. In a very low percentage of compounds, we have seen activity in the cell-based assays that was not discovered using the TR-FRET assay (**10a** and **37a**). It is possible that these results are due to an alternative mechanism of inhibition involving the AF-1 and/or DNA-binding domains of ER, which are present in the full-length protein used in the reporter gene assays but not in the ligand-binding domain of ER employed in the TR-FRET assay. Together, these data provide support that these pyrimidine CBI compounds could be effective as novel inhibitors of ER α -SRC interactions and, thus, ER-mediated transcription.

Modeling of CBI docking in ER α

To better understand the binding mode(s) involved with the pyrimidine-core CBIs, we have performed extensive docking experiments using, as a starting point, the structure of ER-LBD co-crystallized with the agonist diethylstilbestrol and a SRC-2 peptide (see <http://www.rcsb.org> entry 3erd). After work-up of the crystal structure, the coactivator peptide was removed, and the CBIs were docked into the resulting empty binding groove using the FlexiDock module of SYBYL[®] 7.3 from Tripos[™].

As has been noted previously,²² these experiments confirm that the coactivator binding groove of ER is flexible in nature, and modeling that is representative of reality is often complicated by the apparent accommodation of a variety of orientations of a single ligand. This is especially problematic when docking quasi-symmetrical compounds such as **13b**. Fortunately, while analyzing the various docking results, we have been able to apply the empirical binding and activity data described above to produce ER/CBI-binding models that are satisfying chemically, computationally, and experimentally (see Figure 6).

We have been especially interested in comparing the binding orientation of the isopentyl pyrimidine **13b** and the analogous naphthylethyl pyrimidine **13i**, as these compounds show essentially equivalent binding affinity in the TR-FRET assay, yet exhibit opposite selectivity for their corresponding monomethylated aromatic amines. Additionally, the pre-existing knowledge of which N-methylated CBI (N^2 vs. N^4) binds to the surface of the LBD, greatly aids in determination of the binding mode of the unmethylated compound.

In general, the coactivator groove consists of three major binding sites: a small pocket (shown on the right of the binding site in Figure 6), a medium-size pocket (on the left) and a large shelf (bottom center). Another important feature of the binding site is the 'charge clamp' composed of Glu542 and Lys362 of the ER α -LBD, which, in the presence of a coactivator, interact in a

productive manner with the inherent dipole associated with α helical peptide backbone of the LXXLL sequence. As shown in Figures 6a and b, **13b** binds to the ER coactivator groove in such a manner as to optimize its interaction with, not only the three hydrophobic pockets, but also both the carboxyl and amine groups of the charge clamp. The isopentyl alkyl group fills the small pocket on the right, pushing the amine in the 4-position into the medium sized pocket on the left and towards Glu 542, allowing for a positive interaction between partially positively charged N-H of the amine and the negatively charged carboxyl group. The second isobutylamine substituent occupies the coactivator shelf, so that there is minimal steric interaction between the alkyl group and the charged amine of Lys362. This allows for positive electrostatic interaction between Lys362 and the lone pair of the pyrimidinyl ring nitrogen. Additionally, docking of the associated monomethylated products **31a** and **34a** in this orientation allows for rationalization of the binding selectivity observed: When the amine at the 2-position is methylated (**31a**), there is very little rearrangement of either the ligand or the protein, and the interaction between the Lys362 and the pyrimidine nitrogen is maintained. Methylation at the N^4 -position of the pyrimidine (**34a**) completely disrupts the interaction between the N-H and the Glu542, and, consequently, affinity for the receptor is lost.

In contrast to the quasi-symmetric **13b**, the large naphthyl group of **13i** constrains the CBI to only two possible orientations, both of which place the bicyclic aromatic on the large non-polar shelf. Of these two orientations, only that shown in Figures 6c and d is situated so that monomethylation at the 4-position is tolerated while methylation at the 2-position causes disruption of the ER/CBI complex. As seen in the electrostatic rendering of the complex (Figure 6c), this orientation also correctly matches the negatively and positively-charged residues of the 'charge clamp' with the electron-deficient N-H and the electron-rich pyrimidine N. The cut-away rendering in Figure 6d more explicitly shows this orientation. Although not shown, Figure 6d also provides an illustration of the effects of mono-N-methylation of **13i**: While there is ample room for methylation at N^4 (this in effect pushes the CBI to the right, deeper into the small pocket), methylation at N^2 disrupts the pyrimidine nitrogen/Lys362 interaction, causing the CBI to be bumped out of the binding pocket and the lysine residue to be pushed back and to the right.

CONCLUSIONS

In this report, we describe the progressive optimization of the structure of 2,4,6-trisubstituted pyrimidines as inhibitors of the interaction between agonist-liganded estrogen receptor (ER) and a key coactivator protein, steroid receptor coactivator 3 (SRC-3). By inhibiting the interaction of ER with this important mediator of ER transcriptional activity, these coactivator binding inhibitors (CBIs) are able to block ER activity at a point after ligand binding, and we have demonstrated in cell-based reporter gene assays that this inhibition is insurmountable by increasing estrogen concentration. In this sense, inhibition of ER activity by CBIs is direct and distinct from that of conventional estrogen antagonists, which compete for agonist binding and interfere with SRC binding indirectly, by altering the topology of the ER from an agonist conformation that recruits SRCs to an antagonist conformation that does not.

We have achieved this optimization by developing an expedited synthesis of 2,4,6-trisubstituted pyrimidines, which has enabled us to systematically generate a series of focused pyrimidine libraries having alkyl and aralkyl substituents of various size and positioning, linked to the heterocyclic core through carbon and heteroatoms. Additionally, we have probed for the role of potential hydrogen bonding involvement of NH-linking atoms.

Through these studies, we have developed a rather complete structure-activity profile outlining a pharmacophore for the CBI activity of these trisubstituted pyrimidines. This pharmacophore specifies the following:

1. The need for *N*-linked side chains at the 2 and 4-positions of the pyrimidine ring, with a preference for a smaller group (isobutyl) at the 2 position.
2. Ready accommodation of either a C or N-bound moiety at the 6-position of the pyrimidine.
3. A strict size limit to the CBI binding pocket, with no more than two medium (phenyl) groups or one large (naphthyl) group tolerated at one time on the tridentate ligand.
4. Electrostatic effects and/or hydrogen bonding that require at least one free aryl N-H, the preferred position of which being dependant on the size of the alkyl group at the 6-position of the pyrimidine ring.

The best compounds we have obtained have K_i values (as inhibitors of coactivator binding *in vitro*) and IC_{50} values (for inhibition of reporter gene activity in cells) in the low micromolar region, and the vast majority of these compounds show strong selectivity for ER α over ER β . The most promising of these compounds are being evaluated in further cell-based and in other more biologically advanced activity assays. The results of this study suggest that blocking estrogen action using CBIs might provide a viable alternative approach to endocrine therapies.

EXPERIMENTAL SECTION

General Synthetic Methods

All reagents were used as purchased except where noted. THF, Ether, CH_2Cl_2 , and DMF used in reactions were dried using a solvent delivery system (neutral alumina column). Solvents used for extraction and flash chromatography were reagent or ultima grade purchased from either Aldrich or Fisher Scientific. All reactions were run under dry N_2 atmosphere except where noted. Flash column chromatography was performed on Silica P Flash Silica Gel (40–64 μ M, 60A) from SiliCycle[®]. 1H NMR and ^{13}C NMR spectra were obtained on 500 MHz Varian[®] FT-NMR spectrometers. Except where noted, both low and high resolution mass spectra were obtained using electrospray ionization on either a Micromass Q-ToF Ultima or Waters Quattro instrument. HPLC analysis was performed using a Waters 1525 binary HPLC pump equipped with a Waters in-line degasser AF, Waters 2487 Dual γ absorbance detector, and a Waters Symmetry[®] C18 5 μ M, 4.6 X 150 mm column. Microanalysis was performed with a CE 440 CHN analyzer.

Representative Syntheses (For complete synthetic details and HPLC analysis of active compounds please see Supporting Information). 2,4-Dichloro-6-styryl-pyrimidine (1)

Based on the coupling described by Tan et al.²⁹ Trans-2-Phenylvinylboronic acid (2.546 g, 17.2 mmol), K_3PO_4 (7.307 g, 34.4 mmol), and $PdCl_2(PPh_3)_2$ (0.362 g, 0.52 mmol) were dissolved in 100 mL THF. To this mixture, 2,4,6-trichloropyrimidine (3.156 g, 17.2 mmol) dissolved in 20 mL THF was added producing a cloudy yellow suspension. H_2O (15 mL) were added and the now clear solution was heated at reflux for 7 h. Approximately 100 mL of H_2O were added, and the biphasic mixture was extracted three times with ether. The combined organic layers were washed with brine, dried over anhydrous $MgSO_4$, and the solvent removed with a rotary evaporator. The product purified by column chromatography (gradient elution 5–10% EtOAc in hexanes) to provide **1** (3.1613 g, 73%). 1H NMR (500 MHz, $CDCl_3$) δ ppm 6.95 (d, $J=15.87$ Hz, 1 H), 7.22 (s, 1 H), 7.41 (m, 3 H), 7.59 (dd, $J=7.45, 2.08$ Hz, 2 H), 7.96 (d, $J=15.87$ Hz, 1 H). ^{13}C NMR (500 MHz, $CDCl_3$) δ ppm 117.1, 123.0, 128.2, 129.2, 130.6, 134.8, 140.9, 160.7, 162.8, 166.6. HRMS (ESI⁺) m/z calcd for $C_{12}H_9N_2Cl_2^+$ 251.0143, found 251.0101.

***N,N'*-diisobutyl-(6-styryl-pyrimidin-2,4-yl)-diamine (2a)**

Compound **1** (0.111 g, 0.44 mmol) was dissolved in 4 mL of isobutylamine and heated with stirring in a sealed high-pressure tube at 115 °C for 43 h. The reaction was allowed to cool to room temperature and the excess amine removed *in vacuo*. The residue was extracted from H₂O three times with ether. The combined organic layers were washed twice with brine, dried over MgSO₄, and the solvent removed by rotary evaporator. Purification was accomplished with column chromatography (50% EtOAc in hexanes) to give **2a** (67 mg, 47%). ¹H NMR (500 MHz, CDCl₃) δ ppm 0.97 (d, *J*=6.65 Hz, 6 H), 0.98 (d, *J*=6.65 Hz, 6 H), 1.88 (sept, *J*=6.65 Hz, 1 H), 1.89 (sept, *J*=6.65 Hz, 1 H), 3.12 (bs, 2 H), 3.25 (t, *J*=6.32 Hz, 2 H), 4.78 (bs, 1 H), 4.90 (bs, 1 H), 5.74 (s, 1 H), 6.83 (d, *J*=15.87 Hz, 1 H), 7.28 (t, *J*=7.29 Hz, 1 H), 7.35 (t, *J*=7.50 Hz, 2 H), 7.55 (d, *J*=7.50 Hz, 2 H), 7.66 (d, *J*=15.86 Hz, 1 H). ¹³C NMR (500 MHz, CDCl₃) δ ppm 20.5, 20.6, 28.7, 28.8, 49.3, 127.5, 127.7, 128.6, 128.9, 134.0, 136.8, 162.8, 164.4. HRMS (ESI⁺) *m/z* calcd for C₂₀H₂₉N₄⁺ 325.2392, found 325.2393. Anal. (C₂₀H₂₈N₄) H, C: calcd, 74.03; found, 73.44. N: calcd, 17.27; found, 16.82.

2,4-Diisobutoxy-6-styryl-pyrimidine (2c)

Clean Na⁰ (82 mg, 1.4 mmol) was dissolved in 2 mL of isobutylalcohol while heating at 70 °C with stirring (~2 h). To the resulting slightly cloudy solution, 150 mg (0.60 mmol) of **1** were added with stirring forming an opaque pale orange mixture. One more mL of isobutylalcohol was added, and the reaction was stirred at 70°C for 4 h. The reaction was allowed to cool to room temperature, and extracted from H₂O three times with ether. The combined organic layers were washed with brine, dried over anhydrous MgSO₄, and the solvent and excess alcohol removed with a rotary evaporator. Purification was accomplished with column chromatography (10% EtOAc in hexanes) to give **2c** (0.172 g, 88%). ¹H NMR (500 MHz, CDCl₃) δ ppm 1.01 (d, *J*=6.59 Hz, 6 H), 1.06 (d, *J*=6.59 Hz, 6 H), 2.08 (sept, *J*=6.84 Hz, 1 H), 2.19 (sept, *J*=6.84 Hz, 1 H), 4.14 (d, *J*=6.59 Hz, 2 H), 4.18 (d, *J*=6.84 Hz, 2 H), 6.33 (s, 1 H), 6.93 (d, *J*=15.87 Hz, 1 H), 7.32 (t, *J*=7.20 Hz, 1 H), 7.37 (t, *J*=7.32 Hz, 2 H), 7.57 (d, *J*=7.57 Hz, 2 H), 7.82 (d, *J*=15.87 Hz, 1 H). ¹³C NMR (500 MHz, CDCl₃) δ ppm 19.4, 19.6, 28.0, 28.1, 72.9, 73.9, 99.6, 126.0, 127.7, 128.9, 129.1, 136.0, 136.1, 164.3, 165.3, 172.4. HRMS (ESI⁺) *m/z* calcd for C₂₀H₂₇N₂O₂⁺ 327.2073, found 327.2085. Anal. (C₂₀H₂₆N₂O₂) C, H, N.

***N,N'*-dibenzyl-(6-phenethyl-pyrimidin-2,4-yl)-diamine (3b)**

Compound **2b** (80 mg, 0.20 mmol) and 10% Pd/C (22 mg, 0.020 mmol) were dissolved in 16 mL of MeOH. The resulting suspension was stirred under 1 atm H₂ for 1h. The solvent was removed *in vacuo* and the residue purified with column chromatography (25% EtOAc in hexanes) to give **3b** (42 mg, 52%). ¹H NMR (500 MHz, CDCl₃) δ ppm 2.72 (distorted dd, *J*=10.51, 8.36 Hz, 2 H), 2.95 (distorted dd, *J*=10.51, 8.58 Hz, 2 H), 4.48 (d, *J*=4.07 Hz, 2 H), 4.61 (d, *J*=6.00 Hz, 2 H), 4.90 (bs, 1 H), 5.24 (bs, 1 H), 5.56 (s, 1 H), 7.16 7.37 (m, 15 H). ¹³C NMR (500 MHz, CDCl₃) δ ppm 34.9, 39.7, 45.6, 50.4, 126.1, 127.1, 127.6, 127.7, 127.8, 128.5, 128.6, 128.7, 128.9, 140.3, 141.9, 162.4. HRMS (ESI⁺) *m/z* calcd for C₂₆H₂₇N₄⁺ 395.2236, found 395.2245.

2,4-Dichloro-6-phenethyl-pyrimidine (4)

Compound **1** (1.00 g, 4.0 mmol) and 10% Pd/C (118 mg, 0.11 mmol) were dissolved in 40 mL of MeOH. The resulting suspension was stirred under 1 atm H₂ for 1 h. The solvent was removed *in vacuo* and the residue purified with column chromatography (10% EtOAc in hexanes) to give **4** (0.521 mg, 52%). ¹H NMR (500 MHz, CDCl₃) δ ppm 3.06 (s, 4 H), 7.05 (s, 1 H), 7.17 (d, *J*=6.86 Hz, 2 H), 7.22 (t, *J*=7.29 Hz, 1 H), 7.29 (t, *J*=7.40 Hz, 2 H). ¹H NMR (500 MHz, acetone-D₆) δ ppm 3.08 (AA'BB', 2 H) 3.13 (AA'BB', 2 H), 7.20 (t, *J*=6.96 Hz, 1 H), 7.28 (m, 4 H), 7.53 (s, 1 H). ¹³C NMR (500 MHz, CDCl₃) δ ppm 34.4, 39.2, 119.4, 126.7,

128.5, 128.8, 139.9, 160.7, 162.5, 174.6. HRMS (ESI⁺) *m/z* calcd for C₁₂H₁₁N₂Cl₂⁺ 253.0299, found 253.0301.

2,4-Bis-benzyloxy-6-phenethyl-pyrimidine (5a)

Clean Na⁰ (54 mg, 2.3 mmol) was dissolved in 2 mL of benzylalcohol while heating at 70 °C with stirring (~2 h). To the resulting pale yellow solution, 100 mg (0.40 mmol) of **4** were added, and the reaction was stirred at 70 °C for 16 h. The reaction was allowed to cool to room temperature, and extracted from H₂O three times with ether. The combined organic layers were washed with brine, dried over anhydrous MgSO₄, and the solvent and excess alcohol removed *in vacuo* (removal of the alcohol required heating to 80 °C). Purification was accomplished with column chromatography (10% EtOAc in hexanes) to give **5a** (0.130 g, 83%). ¹H NMR (500 MHz, CDCl₃) δ ppm 2.93 (distorted dd, *J*=9.77, 9.03 Hz, 2 H), 3.03 (distorted dd, *J*=10.25, 8.79 Hz, 2 H), 5.40 (s, 2 H), 5.45 (s, 2 H), 6.25 (s, 1 H), 7.20 (m, 3 H), 7.26 7.43 (m, 10 H), 7.51 (d, *J*=7.08 Hz, 2 H). ¹³C NMR (500 MHz, CDCl₃) δ ppm 34.6, 39.3, 68.3, 69.2, 100.6, 126.2, 128.1, 128.2, 128.4, 128.56, 128.6, 128.7, 136.4, 137.0, 141.3, 164.8, 171.5, 172.3. HRMS (ESI⁺) *m/z* calcd for C₂₆H₂₅N₂O₂⁺ 397.1916, found 397.1916. Anal. (C₂₆H₂₄N₂O₂) H, N, C: calcd, 78.76; found, 78.22.

2,4-Bis-isobutylsulfanyl-6-phenethyl-pyrimidine (5b)

To a suspension of 48 mg (1.2 mmol) NaH (60% dispersion in mineral oil) in 5 mL of THF, 2-methyl-1-propanethiol (127 μL, 1.2 mmol) was added and the resulting mixture was stirred for 30 min. To this compound, **4** (0.100 g, 0.40 mmol) in 1 mL THF was added and suspension became a cloudy pink. The reaction was stirred 16 h at room temperature and the extracted from H₂O three times with CH₂Cl₂. The combined organic layers were washed with brine, dried over anhydrous MgSO₄, and the solvent removed with a rotary evaporator. Purification was accomplished with column chromatography (50% to 75% CH₂Cl₂ in hexanes) to give **5b** (0.131 g, 92%). ¹H NMR (500 MHz, CDCl₃) δ ppm 1.04 (d, *J*=6.65 Hz, 6 H), 1.07 (d, *J*=6.65 Hz, 6 H), 1.95 (sept, *J*=6.65 Hz, 1 H), 2.01 (sept, *J*=6.65 Hz, 1 H), 2.86 (distorted dd, *J*=10.29, 9.22 Hz, 2 H), 3.00 (distorted dd, *J*=10.51, 8.79 Hz, 2 H), 3.07 (d, *J*=6.65 Hz, 4 H), 6.60 (s, 1 H), 7.20 (m, 3 H), 7.28 (t, *J*=7.40 Hz, 2 H). ¹³C NMR (500 MHz, CDCl₃) δ ppm 22.1, 22.2, 28.6, 28.7, 34.7, 37.6, 39.2, 39.5, 113.2, 126.3, 128.59, 128.64, 141.2, 167.3, 170.1, 171.5. HRMS (ESI⁺) *m/z* calcd for C₂₀H₂₉N₂S₂⁺ 361.1772, found 361.1781.

2,4-Bis-(2-methyl-propane-1-sulfonyl)-6-phenethyl-pyrimidine (6a)

From the procedure described by Hurst.^{32, 33} mCPBA (77%, 53 mg, 0.24 mmol) and **5b** (18 mg, 0.050 mmol) were dissolved in 1.1 mL CHCl₃ with stirring. The solution was then allowed to stand at room temperature for 36 hours. CHCl₃ (5 mL) was added and the solution was washed 2 times with sat. NaHCO₃ sol. The aqueous layers were extracted once with CHCl₃ and the combined organic layers were washed with sat. NaCl sol. and dried over MgSO₄. The solvent was removed *in vacuo*, and chromatography of the residue (30% EtOAc in hexanes) gave **6a** in quantitative yield. ¹H NMR (500 MHz, CDCl₃) δ ppm 1.10 (d, *J*=6.86 Hz, 6 H), 1.13 (d, *J*=6.86 Hz, 6 H), 2.29 (sept, *J*=6.65 Hz, 1 H), 2.40 (sept, *J*=6.65 Hz, 1 H), 3.16 (t, *J*=7.72 Hz, 2 H), 3.37 (m, 4 H), 3.42 (d, *J*=6.43 Hz, 2 H), 7.16 (d, *J*=7.08 Hz, 2 H), 7.22 (t, *J*=7.40 Hz, 1 H), 7.29 (t, *J*=7.40 Hz, 2 H), 7.91 (s, 1 H). ¹³C NMR (500 MHz, CDCl₃) δ ppm 22.8, 22.9, 24.0, 24.1, 34.4, 40.0, 58.6, 58.7, 118.8, 127.0, 128.6, 129.0, 139.2, 166.4, 167.2, 177.2. HRMS (ESI⁺) *m/z* calcd for C₂₀H₂₉N₂O₄S₂⁺ 425.1569, found 425.1588.

(2-Chloro-6-styryl-pyrimidin-4-yl)-naphthalen-1-ylmethyl-carbamic acid tert-butyl ester (7c)

From the procedure described by Zanda, et al.³⁰ Compound **1** (0.700 g, 2.8 mmol) and Naphthalen-1-ylmethyl-carbamic acid tert-butyl ester (0.745 g, 3.06 mmol) were dissolved in 20 mL DMF. To this solution, NaH (60% dispersion in mineral oil, 0.134 g, 3.3 mmol) was

added under nitrogen causing the solution to become a dark turquoise. The reaction was stirred at room temperature for 1 h. The DMF was removed *in vacuo* with heating and the residue extracted from brine twice with ether and once with CH₂Cl₂. The combined organic layers were washed with sat. NaCl sol. and dried over MgSO₄. The solvent was removed *in vacuo*, and chromatography of the residue (1:1 CH₂Cl₂:hexanes to CH₂Cl₂) gave **7c** (573 mg, 44%). ¹H NMR (500 MHz, CDCl₃) δ ppm 1.33 (s, 9 H), 5.79 (s, 2 H), 7.05 (d, *J*=15.87 Hz, 1 H), 7.21 (d, *J*=7.32 Hz, 1 H), 7.38 (m, 4 H), 7.50 7.62 (m, 4 H), 7.76 (d, *J*=8.06 Hz, 1 H), 7.91 (m, 2 H), 8.09 (d, *J*=8.30 Hz, 1 H), 8.10 (s, 1 H). ¹³C NMR (500 MHz, CDCl₃) δ ppm 28.0, 46.3, 83.5, 109.0, 122.99, 123.03, 125.2, 125.5, 125.8, 126.3, 127.6, 128.0, 128.99, 129.05, 129.7, 131.0, 133.6, 133.8, 135.7, 138.1, 153.4, 160.0, 162.7, 165.5. HRMS (ESI⁺) *m/z* calcd for C₂₈H₂₇ClN₃O₂⁺ 472.1792, found 472.1790.

(2-Benzylamino-6-styryl-pyrimidin-4-yl)-isobutyl-carbamic acid tert-butyl ester (8a)

Compound **7a** (0.059 g, 0.15 mmol) and benzylamine (50 μL, 0.45 mmol) were dissolved in 3 mL DMSO and heated with stirring in a sealed high pressure tube at 90 °C for 16 h. As the reaction had not yet progressed to completion (as shown by TLC), at this point the temperature was raised to 110 °C and the solution was heated an additional 22 h. The DMSO was removed *in vacuo* with heating, and the resulting residue was extracted from brine three times with ether. The combined organic layers were washed with brine and dried over MgSO₄. The solvent was removed *in vacuo*, and chromatography of the residue (5% EtOAc in hexanes) produced **8a** (49 mg, 70%). ¹H NMR (500 MHz, CDCl₃) δ ppm 0.80 (d, *J*=6.59 Hz, 6 H), 1.55 (s, 9 H), 1.98 (sept, *J*=6.84 Hz, 1 H), 3.79 (d, *J*=7.32 Hz, 2 H), 4.65 (d, *J*=5.86 Hz, 2 H), 5.35 (bs, 1 H), 6.94 (d, *J*=16.11 Hz, 1 H), 7.25 (t, *J*=7.20 Hz, 1 H), 7.28 7.39 (m, 8 H), 7.55 (d, *J*=7.57 Hz, 2 H), 7.72 (d, *J*=15.87 Hz, 1 H). ¹³C NMR (500 MHz, CDCl₃) δ ppm 20.4, 28.2, 28.4, 45.8, 52.2, 81.9, 127.2, 127.49, 127.51, 127.6, 128.7, 128.86, 128.91, 135.0, 136.5, 140.0, 154.3, 161.8, 162.4, 163.6. HRMS (ESI⁺) *m/z* calcd for C₂₈H₃₅N₄O₂⁺ 459.2760, found 459.2760.

(2-Benzylamino-6-phenethyl-pyrimidin-4-yl)-isobutyl-carbamic acid tert-butyl ester (9a)

Compound **8a** (6 mg, 0.013 mmol) and 10% Pd/C (2 mg, 0.002 mmol) were dissolved in 2 mL of MeOH and 2 mL CH₂Cl₂. The resulting suspension was stirred under 1 atm H₂ for 1 h. The solvent was removed *in vacuo*, and the residue purified with column chromatography (25% EtOAc in hexanes) to give **9a** in quantitative yield. ¹H NMR (500 MHz, CDCl₃) δ ppm 0.78 (d, *J*=6.84, 6 H), 1.51 (s, 9 H), 1.95 (sept, *J*=6.84 Hz, 1 H), 2.84 (m, 2 H), 2.99 (distorted dd, *J*=11.23, 8.79 Hz, 2 H), 3.76 (d, *J*=7.32 Hz, 2 H), 4.60 (d, *J*=5.86 Hz, 2 H), 5.32 (bs, 1 H), 7.08 (s, 1 H), 7.16 7.35 (m, 10 H). ¹³C NMR (500 MHz, CDCl₃) δ ppm 20.4, 28.2, 28.4, 35.2, 40.2, 45.7, 52.2, 81.8, 102.6, 126.1, 127.2, 127.4, 128.57, 128.65, 128.7, 133.6, 135.0, 140.0, 154.2. HRMS (ESI⁺) *m/z* calcd for C₂₈H₃₇N₄O₂⁺ 461.2917, found 461.2920.

N²-Benzyl-N⁴-isobutyl-6-styryl-pyrimidine-2,4-diamine (10a)

Compound **8a** (16 mg, 0.035 mmol) was dissolved in 1 mL CH₂Cl₂, and, to this solution, 1 mL TFA was added with stirring, causing the solution to become bright yellow. The reaction was stirred at room temperature for 30 min, and the solvent was removed *in vacuo*. The resulting residue was extracted from H₂O three times with ether. The combined organic layers were washed with brine, dried over MgSO₄, and the solvent removed by rotary evaporator. Column chromatography of the residue (40% EtOAc in hexanes) gave **10a** (12 mg, 98%). ¹H NMR (500 MHz, CDCl₃) δ ppm 0.96 (d, *J*=6.59 Hz, 6 H), 1.86 (sept, *J*=6.59 Hz, 1 H), 3.12 (bs, 2 H), 4.66 (d, *J*=5.86 Hz, 2 H), 4.74 (bs, 1 H), 5.12 (bs, 1 H), 5.78 (s, 1 H), 6.83 (d, *J*=15.87 Hz, 1 H), 7.23 7.42 (m, 8 H), 7.54 (d, *J*=7.57 Hz, 2 H), 7.67 (d, *J*=15.87 Hz, 1 H). ¹³C NMR (500 MHz, CDCl₃) δ ppm 20.5, 28.7, 45.8, 127.1, 127.5, 127.6, 127.8, 128.6, 128.9, 134.1, 136.8, 140.4, 162.5, 164.5. HRMS (ESI⁺) *m/z* calcd for C₂₃H₂₇N₄⁺ 359.2236, found 359.2254.

***N*²-Benzyl-*N*⁴-isobutyl-6-phenethyl-pyrimidine-2,4-diamine (11a)**

Compound **10a** (9 mg, 0.025 mmol) and 10% Pd/C (12 mg, 0.011 mmol) were dissolved in 4 mL MeOH. The resulting suspension was stirred under 1 atm H₂ for 1 h. The solvent was removed *in vacuo*, and the residue purified with column chromatography (50% EtOAc in hexanes) to give **11a** in quantitative yield. ¹H NMR (500 MHz, CDCl₃) δ ppm 0.92 (d, *J*=6.59 Hz, 6 H), 1.80 (sept, *J*=6.84 Hz, 1 H), 2.73 (distorted dd, *J*=10.25, 8.30 Hz, 2 H), 2.97 (distorted dd, *J*=10.50, 8.55 Hz, 2 H), 3.03 (bs, 2 H), 4.61 (d, *J*=5.86 Hz, 2 H), 4.63 (bs, 1 H), 5.08 (bs, 1 H), 5.52 (s, 1 H), 7.16 7.34 (m, 8 H), 7.37 (d, *J*=6.84 Hz, 2 H). ¹³C NMR (500 MHz, CDCl₃) δ ppm 20.5, 28.6, 35.0, 39.8, 45.7, 126.0, 127.1, 127.8, 128.5, 128.6, 128.7, 142.0, 162.5, 164.1. HRMS (ESI⁺) *m/z* calcd for C₂₃H₂₉N₄⁺ 361.2392, found 361.2398.

2,4-Dichloro-6-(3-methyl-butyl)-pyrimidine (12b)

Based on methodology described by Furstner et al.^{28, 34, 35} Isopentylmagnesium bromide was formed by slow addition without stirring of isoamylbromide (5.0 mL, 41.7 mmol) to the bottom of a 3-neck flask fitted with a condenser that contained magnesium metal (1.116 g, 45.9 mmol) and 1,2-dibromoethane (500 μL, 5.8 μmol) in ~100 mL of diethyl ether. Once bubbles began to form, the solution was stirred until evolution ceased (1.5 h). Before addition to the following reaction mixture the Grignard was titrated using menthol and 1,10-phenanthroline dissolved in THF. In a separate flask, 2,4,6-trichloropyrimidine (2.20 g, 11.99 mmol), Fe(acac)₃ (0.217 g, 0.614 mmol), and *N*-methyl-2-pyrrolidinone (6.5 ml) were combined in dry THF (85 mL) producing an orange solution. To this solution, the isopentylmagnesium bromide (66 mL, 0.181 M in ether, 11.05 mmol) was added dropwise over the course of 20 minutes, immediately producing a cloudy dark orange precipitate. The reaction was stirred for 1 h at room temperature and then quenched with 1 M aqueous HCl. The mixture was extracted three times with ether, and the combined organic layers were washed with sat. NaHCO₃ sol. and brine, dried over MgSO₄, and the solvent removed *in vacuo*. Purification was accomplished by column chromatography (CH₂Cl₂) to give **12b** as the major product (1.377 g, 52%). ¹H NMR (500 MHz, CDCl₃) δ ppm 0.91 (d, *J*=6.43 Hz, 6 H), 1.58 (m, 3 H), 2.71 (AA'XX', 2 H), 7.14 (s, 1 H). ¹³C NMR (500 MHz, CDCl₃) δ ppm 22.4, 28.0, 35.7, 37.69, 118.9, 160.5, 162.4, 176.4. HRMS (ESI⁺) *m/z* calcd for C₉H₁₃N₂Cl₂⁺ 219.0456, found 219.0462.

2,4-dibenzylamino-6-isopentylpyrimidine (13c)

Compound **12b** (0.071 g, 0.32 mmol) was dissolved in benzylamine (1.5 mL) and heated sequentially with stirring in a sealed high-pressure tube at 110 °C for 5 h, 140 °C for 6h, and finally 155 °C for 13h. The solution was cooled and extracted from sat. NaHCO₃ solution once with CHCl₃ and twice with CH₂Cl₂. The combined organic layers were washed with sat. NaHCO₃ solution, H₂O, and brine, dried over anhydrous MgSO₄ and the solvent was removed with a rotary evaporator. Purification was accomplished with column chromatography (50% EtOAc in hexanes) to give **13c** in quantitative yield. ¹H NMR (500 MHz, CDCl₃) δ ppm 0.91 (d, *J*=6.65 Hz, 6 H), 1.51 (m, 2 H), 1.59 (sept, *J*=6.65 Hz, 1 H), 2.42 (t, *J*=8.15 Hz, 2 H), 4.49 (bs.d, *J*=5.15 Hz, 2 H), 4.59 (d, *J*=6.00 Hz, 2 H), 4.98 (bs, 1 H), 5.20 (bs, 1 H), 5.61 (s, 1 H), 7.21 7.38 (m, 10 H). ¹³C NMR (500 MHz, CDCl₃) δ ppm 22.7, 28.1, 36.0, 37.9, 45.6, 53.3, 105.5, 127.0, 127.1, 127.5, 127.71, 127.74, 128.4, 128.57, 128.6, 128.8, 140.3, 162.4, 163.8, 170.4. HRMS (ESI⁺) *m/z* calcd for C₂₃H₂₉N₄⁺ 361.2392, found 361.2386. Anal. (C₂₃H₂₈N₄) H, N, C, calcd, 76.63; found, 77.36.

2,4-Diisobutoxy-6-(3-methyl-butyl)-pyrimidine (13e)

Clean Na⁰ (63 mg, 2.7 mmol) was dissolved in 2mL of isobutyl alcohol while heating at 70 °C. To this solution, **12b** (0.100 g, 0.46 mmol) dissolved in 0.5 mL of isobutyl alcohol was added and solution became a cloudy pale orange. The reaction was stirred at 70 °C for 12 h

and allowed to cool to room temperature. The solution was extracted from H₂O three times with ether. The combined organic layers were washed with brine, dried over anhydrous MgSO₄, and the solvent removed with a rotary evaporator. Purification was accomplished with column chromatography (10% EtOAc in hexanes) to give **13e** (0.102 g, 76%). ¹H NMR (500 MHz, CDCl₃) δ ppm 0.90 (d, *J*=6.22 Hz, 6 H), 0.97 (d, *J*=6.65 Hz, 6 H), 1.00 (d, *J*=6.65 Hz, 6 H), 1.49 1.64 (m, 3 H), 2.03 (sept, *J*=6.86 Hz, 1 H), 2.10 (sept, *J*=6.65 Hz, 1 H), 2.55 (t, *J*=7.72 Hz, 2 H), 4.06 (d, *J*=6.65 Hz, 2 H), 4.07 (d, *J*=6.65 Hz, 2 H), 6.16 (s, 1 H). ¹³C NMR (500 MHz, CDCl₃) δ ppm 19.4, 19.6, 22.6, 27.97, 28.04, 28.06, 35.70, 35.75, 72.6, 73.7, 99.4, 165.3, 171.9, 173.6. HRMS (ESI⁺) *m/z* calcd for C₁₇H₃₁N₂O₂⁺ 295.2386, found 295.2392. Anal. (C₁₇H₃₀N₂O₂) H, N, C: calcd, 69.35; found, 69.86.

2,4-Bis-isobutylsulfanyl-6-(3-methyl-butyl)-pyrimidine (13g)

To a suspension of 41 mg (1.03 mmol) NaH in 4 mL of THF, 2-methyl-1-propanethiol (93 mg, 1.03 mmol) was added and the resulting mixture was stirred for 20 min. To this, **12b** (0.078 g, 0.35 mmol) in 3 mL THF was added and the suspension became a cloudy yellow. The reaction was stirred 16 h at room temperature and the extracted from H₂O three times with ether. The combined organic layers were washed with brine, dried over anhydrous MgSO₄, and the solvent removed with a rotary evaporator. Purification was accomplished with column chromatography (50% CH₂Cl₂ in hexanes) to give **13g** (0.114 g, 98%). ¹H NMR (500 MHz, CDCl₃) δ ppm 0.91 (d, *J*=6.35 Hz, 6 H), 1.03 (d, *J*=6.59 Hz, 6 H), 1.04 (d, *J*=6.59 Hz, 6 H), 1.49 1.63 (m, 3 H), 1.89 2.03 (m, 2 H), 2.54 (t, *J*=7.81 Hz, 2 H), 3.05 (d, *J*=6.84 Hz, 2 H), 3.08 (d, *J*=6.84 Hz, 2 H), 6.64 (s, 1 H). ¹³C NMR (500 MHz, CDCl₃) δ ppm 22.15, 22.22, 22.6, 28.0, 28.7, 35.6, 37.6, 37.8, 39.5, 112.9, 168.9, 169.8, 171.3. HRMS (ESI⁺) *m/z* calcd for C₁₇H₃₁N₂S₂⁺ 327.1929, found 327.1941.

4-(3-Methyl-butyl)-2,6-bis-(2-methyl-propane-1-sulfonyl)-pyrimidine (14a)

From the procedure described by Hurst.^{32, 33} mCPBA (77%, 142 mg, 0.63 mmol) in 1.5 mL of CHCl₃ was added to a solution of **13g** (43 mg, 0.13 mmol) in 1 mL CHCl₃ with stirring. The solution was then allowed to stand at room temperature for 36 hours. CHCl₃ (10 mL) was added and the solution was washed 2 times with sat. NaHCO₃ sol. The aqueous layers were extracted once with CHCl₃ and the combined organic layers were washed with sat. NaCl sol. and dried over MgSO₄. The solvent was removed *in vacuo*, and chromatography of the residue (25% EtOAc in hexanes) gave **14a** (0.026 g, 50%). ¹H NMR (500 MHz, CDCl₃) δ ppm 0.97 (d, *J*=6.43 Hz, 6 H), 1.13 (d, *J*=6.86 Hz, 6 H), 1.14 (d, *J*=6.86 Hz, 6 H), 1.62 1.72 (m, 3 H), 2.36 (sept, *J*=6.86 Hz, 1 H), 2.41 (sept, *J*=6.86 Hz, 1 H), 3.03 (m, 2 H), 3.39 (d, *J*=6.65 Hz, 2 H), 3.46 (d, *J*=6.65 Hz, 2 H), 8.02 (s, 1 H). ¹³C NMR (500 MHz, CDCl₃) δ ppm 22.5, 22.87, 22.92, 24.0, 24.2, 28.2, 36.7, 37.7, 58.5, 58.7, 118.4, 166.3, 167.2, 179.0. HRMS (ESI⁺) *m/z* calcd for C₁₇H₃₁N₂O₄S₂⁺ 391.1725, found 391.1732.

(2,6-Dichloro-pyrimidin-4-yl)-isobutyl-carbamic acid tert-butyl ester (15a)

Based on the method described by Zanda et al.³⁰ 2,4,6-Trichloropyrimidine (0.500 g, 2.73 mmol) and *N*-isobutyl-tert-butyl carbamate (0.473 g, 2.73 mmol) were dissolved in 15 mL of DMF. NaH (60% dispersion in mineral oil, 0.163 g, 4.07 mmol) was added and the solution turned yellow. The reaction was stirred at room temperature overnight, quenched with sat. NH₄Cl sol, and then extracted three times with ether. The combined organic phases were washed with sat. NaCl sol., and dried over MgSO₄. The solvent was removed *in vacuo*, and column chromatography (1:1 CH₂Cl₂:hexanes) of the residue produced **15a** (0.642 g, 74%). ¹H NMR (500 MHz, CDCl₃) δ ppm 0.89 (d, *J*=6.86 Hz, 6 H), 1.54 (s, 9 H), 2.03 (sept, *J*=6.86 Hz, 1 H), 3.87 (d, *J*=7.29 Hz, 2 H), 8.08 (s, 1 H). ¹³C NMR (500 MHz, CDCl₃) δ ppm 20.3, 28.0, 28.2, 52.7, 83.8, 110.4, 153.3, 158.9, 162.0, 163.0. HRMS (ESI⁺) *m/z* calcd for C₁₃H₂₀N₃O₂Cl₂⁺ 320.0933, found 320.0939.

[2-Chloro-6-(3-methyl-butyl)-pyrimidin-4-yl]-isobutyl-carbamic acid tert-butyl ester (16b)

Based on methodology described by Furstner et al.^{28, 34, 35} Isopentylmagnesium bromide was formed by slow addition without stirring of isoamylbromide (0.700 mL, 5.84 mmol) to the bottom of a 3-neck flask fitted with a condenser that contained magnesium metal (0.50 g, 20.6 mmol) and 1,2-dibromoethane (75 μ L, 0.87 μ mol) in ~20 mL of diethyl ether. Once bubbles began to form, the solution was stirred until evolution ceased (1.5 h). Before addition to the following reaction mixture, the Grignard was titrated using menthol and 1,10-phenanthroline dissolved in THF. Compound **15a** (0.220 g, 0.69 mmol), Fe(acac)₃ (0.017 g, 0.048 mmol), and N-methyl-2-pyrrolidinone (0.4 mL) were combined in dry THF (5.0 mL). To this solution, isopentylmagnesium bromide (0.29 M in ether, 3.55 mL, 1.03 mmol) was added dropwise, causing a progression from the starting brown solution to a cloudy orange followed by a dark brown and finally a clear solution containing solid salts. The reaction was stirred for 4 h at room temperature and then quenched with 1 M aqueous HCl. The mixture was extracted three times with ether, and the combined organic layers were washed with brine, dried over MgSO₄, and the solvent removed *in vacuo*. Purification was accomplished by column chromatography (CH₂Cl₂ followed by 3% EtOAc in CH₂Cl₂) to give **16b** (128 mg, 52%). ¹H NMR (500 MHz, CDCl₃) δ ppm 0.88 (d, *J*=6.59 Hz, 6 H), 0.92 (d, *J*=6.35 Hz, 6 H), 1.52 1.67 (m, 12 H), 2.03 (sept, *J*=6.84 Hz, 1 H), 2.66 (m, 2 H), 3.87 (d, *J*=7.08 Hz, 2 H), 7.78 (s, 1 H). ¹³C NMR (500 MHz, CDCl₃) δ ppm 20.3, 22.6, 28.2, 28.3, 36.3, 37.2, 38.2, 52.5, 82.9, 109.8, 153.7, 159.3, 162.6, 174.4. HRMS (ESI⁺) *m/z* calcd for C₁₈H₃₁N₃O₂Cl⁺ 356.2105, found 356.2114.

[2-Benzylamino-6-(3-methyl-butyl)-pyrimidin-4-yl]-isobutyl-carbamic acid tert-butyl ester (17a)

Compound **16b** (0.020 g, 0.056 mmol) was dissolved in benzylamine (1 mL) and heated with stirring in a sealed high-pressure tube at 100 °C for 24 h. The solution was cooled and the excess amine removed *in vacuo* with heating. The residue was extracted from sat. NaHCO₃ solution three times with CH₂Cl₂. The combined organic layers were washed with H₂O and brine, dried over anhydrous MgSO₄ and the solvent removed with a rotary evaporator. Purification was accomplished with column chromatography (15% EtOAc in hexanes) to give **17a** in quantitative yield. ¹H NMR (500 MHz, CDCl₃) δ ppm 0.78 (d, *J*=6.86 Hz, 6 H), 0.92 (d, *J*=6.43 Hz, 6 H), 1.50 1.66 (m, 12 H), 1.95 (sept, *J*=6.86 Hz, 1 H), 2.53 (m, 2 H), 3.75 (d, *J*=7.29 Hz, 2 H), 4.58 (d, *J*=6.00 Hz, 2 H), 5.31 (bs, 1 H), 7.06 (s, 1 H), 7.21 7.34 (m, 5 H). ¹³C NMR (500 MHz, CDCl₃) δ ppm 20.3, 22.7, 28.2, 28.3, 28.4, 36.5, 38.3, 45.6, 52.2, 81.7, 127.1, 127.4, 128.7, 140.0, 145.3, 154.3, 161.7, 161.8, 172.6. HRMS (ESI⁺) *m/z* calcd for C₂₅H₃₉N₄O₂⁺ 427.3073, found 427.3068.

N⁴-Benzyl-N²-isobutyl-6-(3-methyl-butyl)-pyrimidine-2,4-diamine (18d)

Compound **17c** (0.030 g, 0.071 mmol) was dissolved in 1.5 mL CH₂Cl₂ followed by addition of 1.5 mL TFA with stirring. The reaction was stirred at room temperature for 1.5 h, and the solvent and excess TFA were removed by rotary evaporator. Direct purification of the residue was accomplished with column chromatography (20% EtOAc and 2% TEA in hexanes) to give **18d** in quantitative yield. ¹H NMR (500 MHz, CDCl₃) δ ppm 0.90 (d, *J*=6.65 Hz, 6 H), 0.93 (d, *J*=6.86 Hz, 6 H), 1.49 (m, 2 H), 1.58 (sept, *J*=6.65 Hz, 1 H), 1.82 (sept, *J*=6.65 Hz, 1 H), 2.39 (m, 2 H), 3.18 (t, *J*=6.32 Hz, 2 H), 4.50 (d, *J*=5.15 Hz, 2 H), 4.84 (bs, 1 H), 4.88 (bs, 1 H), 5.56 (s, 1 H), 7.30 (m, 5 H). ¹³C NMR (500 MHz, CDCl₃) δ ppm 20.5, 22.7, 28.2, 28.8, 36.1, 38.0, 45.5, 49.2, 91.9, 127.5, 127.7, 128.8, 162.8, 163.8. HRMS (ESI⁺) *m/z* calcd for C₂₀H₃₁N₄⁺ 327.2549, found 327.2553.

[6-Chloro-2-(3-methyl-butyl)-pyrimidin-4-yl]-isobutyl-carbamic acid tert-butyl ester (19a)

Formed as a byproduct from the synthesis of **16b** (30 mg, 12%). ¹H NMR (500 MHz, CDCl₃) δ ppm 0.89 (d, *J*=6.84 Hz, 6 H), 0.93 (d, *J*=6.35 Hz, 6 H), 1.55 (s, 9 H), 1.60 (sept, *J*=6.59 Hz, 1 H), 1.66 (m, 2 H), 2.02 (sept, *J*=6.84 Hz, 1 H), 2.82 (distorted t, *J*=8.06 Hz, 2 H), 3.92 (d, *J*=7.08 Hz, 2 H), 7.88 (s, 1 H). ¹³C NMR (500 MHz, CDCl₃) δ ppm 20.4, 22.7, 27.9, 28.2, 28.3, 37.26, 37.32, 52.5, 82.9, 109.7, 153.8, 160.9, 161.6, 171.1. HRMS (ESI⁺) *m/z* calcd for C₁₈H₃₁N₃O₂Cl⁺ 356.2105, found 356.2099.

Isobutyl-[6-isobutylamino-2-(3-methyl-butyl)-pyrimidin-4-yl]-carbamic acid tert-butyl ester (20a)

Compound **19a** (0.019 g, 0.053 mmol) was dissolved in isobutylamine (2 mL) and heated with stirring in a sealed high-pressure tube at 100 °C for 16 h. The solution was cooled and the excess amine removed *in vacuo*. Direct purification of the residue was accomplished with column chromatography (15% EtOAc in hexanes) to give **20a** (18 mg, 88%). ¹H NMR (500 MHz, CDCl₃) δ ppm 0.86 (d, *J*=6.84 Hz, 6 H), 0.92 (d, *J*=6.35 Hz, 6 H), 0.98 (d, *J*=6.84 Hz, 6 H), 1.52 (s, 9 H), 1.62 (m, 3 H), 1.86 (sept, *J*=6.59 Hz, 1 H), 1.95 (m, *J*=6.84 Hz, 1 H), 2.63 (distorted t, *J*=8.06 Hz, 2 H), 3.06 (t, *J*=5.74 Hz, 2 H), 3.87 (d, *J*=7.32 Hz, 2 H), 4.89 (bs, 1 H), 6.68 (s, 1 H). ¹³C NMR (500 MHz, CDCl₃) δ ppm 20.4, 20.6, 22.8, 28.0, 28.4, 28.51, 28.54, 37.4, 49.5, 52.4, 81.4, 110.0, 157.3, 164.1.

***N,N'*-Diisobutyl-2-(3-methyl-butyl)-pyrimidine-4,6-diamine (21a)**

Compound **20a** (0.018 g, 0.047 mmol) was dissolved in 2 mL CH₂Cl₂ followed by addition of 2 mL TFA with stirring. The reaction was stirred at room temperature for 1 h, and the solvent and excess TFA were removed by rotary evaporator. Direct purification of the residue was accomplished with column chromatography (25% EtOAc and 2% TEA in hexanes) to give **21a** (6 mg, 47%). ¹H NMR (500 MHz, CDCl₃) δ ppm 0.92 (d, *J*=6.35 Hz, 6 H), 0.99 (d, *J*=6.84 Hz, 12 H), 1.61 (m, 3 H), 1.87 (sept, *J*=6.84 Hz, 2 H), 2.51 (m, 2 H), 2.98 (t, *J*=6.10 Hz, 4 H), 4.83 (bs, 2 H), 5.05 (s, 1 H). ¹³C NMR (500 MHz, CDCl₃) δ ppm 20.6, 22.8, 28.48, 28.54, 37.7, 37.9, 49.8, 110.0, 163.6. HRMS (ESI⁺) *m/z* calcd for C₁₇H₃₃N₄⁺ 293.2705, found 293.2696.

2-Chloro-4,6-distyryl-pyrimidine (22a)

Based on the coupling described by Tan et al.²⁹ Trans-2-Phenylvinylboronic acid (0.148 g, 1.00 mmol), K₃PO₄ (0.430 g, 2.03 mmol), and PdCl₂(PPh₃)₂ (0.010 g, 0.015 mmol) were combined in a 25 ml round-bottom flask. To this mixture, 2,4,6-trichloropyrimidine (0.093 g, 0.50 mmol) dissolved in THF (1.5 mL) was added producing a cloudy suspension. More THF (4.5 ml) and H₂O (0.11 mL) was added, producing a white cloudy suspension, which was heated at reflux for 19 h. 0.5 mL more of H₂O were added, eventually causing the precipitate to dissolve and the solution to turn dark orange. After 5 more hours at reflux, the solution was allowed to cool to room temperature. 35 mL of H₂O were added and the biphasic mixture was extracted three times with ether. The combined organic layers were washed with brine, dried over anhydrous MgSO₄, and the solvent removed with a rotary evaporator. The product was recrystallized from 5% EtOAc/hexanes and the filtrate purified with by column chromatography (5% EtOAc/hexanes) to provide **22a** (0.084 g, 52%). ¹H NMR (500 MHz, CDCl₃) δ ppm 7.04 (d, *J*=15.87 Hz, 2 H), 7.20 (s, 1 H), 7.36 7.45 (m, 6 H), 7.62 (d, *J*=6.84 Hz, 4 H), 7.95 (d, *J*=15.87 Hz, 2 H). ¹³C NMR (500 MHz, CDCl₃) δ ppm 114.9, 124.6, 128.1, 129.2, 130.0, 135.5, 139.0, 161.7, 165.9. HRMS (ESI⁺) *m/z* calcd for C₂₀H₁₆N₂Cl⁺ 319.1002, found 319.1005.

2-Chloro-4,6-bis-(3-methyl-butyl)-pyrimidine (22b)

Formed as a byproduct from the synthesis of **12b** (279 mg, 9%). ¹H NMR (500 MHz, CDCl₃) δ ppm 0.91 (d, *J*=6.22 Hz, 12 H), 1.53 1.63 (m, 6 H), 2.67 (distorted t, *J*=8.36 Hz, 4 H), 6.93 (s, 1 H). ¹³C NMR (500 MHz, CDCl₃) δ ppm 22.5, 28.2, 35.8, 38.0, 117.5, 161.0, 174.6. HRMS (ESI⁺) *m/z* calcd for C₁₄H₂₄N₂Cl⁺ 255.1628, found 255.1620.

[4,6-Bis-(3-methyl-butyl)-pyrimidin-2-yl]-isobutylamine (23a)

Compound **22b** (0.050 g, 0.20 mmol) was added to 1.5 mL of isobutylamine immediately forming a bright yellow solution. With stirring at room temperature (~5 min), the solution became a light brown. The reaction mixture was heated in a sealed high-pressure tube at 95 °C for 16 h. The reaction was cooled and the excess isobutylamine was removed *in vacuo*. The resulting residue was extracted from H₂O three times with ether. The combined organic layers were washed with brine, dried over anhydrous MgSO₄, and the solvent removed with a rotary evaporator. Purification was accomplished with column chromatography (10% EtOAc in hexanes) to give **23a** in quantitative yield. ¹H NMR (500 MHz, CDCl₃) δ ppm 0.92 (d, *J*=6.35 Hz, 12 H), 0.95 (d, *J*=6.84 Hz, 6 H), 1.50 1.64 (m, 6 H), 1.85 (sept, *J*=6.59 Hz, 1 H), 2.50 (m, 4 H), 3.24 (dd, *J*=6.71, 5.98 Hz, 2 H), 4.99 (bt, *J*=5.37 Hz, 1 H), 6.24 (s, 1 H). ¹³C NMR (500 MHz, CDCl₃) δ ppm 20.5, 22.7, 28.1, 28.8, 36.0, 38.0, 49.2, 108.1, 162.8, 171.7. HRMS (ESI⁺) *m/z* calcd for C₁₈H₃₄N₃⁺ 292.2753, found 292.2755.

(4,6-Diphenethyl-pyrimidin-2-yl)-isobutylamine (24a)

Compound **23d** (0.089 g, 0.25 mmol) was dissolved in suspension of 13 mg (0.012 mmol) 10% Pd/C in 20 mL of MeOH, forming a bright yellow mixture. The suspension was stirred under 1 atm of H₂ for 45 min. producing a clear mixture. The MeOH was removed *in vacuo* and the residue purified with column chromatography (25% EtOAc in hexanes) to give **24a** (57 mg, 64%). ¹H NMR (500 MHz, CDCl₃) δ ppm 1.00 (d, *J*=6.65 Hz, 6 H), 1.90 (sept, *J*=6.65 Hz, 1 H), 2.82 (distorted dd, *J*=10.29, 8.79 Hz, 4 H), 2.98 (distorted dd, *J*=10.29, 8.79 Hz, 4 H), 3.30 (t, *J*=6.22 Hz, 2 H), 5.10 (t, *J*=5.15 Hz, 1 H), 6.19 (s, 1 H), 7.20 (m, 6 H), 7.29 (m, 4 H). ¹³C NMR (500 MHz, CDCl₃) δ ppm 20.5, 28.8, 34.9, 39.6, 49.2, 108.7, 126.2, 128.56, 128.62, 141.7, 162.9, 170.3. HRMS (ESI⁺) *m/z* calcd for C₂₄H₃₀N₃⁺ 360.2440, found 360.2435. Anal. (C₂₄H₂₉N₃) C, H, N.

***N,N,N'*-Triisobutyl-pyrimidine-2,4,6-triamine (25a)**

2,4,6-trichloropyrimidine (0.182 g, 0.11 mmol) was added to 4 mL of isobutylamine, producing a violent reaction accompanied by the evolution of light smoke. The reaction mixture was heated with stirring in a sealed high-pressure tube at 115 °C for 43 h. The reaction was removed from the heat, allowed to cool to room temperature, and the excess amine was removed *in vacuo*. The resulting residue was extracted from H₂O three times with CH₂Cl₂. The combined organic layers were washed with sat. NaHCO₃ and brine and dried over anhydrous MgSO₄. The solvent was removed with a rotary evaporator and purification of the residue was accomplished with column chromatography (100% EtOAc) to give **25a** (175 mg, 60%). ¹H NMR (500 MHz, CDCl₃) δ ppm 0.91 (d, *J*=6.84 Hz, 6 H), 0.94 (d, *J*=6.59 Hz, 12 H), 1.81 (m, 3 H), 2.96 (t, *J*=6.35 Hz, 4 H), 3.12 (t, *J*=6.59 Hz, 2 H), 4.52 (m, 3 H), 4.74 (s, 1 H). ¹³C NMR (500 MHz, CDCl₃) δ ppm 20.5, 20.6, 28.6, 28.8, 49.1, 49.6, 71.6, 162.4, 164.5. HRMS (ESI⁺) *m/z* calcd for C₁₆H₃₂N₅⁺ 294.2658, found 294.2656. Anal. (C₁₆H₃₁N₅) C, H, N.

2,4,6-Triisobutoxy-pyrimidine (25c)

Clean Na⁰ (83 mg, 3.6 mmol) was dissolved in 4 mL of isobutylalcohol while heating at 70 °C. The resulting solution was cooled to room temperature and 104 mg (0.57 mmol) 2,4,6-trichloropyrimidine dissolved in 0.5 mL of isobutyl alcohol were added with stirring, causing the solution to immediately become cloudy. The reaction was stirred at room temperature for

1 h and then at 60 °C for 24 h. The reaction was allowed to cool to room temperature, extracted from H₂O twice with ether and once with CH₂Cl₂. The combined organic layers were washed with brine, dried over anhydrous MgSO₄, and the solvent and excess alcohol removed with a rotary evaporator. Purification was accomplished with column chromatography (5% EtOAc in hexanes) to give **25c** (0.151 g, 90%). ¹H NMR (500 MHz, CDCl₃) δ ppm 0.96 (d, *J*=6.65 Hz, 12 H), 0.99 (d, *J*=6.65 Hz, 6 H), 2.03 (sept, *J*=6.65 Hz, 2 H), 2.11 (sept, *J*=6.65 Hz, 1 H), 4.02 (d, *J*=6.86 Hz, 4 H), 4.05 (d, *J*=6.86 Hz, 2 H), 5.66 (s, 1 H). ¹³C NMR (500 MHz, CDCl₃) δ ppm 19.4, 19.5, 28.0, 28.1, 73.1, 73.9, 83.4, 164.9, 172.8. HRMS (ESI⁺) *m/z* calcd for C₁₆H₂₉N₂O₃⁺ 297.2178, found 297.2179. Anal. (C₁₆H₂₈N₂O₃) H, N, C: calcd, 64.83; found, 65.26.

2,4,6-Tris-isobutylsulfanyl-pyrimidine (25e)

To a suspension of 147 mg NaH (3.67 mmol, 60% dispersion in mineral oil) in 15 mL of THF, 2-methyl-propane-1-thiol (0.35 mL, 3.3 mmol) was added dropwise and the resulting mixture was stirred for 20 min. To this, 2,4,6-trichloropyrimidine (0.150 g, 0.82 mmol) was added. The reaction was stirred 16 h at room temperature, quenched with H₂O, and extracted three times with ether. The combined organic layers were washed with brine, dried over anhydrous MgSO₄, and the solvent removed with a rotary evaporator. Purification was accomplished with column chromatography (50% CH₂Cl₂ in hexanes) to give **25e** (0.226 g, 94%). ¹H NMR (500 MHz, CDCl₃) δ ppm 1.01 (d, *J*=6.65 Hz, 12 H), 1.04 (d, *J*=6.65 Hz, 6 H), 1.92 (sept, *J*=6.65 Hz, 2 H), 1.98 (sept, *J*=6.65 Hz, 1 H), 3.02 (d, *J*=6.86 Hz, 2 H), 3.03 (d, *J*=6.86 Hz, 4 H), 6.64 (s, 1 H). ¹³C NMR (500 MHz, CDCl₃) δ ppm 22.1, 22.2, 28.6, 28.7, 37.8, 39.5, 110.8, 168.0, 170.9. HRMS (ESI⁺) *m/z* calcd for C₁₆H₂₉N₂S₃⁺ 345.1493, found 345.1479. Anal. (C₁₆H₂₈N₂S₃) C, H, N.

2,4-diisobutylamino-6-chloropyrimidine (26)

Isobutylamine (1 mL) was added dropwise to 0.337 g (1.8 mmol) of 2,4,6-trichloropyrimidine producing a violent reaction accompanied by the evolution of white smoke. The resulting mixture was heated in a sealed pressure tube at 75 °C for 1 h. The reaction was cooled to room temperature and extracted three times from sat. NaHCO₃ solution with CH₂Cl₂. The combined organic layers were washed with brine, dried over anhydrous MgSO₄, and the solvent removed with a rotary evaporator. Purification was accomplished with column chromatography (5% EtOAc in hexanes) to give **26** (0.216 g, 45%). ¹H NMR (500 MHz, CDCl₃) δ ppm 0.90 (d, *J*=6.59 Hz, 6 H), 0.92 (d, *J*=6.59 Hz, 6 H), 1.76 1.88 (m, 2 H), 3.03 (bs, 2 H), 3.15 (t, *J*=6.35 Hz, 2 H), 4.98 (bs, 1 H), 5.16 (bs, 1 H), 5.66 (s, 1 H). ¹³C NMR (500 MHz, CDCl₃) δ ppm 20.4, 28.5, 28.6, 49.0, 162.1, 164.4. HRMS (ESI⁺) *m/z* calcd for C₁₂H₂₂N₄Cl⁺ 257.1533, found 257.1522.

2,4-diisobutylamino-pyrimidine (27d)

Compound **26** (0.035 g, 0.14 mmol) was dissolved in a suspension of 3 mL MeOH, 23 μL Et₃N, and 24 mg (0.022 mmol) 10% Pd/C. The suspension was stirred under 1 atm of H₂ for 24 h. The reaction was filtered using a 2 μm syringe filter and the solvent removed using a rotary evaporator. The residue was extracted three times from H₂O with CH₂Cl₂. The combined organic layers were washed with brine, dried over anhydrous MgSO₄, and the solvent removed *in vacuo*. Purification was accomplished with column chromatography (5% EtOAc and 1% TEA in hexanes) to give **27d** (19 mg, 63%). ¹H NMR (500 MHz, CDCl₃) δ ppm 0.95 (d, *J*=6.84 Hz, 6 H), 0.95 (d, *J*=6.59 Hz, 6 H), 1.80 1.90 (m, 2 H), 3.07 (bs, 2 H), 3.17 (dd, *J*=6.71, 5.98 Hz, 2 H), 4.73 (bs, 1 H), 4.86 (s, 1 H), 5.66 (d, *J*=5.86 Hz, 1 H), 7.81 (bs, 1 H). ¹³C NMR (500 MHz, CDCl₃) δ ppm 20.47, 20.51, 28.6, 28.7, 49.1, 156.3, 162.6, 163.4. HRMS (ESI⁺) *m/z* calcd for C₁₂H₂₃N₄⁺ 223.1923, found 223.1915.

***N*²,*N*⁴-dimethyl-*N*²,*N*⁴-diisobutyl-(6-isopentyl-pyrimidin-2,4-yl)-diamine (29a)**

N-methylisobutylamine (1 mL) was added dropwise to **12b** (0.055 g, 0.22 mmol), causing the immediate formation of a precipitate. The reaction mixture was stirred in a sealed high-pressure tube at 80 °C for 16h, allowed to cool to room temperature, and extracted three times from aq. NaHCO₃ with CH₂Cl₂. The combined organic layers were washed with brine, dried over anhydrous MgSO₄, and the solvent removed *in vacuo*. Purification was accomplished with column chromatography (10% EtOAc in hexanes) to give **29a** (25 mg, 31%). ¹H NMR (500 MHz, CDCl₃) δ ppm 0.89 (d, *J*=6.65 Hz, 12 H), 0.92 (d, *J*=6.43 Hz, 6 H), 1.52 1.66 (m, 3 H), 2.06 (nonet, *J*=6.86 Hz, 2 H), 2.45 (t, *J*=7.93 Hz, 2 H), 2.99 (s, 3 H), 3.12 (s, 3 H), 3.28 (d, *J*=6.22 Hz, 2 H), 3.39 (d, *J*=7.29 Hz, 2 H), 5.57 (s, 1 H). ¹³C NMR (500 MHz, CDCl₃) δ ppm 20.58, 20.63, 22.8, 27.7, 27.8, 28.0, 36.2, 36.5, 36.7, 38.1, 57.0, 57.2, 89.6, 162.2, 163.2, 169.7. HRMS (ESI⁺) *m/z* calcd for C₁₉H₃₇N₄⁺ 321.3018, found 321.3014.

Isobutyl-[2-(isobutyl-methyl-amino)-6-styryl-pyrimidin-4-yl]-carbamic acid tert-butyl ester (31b0)

Compound **7a** (0.063 g, 0.16 mmol) was dissolved in 1.5 mL of *N*-methylisobutylamine and heated with stirring in a sealed high-pressure tube at 100 °C for 16 h. The reaction was allowed to cool to room temperature and the excess amine removed *in vacuo*. The resulting residue was extracted three times from H₂O with ether. The combined organic layers were washed with brine, dried over anhydrous MgSO₄, and the solvent removed by rotary evaporator. Purification was accomplished with column chromatography (CH₂Cl₂ followed by 10% EtOAc in hexanes) to give **31b0** (32 mg, 45%). ¹H NMR (500 MHz, CDCl₃) δ ppm 0.90 (d, *J*=6.84 Hz, 6 H), 0.93 (d, *J*=6.84 Hz, 6 H), 1.56 (s, 9 H), 2.11 (m, 2 H), 3.21 (s, 3 H), 3.45 (d, *J*=7.08 Hz, 2 H), 3.87 (d, *J*=7.32 Hz, 2 H), 6.95 (d, *J*=15.63 Hz, 1 H), 7.17 (s, 1 H), 7.29 (t, *J*=7.32 Hz, 1 H), 7.37 (t, *J*=7.45 Hz, 2 H), 7.56 (d, *J*=7.57 Hz, 2 H), 7.76 (d, *J*=15.87 Hz, 1 H). ¹³C NMR (500 MHz, CDCl₃) δ ppm 20.5, 20.6, 27.6, 28.2, 28.5, 36.4, 52.3, 57.2, 81.7, 100.9, 127.6, 128.3, 128.6, 128.9, 134.4, 136.8, 154.4, 161.7, 161.8, 162.9. HRMS (ESI⁺) *m/z* calcd for C₂₆H₃₉N₄O₂⁺ 439.3073, found 439.3076.

***N*²-methyl-*N*²,*N*⁴-diisobutyl-(6-styryl-pyrimidin-2,4-yl)-diamine (31b)**

Compound **31b0** (0.032 g, 0.073 mmol) was dissolved in 1.5 mL CH₂Cl₂ and to this solution 1.5 mL of TFA was added dropwise with stirring. The reaction was allowed to stir at room temperature for 2.5 h. The solvent was removed *in vacuo*, and the resulting residue was directly purified by column chromatography (5% EtOAc and 1% TEA in hexanes) to give **31b** in quantitative yield. ¹H NMR (500 MHz, CDCl₃) δ ppm 0.93 (d, *J*=6.59 Hz, 6 H), 0.97 (d, *J*=6.84 Hz, 6 H), 1.90 (sept, *J*=6.84 Hz, 1 H), 2.12 (sept, *J*=6.59 Hz, 1 H), 3.15 (bs, 2 H), 3.19 (s, 3 H), 3.45 (d, *J*=7.32 Hz, 2 H), 4.64 (bs, 1 H), 5.67 (s, 1 H), 6.83 (d, *J*=15.87 Hz, 1 H), 7.28 (t, *J*=7.32 Hz, 1 H), 7.35 (t, *J*=7.57 Hz, 2 H), 7.55 (d, *J*=7.32 Hz, 2 H), 7.71 (d, *J*=15.87 Hz, 1 H). ¹³C NMR (500 MHz, CDCl₃) δ ppm 20.57, 20.64, 27.7, 28.8, 36.3, 49.2, 57.1, 127.5, 128.37, 128.43, 128.8, 133.5, 162.4. HRMS (ESI⁺) *m/z* calcd for C₂₁H₃₁N₄⁺ 339.2549, found 339.2542.

***N*²-methyl-*N*²,*N*⁴-diisobutyl-(6-phenethyl-pyrimidin-2,4-yl)-diamine (32)**

Compound **31b** (0.022 g, 0.064 mmol) was dissolved in a suspension of 16 mg (0.015 mmol) 10% Pd/C in 4 mL MeOH. The reaction was stirred under 1 atm of H₂ for 45 min. The solvent was removed *in vacuo* and residue was purified directly by column chromatography (10% EtOAc in hexanes) to give **32** (16 mg, 73%). ¹H NMR (500 MHz, CDCl₃) δ ppm 0.90 (d, *J*=6.59 Hz, 6 H), 0.94 (d, *J*=6.59 Hz, 6 H), 1.85 (sept, *J*=6.59 Hz, 1 H), 2.07 (sept, *J*=6.59 Hz, 1 H), 2.74 (bt, *J*=6.84 Hz, 2 H), 3.00 (dd, *J*=9.28, 6.84 Hz, 2 H), 3.06 (bs, 2 H), 3.12 (s, 3 H), 3.42 (d, *J*=7.32 Hz, 2 H), 4.52 (bs, 1 H), 5.44 (s, 1 H), 7.17 (t, *J*=7.20 Hz, 1 H), 7.22 (distorted

d, $J=6.84$ Hz, 2 H), 7.27 (t, $J=7.57$ Hz, 2 H). HRMS (ESI⁺) m/z calcd for C₂₁H₃₃N₄⁺ 341.2705, found 341.2705.

(2-Chloro-6-styryl-pyrimidin-4-yl)-isobutyl-methyl-amine (33b)

Compound **1** (50 mg, 0.20 mmol) and K₂CO₃ (82 mg, 0.60 mmol) were mixed in 2.5 mL of DMF. To this suspension, 24 μ L (0.20 mmol) of *N*-methylisobutylamine were added with stirring at room temperature. Consumption of starting material was observed by TLC after 3 h. The reaction mixture was diluted with H₂O and extracted three times with ether. The combined organic layers were washed with brine, dried over MgSO₄, and the solvent removed by rotary evaporator. Purification of the residue by column chromatography (CH₂Cl₂ followed by 10% EtOAc in hexanes) afforded **33b** (50 mg, 84%). ¹H NMR (500 MHz, CDCl₃) δ ppm 0.94 (d, $J=6.35$ Hz, 6 H), 2.08 (sept, $J=6.84$ Hz, 1 H), 3.11 (bs, 3 H), 3.42 (bs, 2 H), 6.25 (s, 1 H), 6.88 (d, $J=15.87$ Hz, 1 H), 7.32 (t, $J=7.20$ Hz, 1 H), 7.37 (t, $J=7.32$ Hz, 2 H), 7.56 (d, $J=7.32$ Hz, 2 H), 7.80 (d, $J=15.87$ Hz, 1 H). ¹³C NMR (500 MHz, CDCl₃) δ ppm 20.3, 27.5, 37.1, 125.6, 127.7, 129.0, 129.2, 136.1, 136.3 164.1. HRMS (ESI⁺) m/z calcd for C₁₇H₂₁N₃Cl⁺ 302.1424, found 302.1421.

*N*⁴-methyl-*N*²,*N*⁴-diisobutyl-(6-styryl-pyrimidin-2,4-yl)-diamine (34b)

Compound **33b** (0.050 g, 0.17 mmol) was dissolved in 2.5 mL of isobutylamine and heated with stirring in a sealed high-pressure tube at 100 °C for 24 h. The reaction was allowed to cool to room temperature and the excess amine removed *in vacuo*. Purification was accomplished with column chromatography (5% EtOAc and 1% TEA in hexanes) to give **34b** (27 mg, 47%). ¹H NMR (500 MHz, CDCl₃) δ ppm 1H 0.92 (d, $J=6.59$ Hz, 6 H), 0.98 (d, $J=6.59$ Hz, 6 H), 1.91 (sept, $J=6.59$ Hz, 1 H), 2.08 (sept, $J=6.84$ Hz, 1 H), 3.06 (s, 3 H), 3.25 (t, $J=6.35$ Hz, 2 H), 3.33 (bs, 2 H), 4.93 (bs, 1 H), 5.83 (s, 1 H), 6.85 (d, $J=15.87$ Hz, 1 H), 7.28 (t, $J=7.32$ Hz, 1 H), 7.35 (t, $J=7.57$ Hz, 2 H), 7.55 (d, $J=7.32$ Hz, 2 H), 7.66 (d, $J=15.87$ Hz, 1 H). ¹³C NMR (500 MHz, CDCl₃) δ ppm 20.5, 20.6, 27.8, 28.9, 36.8, 49.4, 57.3, 92.2, 127.4, 128.1, 128.4, 128.8, 133.5, 136.9, 162.5, 163.8. HRMS (ESI⁺) m/z calcd for C₂₁H₃₁N₄⁺ 339.2549, found 339.2562.

*N*⁴-methyl-*N*²,*N*⁴-diisobutyl-6-[(2-naphthalen-1-yl-ethyl)-pyrimidin-2,4-yl]-diamine (34c)

Compound **33c** (0.012 g, 0.03 mmol) was dissolved in 4 mL of isobutylamine and heated with stirring in a sealed high-pressure tube at 95 °C for 20 h. The reaction was allowed to cool to room temperature and the excess amine removed *in vacuo*. The resulting residue was extracted three times from H₂O with CH₂Cl₂. The combined organic layers were washed with brine, dried over anhydrous MgSO₄, and the solvent removed by rotary evaporator. Purification was accomplished with column chromatography (10% EtOAc and 1% TEA in hexanes) to give **34c** (3 mg, 21%). ¹H NMR (500 MHz, CDCl₃) δ ppm 0.86 (d, $J=6.59$ Hz, 6 H), 0.98 (d, $J=6.84$ Hz, 6 H), 1.87 2.03 (m, 2 H), 2.86 (m, 2 H), 2.97 (s, 3 H), 3.24 (t, $J=6.35$ Hz, 4 H), 3.44 (distorted t, $J=8.30$ Hz, 2 H), 5.03 (bs, 1 H), 5.52 (s, 1 H), 7.37 (m, 2 H), 7.45 7.54 (m, 2 H), 7.71 (d, $J=7.57$ Hz, 1 H), 7.85 (dd, $J=7.93, 1.34$ Hz, 1 H), 8.15 (d, $J=8.30$ Hz, 1 H). HRMS (ESI⁺) m/z calcd for C₂₅H₃₅N₄⁺ 391.2862, found 391.2863.

*N*⁴-dimethyl-*N*²,*N*⁴-diisobutyl-(6-phenethyl-pyrimidin-2,4-yl)-diamine (35)

Compound **34b** (0.016 g, 0.05 mmol) was dissolved in a suspension of 10 mg (0.009 mmol) 10% Pd/C in 2 mL MeOH. The reaction was stirred under 1 atm of H₂ for 45 min. The solvent was removed *in vacuo* and residue was purified directly by column chromatography (10% EtOAc and 1% TEA in hexanes) to give **35** (14 mg, 85%). ¹H NMR (500 MHz, CDCl₃) δ ppm 0.88 (d, $J=6.59$ Hz, 6 H), 0.96 (d, $J=6.59$ Hz, 6 H), 1.88 (sept, $J=6.84$ Hz, 1 H), 2.00 (sept, $J=6.59$ Hz, 1 H), 2.72 (m, 2 H), 2.97 (m, 5 H), 3.21 (t, $J=6.47$ Hz, 2 H), 3.26 (bs, 2 H), 4.92 (bs, 1 H), 5.55 (s, 1 H), 7.18 (t, $J=7.20$ Hz, 1 H), 7.22 (d, $J=6.84$ Hz, 2 H), 7.27 (t, $J=7.57$ Hz,

2 H). ^{13}C NMR (500 MHz, CDCl_3) δ ppm 20.5, 20.6, 27.7, 28.8, 35.4, 36.7, 40.0, 49.4, 57.2, 91.3, 126.0, 128.5, 128.7, 142.1, 162.3, 163.4. HRMS (ESI⁺) m/z calcd for $\text{C}_{21}\text{H}_{33}\text{N}_4^+$ 341.2705, found 341.2713.

Isobutyl-[2-isobutylsulfanyl-6-(3-methyl-butyl)-pyrimidin-4-yl]-carbamic acid tert-butyl ester (36b)

To a suspension of 45 mg (1.1 mmol,) NaH (60% dispersion in mineral oil) in 3 mL of THF, 2-methyl-propane-1-thiol (122 μL , 1.1 mmol) was added dropwise and the resulting mixture was stirred for 15 min. To this mixture, **16b** (0.040 g, 0.11 mmol) was added dissolved in 1 mL THF. The reaction was stirred 16 h at room temperature, quenched with H_2O , and extracted three times with ether. The combined organic layers were washed with brine, dried over anhydrous MgSO_4 , and the solvent removed with a rotary evaporator. Purification was accomplished with column chromatography (10% EtOAc in hexanes) to give **36b** (0.036 g, 78%). ^1H NMR (500 MHz, CDCl_3) δ ppm 0.88 (d, $J=6.84$ Hz, 6 H), 0.92 (d, $J=5.86$ Hz, 6 H), 1.04 (d, $J=6.59$ Hz, 6 H), 1.54 (s, 9 H), 1.58 (bs, 3 H), 1.95 (sept, $J=6.84$ Hz, 1 H), 2.04 (sept, $J=6.84$ Hz, 1 H), 2.62 (bt, $J=7.32$ Hz, 2 H), 3.00 (d, $J=6.35$ Hz, 2 H), 3.89 (d, $J=7.57$ Hz, 2 H), 7.44 (s, 1 H). ^{13}C NMR (500 MHz, CDCl_3) δ ppm 20.3, 22.3, 22.7, 28.1, 28.3, 28.4, 28.7, 36.3, 38.1, 39.5, 52.2, 82.3, 107.4, 154.0, 160.7, 170.3, 171.8. HRMS (ESI⁺) m/z calcd for $\text{C}_{16}\text{H}_{29}\text{N}_2\text{S}_3^+$ 345.1493, found 345.1479.

[2-Isobutoxy-6-(3-methyl-butyl)-pyrimidin-4-yl]-isobutylamine (37a)

NaH (60% dispersion in mineral oil, 34 mg, 0.85 mmol) was added to 3 mL of isobutanol and stirred for 30 minutes at room temperature. To this solution, 28 mg (0.078 mmol) of **16b** dissolved in 3 mL of isobutanol were added. The resulting solution was heated with stirring in a sealed high-pressure tube at 100 °C for 4 h. The solution was allowed to cool to room temperature and stirred an additional 16 h. Extraction of the reaction mixture was performed three times from H_2O with ether, and the combined organic layers were washed with brine, dried over MgSO_4 , and the solvent removed by rotary evaporator. The resulting residue was dissolved in 2 mL CH_2Cl_2 and 2 mL of TFA were added with stirring. The reaction was stirred for 1.5 h at room temperature and the solvent was removed *in vacuo*. Purification of the residue was accomplished with column chromatography (10% EtOAc and 2% TEA in hexanes) to give **37a** (22 mg, 98%). ^1H NMR (500 MHz, CDCl_3) δ ppm 0.92 (d, $J=6.35$ Hz, 6 H), 0.96 (d, $J=6.84$ Hz, 6 H), 1.00 (d, $J=6.59$ Hz, 6 H), 1.51 1.64 (m, 3 H), 1.86 (sept, $J=6.84$ Hz, 1 H), 2.08 (sept, $J=6.59$ Hz, 1 H), 2.50 (distorted t, $J=8.06$ Hz, 2 H), 3.09 (bs, 2 H), 4.02 (d, $J=6.84$ Hz, 2 H), 4.90 (bs, 1 H), 5.81 (s, 1 H). ^{13}C NMR (500 MHz, CDCl_3) δ ppm 19.6, 20.5, 22.7, 28.16, 28.18, 28.6, 37.9, 73.3, 165.0. HRMS (ESI⁺) m/z calcd for $\text{C}_{17}\text{H}_{32}\text{N}_3\text{O}^+$ 294.2545, found 294.2538.

Isobutyl-[2-isobutylsulfanyl-6-(3-methyl-butyl)-pyrimidin-4-yl]-amine (37b)

Compound **36b** (18 mg, 0.043 mmol) was dissolved in 2 mL CH_2Cl_2 , to which 2 mL of TFA were added with stirring. The reaction was stirred for 1.5 h at room temperature and the solvent was removed *in vacuo*. Purification of the residue was accomplished with column chromatography (10% EtOAc and 2% TEA in hexanes) to give **37b** in quantitative yield. ^1H NMR (500 MHz, CDCl_3) δ ppm 0.89 (d, $J=6.35$ Hz, 6 H), 0.95 (d, $J=6.59$ Hz, 6 H), 1.02 (d, $J=6.59$ Hz, 6 H), 1.47 1.61 (m, 3 H), 1.86 2.01 (m, 2 H), 2.52 (distorted t, $J=7.81$ Hz, 2 H), 3.01 (d, $J=6.59$ Hz, 2 H), 3.22 (bs, 2 H), 6.09 (bs, 1 H). HRMS (ESI⁺) m/z calcd for $\text{C}_{17}\text{H}_{32}\text{N}_3\text{S}^+$ 310.2317, found 310.2309.

Isobutyl-[6-(3-methyl-butyl)-2-(2-methyl-propane-1-sulfonyl)-pyrimidin-4-yl]-carbamic acid tert-butyl ester (**38**)

From the procedure described by Hurst, et al.^{32, 33} mCPBA (77%, 27 mg, 0.12 mmol) and 20 mg of **36b** were dissolved in 2 mL of CHCl₃ and mixed well. The solution was then allowed to stand at room temperature for 16 hours. 20 mL of CHCl₃ was added and the solution was washed 3 times with sat. NaHCO₃ sol. The aqueous layers were extracted twice with CHCl₃ and the combined organic layers were washed with sat. NaCl sol. and dried over MgSO₄. The solvent was removed *in vacuo*, and chromatography of the residue (10% EtOAc in hexanes) gave **38** (9 mg, 40%). ¹H NMR (500 MHz, CDCl₃) δ ppm 0.91 (d, *J*=6.59 Hz, 6 H), 0.94 (d, *J*=6.59 Hz, 6 H), 1.10 (d, *J*=6.84 Hz, 6 H), 1.57 (s, 9 H), 1.59 1.67 (m, 3 H), 2.07 (sept, *J*=6.84 Hz, 1 H), 2.37 (sept, *J*=6.59 Hz, 1 H), 2.80 (m, 2 H), 3.39 (d, *J*=6.59 Hz, 2 H), 3.94 (d, *J*=7.32 Hz, 2 H), 8.05 (s, 1 H). ¹³C NMR (500 MHz, CDCl₃) δ ppm 20.4, 22.6, 23.0, 24.1, 28.18, 28.24, 28.3, 36.3, 38.1, 52.8, 58.4, 83.4, 113.3, 153.7, 161.8, 164.5, 173.6.

Isobutyl-[6-(3-methyl-butyl)-2-(2-methyl-propane-1-sulfonyl)-pyrimidin-4-yl]-amine (**39**)

Compound **38** (9 mg, 0.019 mmol) was dissolved in 2 mL CH₂Cl₂, to which 2 mL of TFA were added with stirring. The reaction was stirred for 2.5 h at room temperature and the solvent was removed *in vacuo*. Purification of the residue was accomplished with column chromatography (25% EtOAc and 2% TEA in hexanes) to give **39** in quantitative yield. ¹H NMR (500 MHz, CDCl₃) δ ppm 0.93 (d, *J*=6.35 Hz, 6 H), 0.99 (d, *J*=6.59 Hz, 6 H), 1.10 (d, *J*=6.59 Hz, 6 H), 1.54 1.65 (m, 3 H), 1.89 (sept, *J*=6.59 Hz, 1 H), 2.37 (sept, *J*=6.59 Hz, 1 H), 2.66 (distorted t, *J*=8.06 Hz, 2 H), 3.06 (bs, 2 H), 3.37 (d, *J*=6.35 Hz, 2 H), 5.55 (bs, 1 H), 6.23 (s, 1 H). HRMS (ESI⁺) *m/z* calcd for C₁₇H₃₂N₃O₂S⁺ 342.2215, found 342.2209.

Biological Methods

TR-FRET CBI Assay

Purified ER α -417, labeled site-specifically with maleimide-biotin (Quanta BioDesign) and SRC-3-NRD, labeled non-specifically through cysteine residues with iodoacetamide-fluorescein (Invitrogen), were used in the time-resolved FRET assays.⁴² A 5- μ L volume of a stock solution mix of ER α -417 (8 nM), estradiol (4 μ M), and LanthaScreen Streptavidin-Terbium (Invitrogen) (2 nM) in TR-FRET buffer (20 mM Tris, pH 7.5, 0.01% NP40, 50 mM NaCl) were placed in separate wells of a black 96-well Molecular Devices HE high efficiency microplate (Molecular Devices, Inc., Sunnyvale, CA). In a second 96-well Nunc polypropylene plate (Nalge Nunc International, Rochester, NY), a 0.02 M solution of each coactivator binding inhibitor was serially diluted in a 1:10 fashion into DMF. Each concentration of coactivator binding inhibitor or vehicle was then diluted 1:10 into TR-FRET buffer, and 10 μ L of this solution was added to the stock ER α solution in the 96-well plate. After a twenty-minute incubation, 5 μ L of 200 nM fluorescein-SRC-3-NRD was added to each well. This mixture was allowed to incubate for 1 h at room temperature in the dark. TR-FRET was measured using an excitation filter at 340/10 nm, and emission filters for terbium and fluorescein at 495/20 and 520/25 nm, respectively. The final concentrations of the reagents were as follows: ER α -417 (2 nM), streptavidin-terbium (0.5 nM), estradiol (1 μ M), coactivator binding inhibitor (0–1 mM), SRC-3-NRD (50 nM).

Luciferase Reporter Gene Assay

Human endometrial cancer (HEC-1) cells were maintained in culture and transfected in 24 well plates as previously described.⁴³ HBSS (50 μ L/well), Holo-transferrin (Sigma T1408) (20 μ L/well), and lipofectin (Invitrogen #18292–011) (5 μ L/well) were incubated together at room temperature for 5 minutes. A DNA mixture containing 200 ng of pCMV β -galactosidase as an internal control, 500 ng of the estrogen responsive reporter gene plasmid 2ERE Luc, and 100

ng of full-length ER alpha expression vector with 75 μ L HBSS per well was added to the first mixture and allowed to incubate for 20 minutes at room temperature. After changing the cell media to Opti-MEM (350 μ L/well), 150 μ L of the transfection mixture was added to each well. The cells were incubated at 37 °C in a 5% CO₂ containing incubator for 6 h before the medium was replaced with fresh medium containing 5% charcoal-dextran-treated calf serum and the desired concentrations of ligands. Luciferase reporter gene activity was assayed 24 h after ligand addition as described.⁴³

In the initial screen, compounds were assayed in a dose-response format at concentrations ranging from 20 μ M to 0.6 μ M; their inhibitory potential was determined by performing the assay in the presence of 10⁻⁹ M estradiol (E₂). Upon validation of antagonistic activity, mechanism of action was examined by repeating the compound titration in the presence of both 10⁻⁷ and 10⁻⁹ M E₂ with an expectation that changing the concentration of E₂ 100-fold would not change the IC₅₀ of true coactivator binding inhibitors.

Estrogen Receptor-Relative Binding Affinity Assay

Relative binding affinities were determined using a modification of a competitive radiometric binding assay as previously described, using 2 nM [³H]estradiol as tracer ([2,4,6,7-³H]estra-1,3,5[10]-triene-3,17 β -diol, 84–85 Ci/mmol, Amersham/GE Health Care, Piscataway, NJ); purified full-length human ER α and ER β were purchased from PanVera/Invitrogen (Carlsbad, CA). Incubations were conducted for 18–24 hr at 0 °C. Hydroxyapatite (BioRad, Hercules, CA) was used to absorb the receptor-ligand complexes, and free ligand was washed away. The binding affinities are expressed as relative binding affinity (RBA) values with the RBA of estradiol set to 100%. Estradiol binds to ER α with a K_d of 0.2 nM and to ER β with a K_d of 0.5 nM.^{44,45}

Molecular Modeling of the CBI/ER Interaction

All Modeling of the ER-LBD was performed using the Sybyl[®] 7.3 module from Tripos. The crystal structure of ER-LBD co-crystallized with diethylstilbestrol and an NR-box II (LXXLL motif) containing peptide from the steroid receptor coactivator 2 (SRC-2) was used as the basis for coactivator groove modeling (<http://www.rcsb.org> ID 3erd). The crystal structure was prepared for docking experiments by addition of the missing internal amino acids of the LBD using information contained in RCSB website and the loop search (PRODAT database) feature of Sybyl[®]. Hydrogens, missing sidechains, and charged end groups were added to the protein and peptide, and the ER/SRC-2 structure was minimized using MMFF94 calculated charges and an MMFF94s force field in three steps (inserted loops, water molecules, entire protein) with appropriate aggregates applied for each. CBI structures were minimized using the Tripos forcefield to termination gradient of 0.05 kcal/(mol*Å). Initial placement of the CBI was performed using least squares multiple atom fitting of the alkyl groups on the CBI with the ER-interacting leucine residues of the SRC-2 peptide. Subsequent CBI orientations used for docking were manipulated into the coactivator groove by hand. Before docking, the SRC-2 peptide and all water molecules were removed from the ER-LBD structure. Docking experiments were performed using the Sybyl[®] FlexiDock module, with all bonds in the CBI and all sidechains within 10 Å of the coactivator groove designated as rotatable. H-bond donor and acceptor sites were designated for the appropriate atoms in the CBI as well as for Glu542 and Lys362. Docking runs were begun from a random seed and allowed to proceed for 100,000 iterations. In most instances, duplicate runs were performed to ensure validity of the docking results. The lowest energy conformation of CBI/receptor thus produced was then further minimized with the MMFF94s force field to a termination gradient of 0.10 kcal/(mol*Å), following a four step procedure to produce the final structures [(1) 10 Å surrounding CBI with CBI and backbone static, (2) 10 Å surrounding CBI with backbone static, (3) 10 Å surrounding CBI with CBI static, and (4) 10 Å surrounding CBI].

Supplementary Material

Refer to Web version on PubMed Central for supplementary material.

Acknowledgements

We greatly acknowledge support of this research from the National Institutes of Health (PHS 5R37DK15556). JRG was supported by a David Robertson Fellowship and an NIH Fellowship NRSA 1 F30 ES016484-01 and Training Grant NRSA 5 T32 GM070421. AAP received support from an Illinois Distinguished Fellowship and a Robert D. Doolen Fellowship. We are grateful for the helpful suggestions of Dr. Sung Hoon Kim.

Abbreviations

ER	estrogen receptor
LBD	ligand binding domain
SRC	steroid receptor coactivator
CBI	coactivator binding inhibitor
TR-FRET	time-resolved fluorescence resonance energy transfer
RBA	relative binding affinity

References

1. Heldring N, Pike A, Andersson S, Matthews J, Cheng G, Hartman J, Tujague M, Stroem A, Treuter E, Warner M, Gustafsson JA. Estrogen receptors: how do they signal and what are their targets. *Physiol Rev* 2007;87:905–931. [PubMed: 17615392]
2. Gustafsson JA. What pharmacologists can learn from recent advances in estrogen signalling. *Trends Pharmacol Sci* 2003;24:479–485. [PubMed: 12967773]
3. Hess RA. Estrogen in the adult male reproductive tract: a review. *Rep Biol Endocrinol* 2003;1(52):1–14.
4. Hewitt SC, Korach KS. Estrogen receptor knockout mice: Roles for estrogen receptors a and b in reproductive tissues. *Reproduction (Cambridge, United Kingdom)* 2003;125:143–149.
5. Lakoski SG, Herrington DM. Effects of oestrogen receptor-active compounds on lipid metabolism. *Diabetes, Obesity and Metabolism* 2005;7:471–477.
6. Schneider JG, Tompkins C, Blumenthal Roger S, Mora S. The metabolic syndrome in women. *Cardiol Rev* 2006;14:286–291. [PubMed: 17053375]
7. Tikkanen MJ. Estrogens, progestins and lipid metabolism. *Maturitas* 1996;23:S51–S55. [PubMed: 8865140]
8. Syed F, Khosla S. Mechanisms of sex steroid effects on bone. *Biochem Biophys Res Commun* 2005;328:688–696. [PubMed: 15694402]
9. Jaervinen TLN, Kannus P, Sievaenen H. Estrogen and bone—a reproductive and locomotive perspective. *J Bone Miner Res* 2003;18:1921–1931. [PubMed: 14606503]
10. Carruba G. Estrogens and mechanisms of prostate cancer progression. *Ann N Y Acad Sci* 2006;1089:201–217. [PubMed: 17261768]

11. Vergote I, Neven P, van Dam P, Serreyn R, De Prins F, De Sutter P, Albertyn G. The estrogen receptor and its selective modulators in gynecological and breast cancer. *Eur J Cancer* 2000;36:S1–S9. [PubMed: 11056296]
12. Hanstein B, Djahansouzi S, Dall P, Beckmann MW, Bender HG. Insights into the molecular biology of the estrogen receptor define novel therapeutic targets for breast cancer. *Eur J Endocrinol* 2004;150:243–255. [PubMed: 15012607]
13. Nicholson RI, Johnston SR. Endocrine therapy - current benefits and limitations. *Breast Cancer Res Treat* 2005;93:S3–S10. [PubMed: 16247594]
14. Katzenellenbogen BS, Katzenellenbogen JA. Estrogen receptor transcription and transactivation. Estrogen receptor alpha and estrogen receptor beta. Regulation by selective estrogen receptor modulators and importance in breast cancer. *Breast Cancer Res* 2000;2:335–344. [PubMed: 11250726]
15. McKenna NJ, O'Malley BW. Minireview: nuclear receptor coactivators-an update. *Endocrinology* 2002;143:2461–2465. [PubMed: 12072374]
16. Hall Julie M, McDonnell Donald P. Coregulators in nuclear estrogen receptor action: from concept to therapeutic targeting. *Mol Interv* 2005;5:343–357. [PubMed: 16394250]
17. Brzozowski AM, Pike ACW, Dauter Z, Hubbard RE, Bonn T, Engstrom O, Ohman L, Greene GL, Gustafsson JA, Carlquist M. Molecular basis of agonism and antagonism in the estrogen receptor. *Nature (London)* 1997;389:753–758. [PubMed: 9338790]
18. Swain SM. Tamoxifen: the long and short of it. *J Natl Cancer Inst* 1996;88:1510–1512. [PubMed: 8901846]
19. Fisher B, Dignam J, Bryant J, DeCillis A, Wickerham DL, Wolmark N, Costantino J, Redmond C, Fisher ER, Bowman DM, Deschenes L, Dimitrov NV, Margolese RG, Robidoux A, Shibata H, Terz J, Paterson AHG, Feldman MI, Farrar W, Evans J, Lickley HL. Five versus more than five years of tamoxifen therapy for breast cancer patients with negative lymph nodes and estrogen receptor-positive tumors. *J Nat Cancer Inst* 1996;88:1529–1542. [PubMed: 8901851]
20. Normanno N, Di Maio M, De Maio E, De Luca A, de Matteis A, Giordano A, Perrone F. Mechanisms of endocrine resistance and novel therapeutic strategies in breast cancer. *Endocr Rel Cancer* 2005;12:721–747.
21. Schiff R, Osborne CK. New insight into estrogen receptor-a function and its implication for endocrine therapy resistance in breast cancer. *Breast Cancer Res* 2005;7:205–211. [PubMed: 16168139]
22. Rodriguez AL, Tamrazi A, Collins ML, Katzenellenbogen JA. Design, Synthesis, and in Vitro Biological Evaluation of Small Molecule Inhibitors of Estrogen Receptor a Coactivator Binding. *J Med Chem* 2004;47:600–611. [PubMed: 14736241]
23. Shao D, Berrodin TJ, Manas E, Hauze D, Powers R, Bapat A, Gonder D, Winneker RC, Frail DE. Identification of novel estrogen receptor a antagonists. *J Steroid Biochem Mol Biol* 2004;88:351–360. [PubMed: 15145444]
24. Zhou HB, Collins ML, Gunther JR, Comminos JS, Katzenellenbogen JA. Bicyclo[2.2.2]octanes: Close structural mimics of the nuclear receptor-binding motif of steroid receptor coactivators. *Bioorg Med Chem Lett* 2007;17:4118–4122. [PubMed: 17560105]
25. Becerril J, Hamilton AD. Helix mimetics as inhibitors of the interaction of the estrogen receptor with coactivator peptides. *Ange Chem, Int Ed Engl* 2007;46:4471–4473.
26. Gunther JR, Moore TW, Collins ML, Katzenellenbogen JA. Amphipathic Benzenes Are Designed Inhibitors of the Estrogen Receptor a/Steroid Receptor Coactivator Interaction. *ACS Chem Biol* 2008;3:282–286. [PubMed: 18484708]
27. Shiau AK, Barstad D, Loria PM, Cheng L, Kushner PJ, Agard DA, Greene GL. The structural basis of estrogen receptor/coactivator recognition and the antagonism of this interaction by tamoxifen. *Cell (Cambridge, Massachusetts)* 1998;95:927–937.
28. Scheiper B, Bonnekessel M, Krause H, Fuerstner A. Selective Iron-Catalyzed Cross-Coupling Reactions of Grignard Reagents with Enol Triflates, Acid Chlorides, and Dichloroarenes. *J Org Chem* 2004;69:3943–3949. [PubMed: 15153029]
29. Tan J, Chang J, Deng M. The facile route to stereo-defined alkenyl-substituted pyrimidines. *Synth Commun* 2004;34:3773–3783.

30. Zanda M, Talaga P, Wagner A, Mioskowski C. Efficient and regioselective 4-aminodechlorination of 2,4,6-trichloropyrimidine with N-sodium carbamates. *Tetrahedron Lett* 2000;41:1757–1761.
31. Schroeter S, Stock C, Bach T. Regioselective cross-coupling reactions of multiple halogenated nitrogen-, oxygen-, and sulfur-containing heterocycles. *Tetrahedron* 2005;61:2245–2267.
32. Harnden MR, Hurst DT. The chemistry of pyrimidinethiols. III. The synthesis of some substituted pyrimidinethiols and some thiazolo[5,4-d]pyrimidines. *Aust J Chem* 1990;43:55–62.
33. Hurst DT. The synthesis and chemistry of 2-methylpyrimidine-4,6-dithiol and some related compounds. *Aust J Chem* 1983;36:1477–82.
34. Fuerstner A, Leitner A, Mendez M, Krause H. Iron-Catalyzed Cross-Coupling Reactions. *J Am Chem Soc* 2002;124:13856–13863. [PubMed: 12431116]
35. Furstner A, Leitner A. Iron-catalyzed cross-coupling reactions of alkyl-Grignard reagents with aryl chlorides, tosylates, and triflates. *Angew Chem, Int Ed Engl* 2002;41:609–612.
36. Galande AK, Bramlett KS, Trent JO, Burris TP, Wittliff JL, Spatola AF. Potent inhibitors of LXXLL-based protein-protein interactions. *ChemBioChem* 2005;6:1991–1998. [PubMed: 16222726]
37. Geistlinger TR, McReynolds AC, Guy RK. Ligand-Selective Inhibition of the Interaction of Steroid Receptor Coactivators and Estrogen Receptor Isoforms. *Chem Biol* 2004;11:273–281. [PubMed: 15123288]
38. Geistlinger TR, Guy RK. Novel Selective Inhibitors of the Interaction of Individual Nuclear Hormone Receptors with a Mutually Shared Steroid Receptor Coactivator 2. *J Am Chem Soc* 2003;125:6852–6853. [PubMed: 12783522]
39. Ellem SJ, Risbridger GP. Treating prostate cancer: a rationale for targeting local oestrogens. *Nature Rev Cancer* 2007;7:621–627. [PubMed: 17611544]
40. Murphy LC, Watson PH. Is oestrogen receptor-b a predictor of endocrine therapy responsiveness in human breast cancer? . *Endocr Relat Cancer* 2006;13:327–334. [PubMed: 16728566]
41. Saji S, Hirose M, Toi M. Clinical significance of estrogen receptor b in breast cancer. *Cancer Chemother Pharmacol* 2005;56:s21–s26.
42. Tamrazi A, Carlson KE, Daniels JR, Hurth KM, Katzenellenbogen JA. Estrogen Receptor Dimerization: Ligand Binding Regulates Dimer Affinity and DimerDissociation Rate. *Mol Endocrinol* 2002;16:2706–2719. [PubMed: 12456792]
43. Sun J, Meyers MJ, Fink BE, Rajendran R, Katzenellenbogen JA, Katzenellenbogen BS. Novel ligands that function as selective estrogens or antiestrogens for estrogen receptor-alpha or estrogen receptor-beta. *Endocrinology* 1999;140:800–804. [PubMed: 9927308]
44. Carlson KE, Choi I, Gee A, Katzenellenbogen BS, Katzenellenbogen JA. Altered ligand binding properties and enhanced stability of a constitutively active estrogen receptor: Evidence that an open pocket conformation is required for ligand interaction. *Biochemistry* 1997;36:14897–14905. [PubMed: 9398213]
45. Katzenellenbogen JA, Johnson HJ Jr, Myers HN. Photoaffinity labels for estrogen binding proteins of rat uterus. *Biochemistry* 1973;12:4085–4092. [PubMed: 4745660]

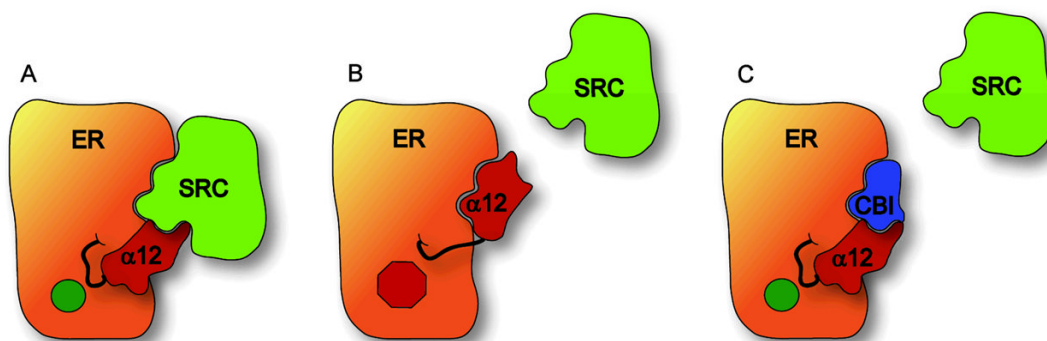


Figure 1. Cartoon representation of classical vs. CBI antagonism of ER. **A.** Conformation of agonist-bound ER with helix 12 forming part of the steroid receptor coactivator (SRC) binding site; **B.** Conformation of antagonist-bound ER in which helix 12 occupies the SRC binding site, disrupting the ER/SRC interaction indirectly; **C.** Conformation of agonist-bound ER in which a CBI occupies the SRC binding site, disrupting ER/SRC interaction directly.

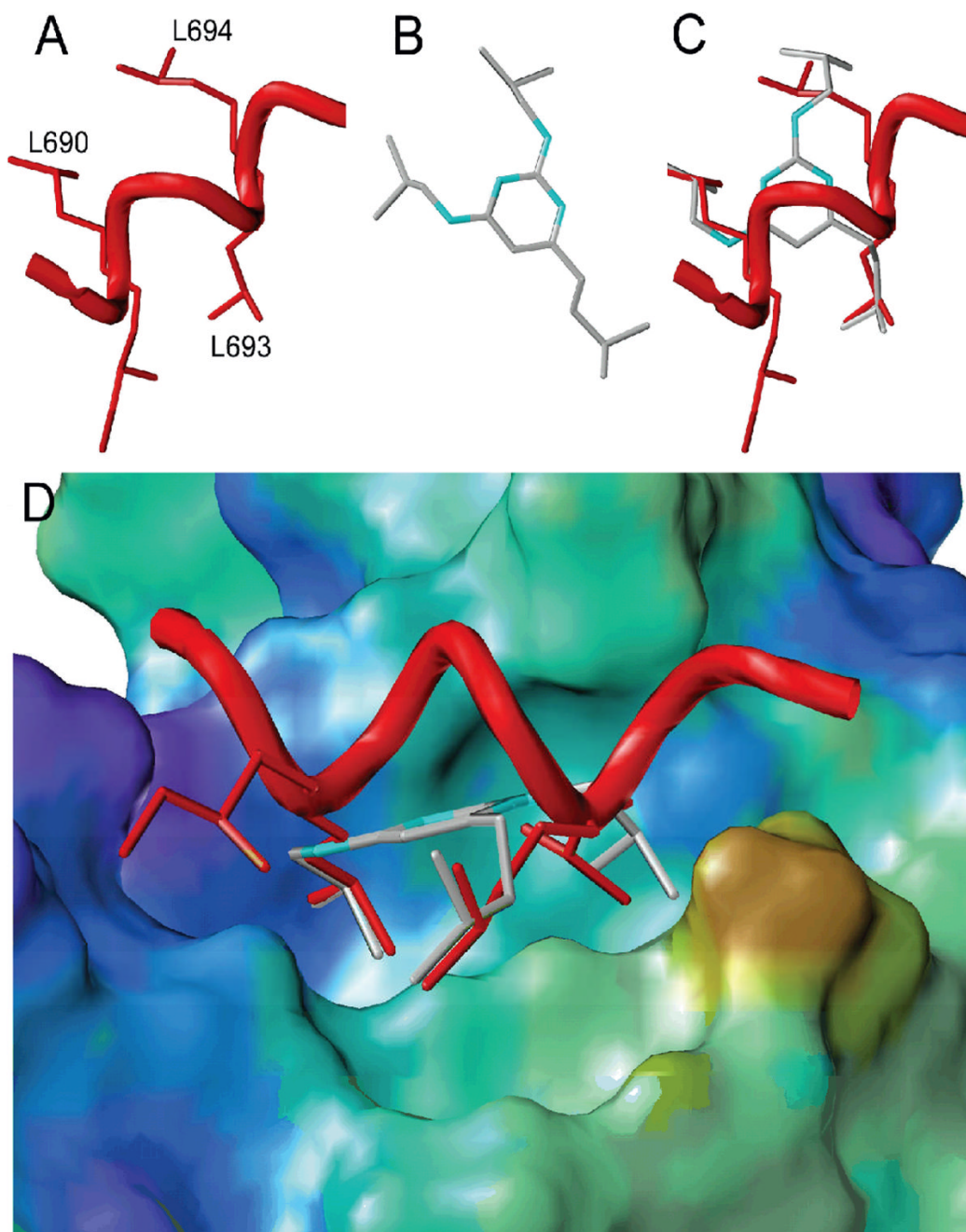


Figure 2. Structure-based design of pyrimidine core molecules based on the ER/SRC-2 interaction (3erd). **A**, Rendering of SRC-2 peptide from 3erd crystal structure (the internal H691 and R692 residues are deleted for clarity); **B**, Minimized structure of CBI 2,4-diiisobutylamino-6-isopentylpyrimidine; **C**, Overlay of the SRC-2 peptide and CBI; **D**, Side-view of SRC-2 peptide and CBI overlay in coactivator groove.

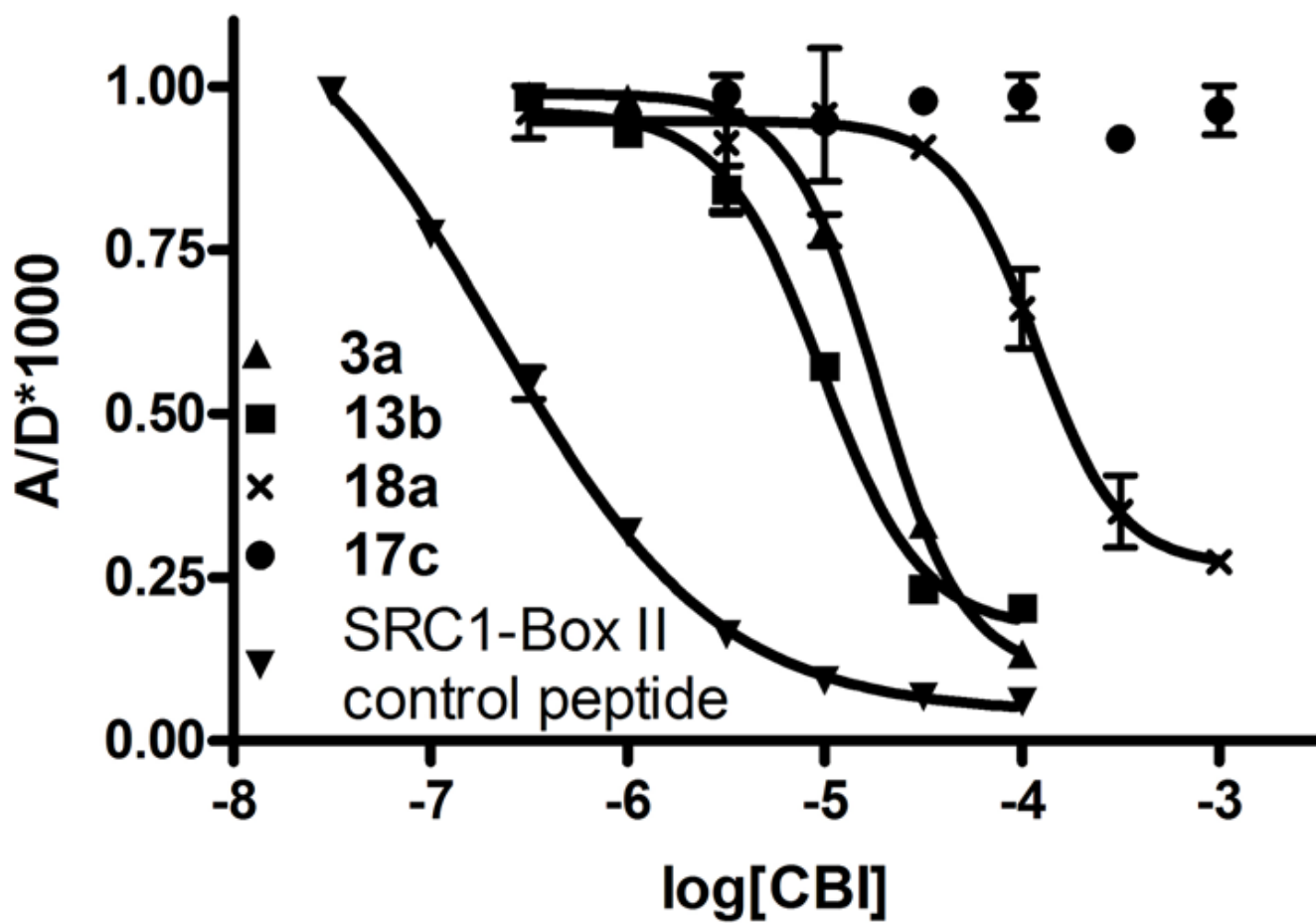


Figure 3. In vitro coactivator binding inhibition assay. TR-FRET assay shows displacement of SRC-3-NRD-FI by control peptide and pyrimidine CBIs.

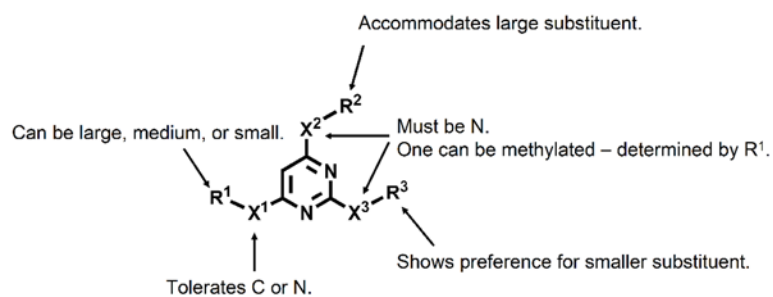


Figure 4.
Summary of the structure-activity relationships of the pyrimidine-core CBIs.

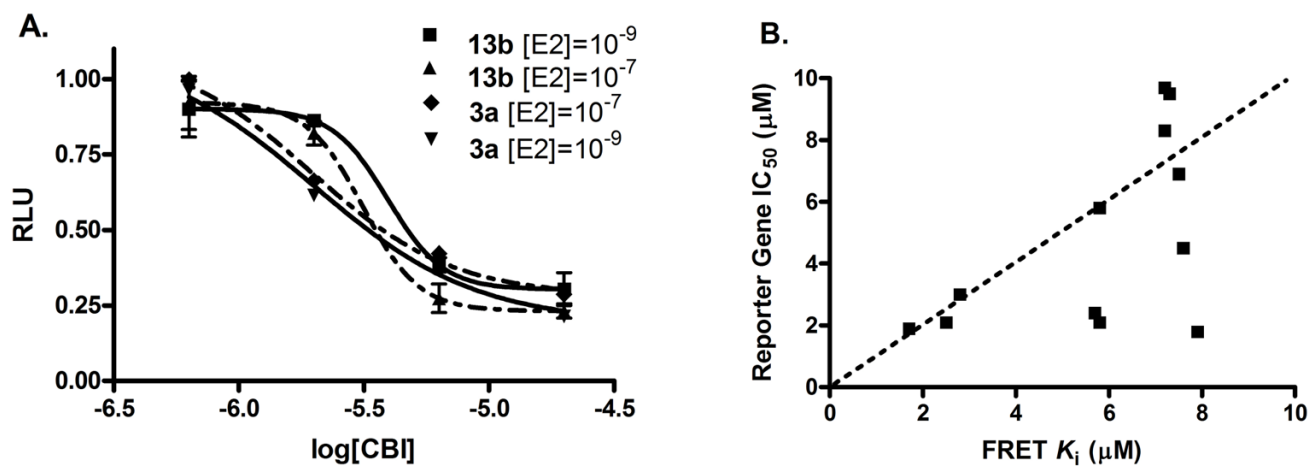


Figure 5. Coactivator binding inhibition assays. **A**, Dose-response of CBI inhibition of ER-mediated transcription in cell-based reporter gene assay run at two concentrations of estradiol; **B**, Plot of CBI K_i (μM) as calculated from *in vitro* TR-FRET assay vs. CBI IC₅₀ as determined by cell-based reporter gene assay.

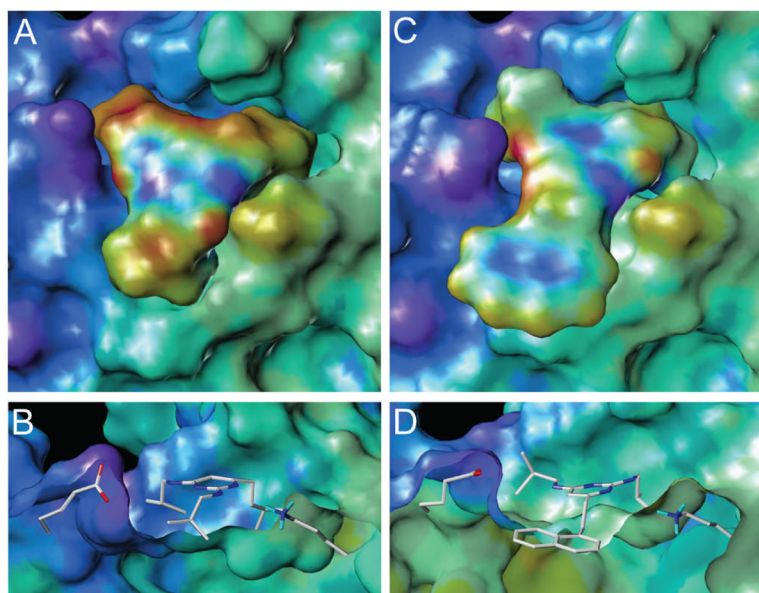
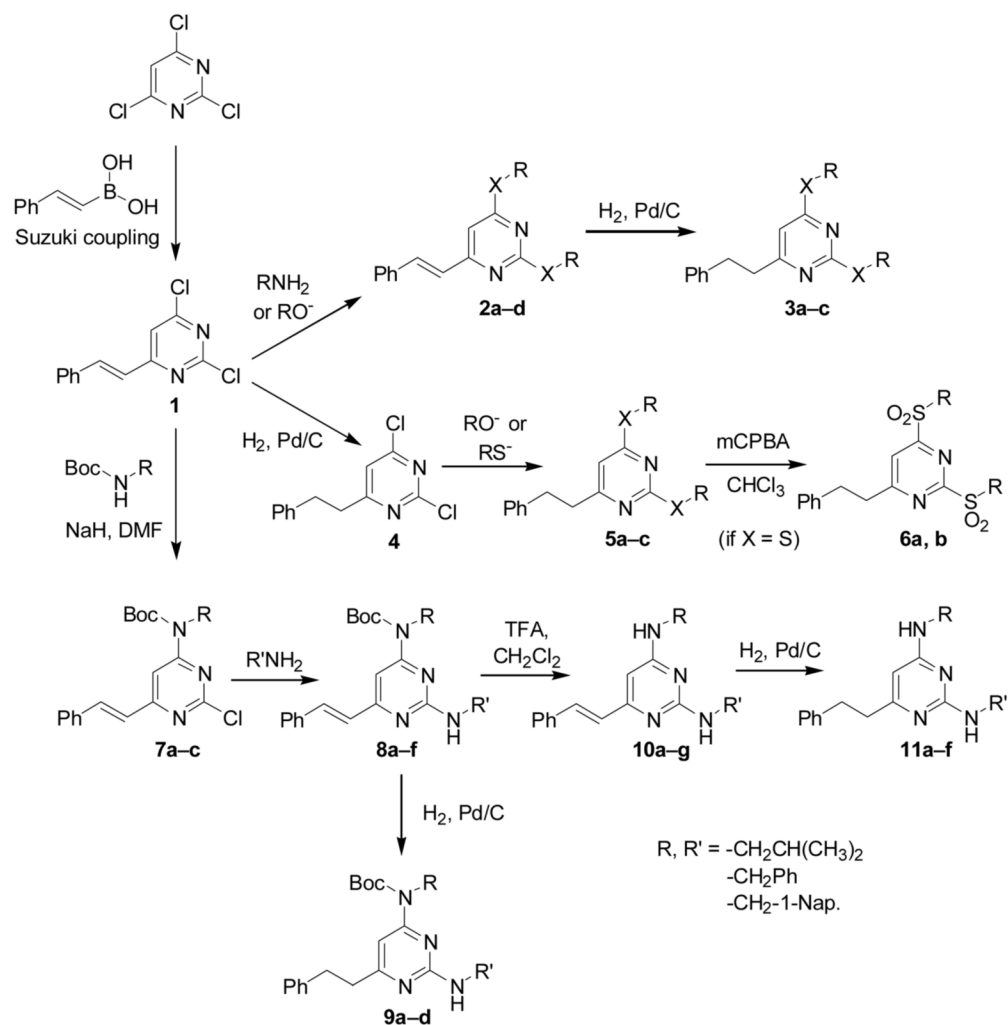
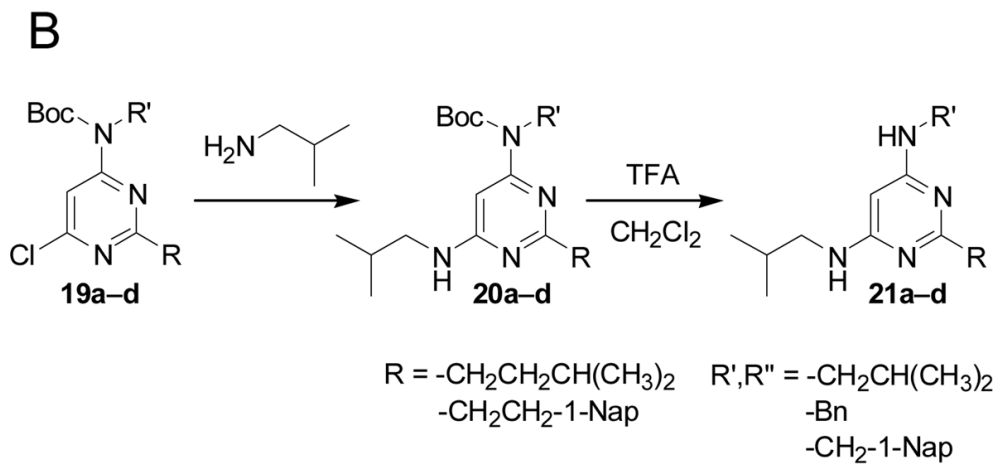
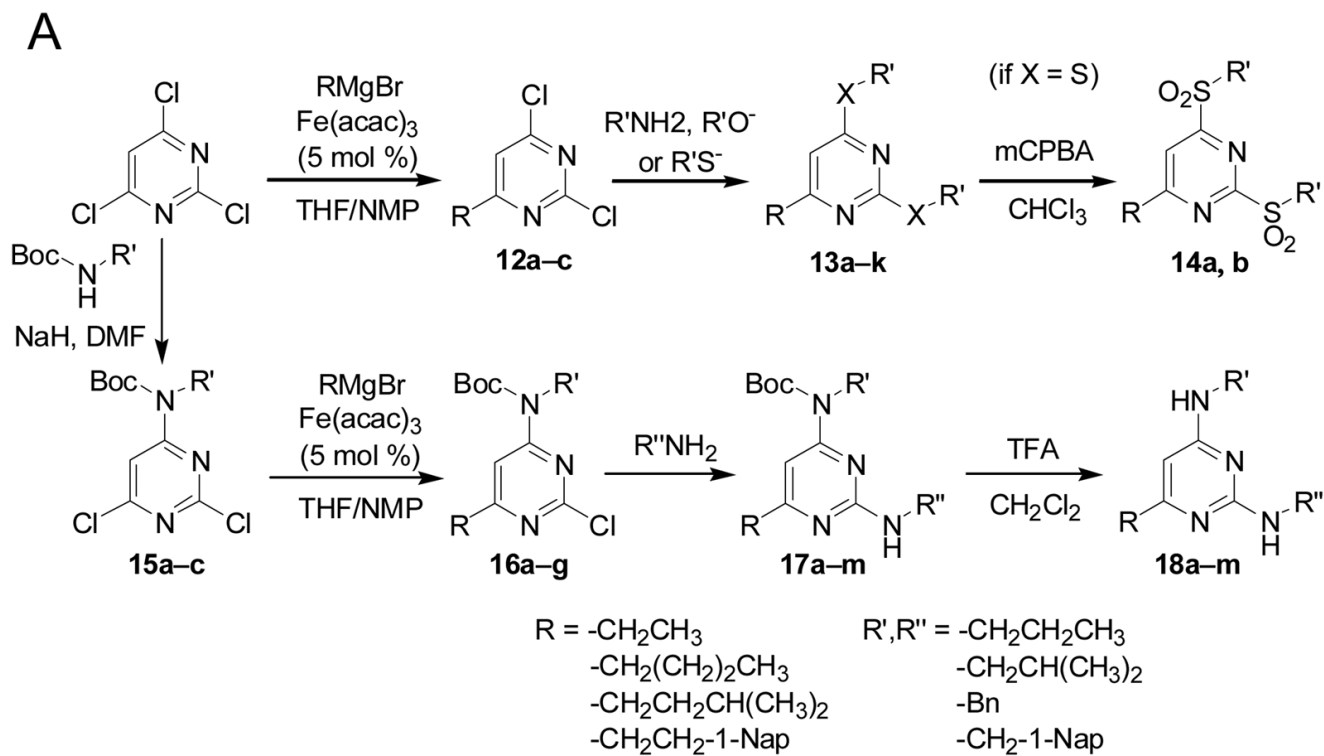


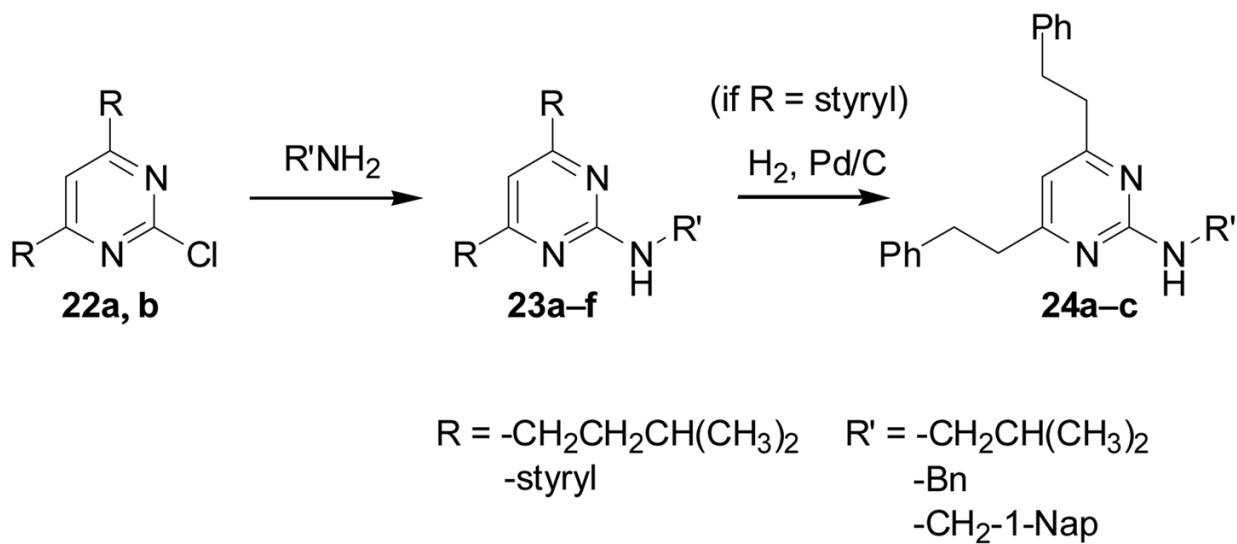
Figure 6. Docking of pyrimidine-core CBIs into the coactivator groove of ER α -LBD. **A**, electrostatic rendering of **13b** bound to ER α -LBD; **B**, cut-away showing the interaction of Glu542 and Lys362 with **13b**; **C**, electrostatic rendering of **13i** bound to ER α -LBD; **D**, cut-away showing the interaction of Glu542 and Lys362 with **13i**.



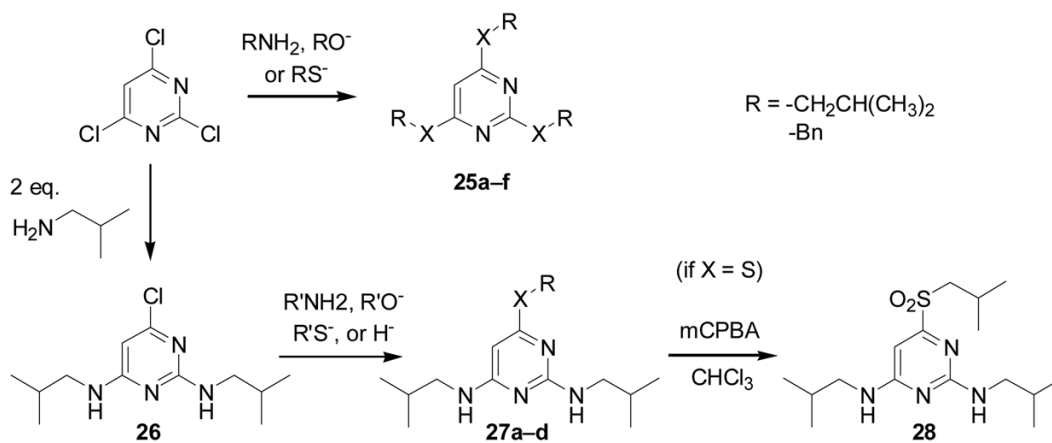
Scheme 1.
 Synthesis of 'symmetric' and unsymmetric 2,4-diamino-6-phenethylpyrimidines

**Scheme 2.**

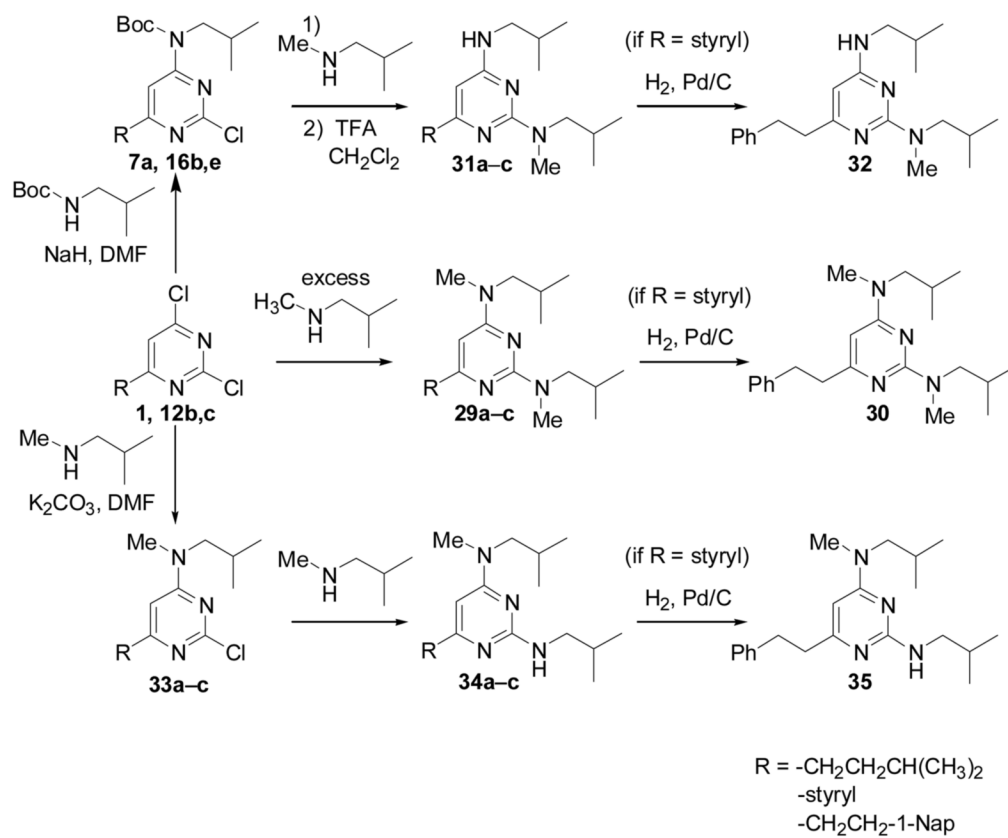
Synthesis of alkyipyrimidines: **A**, synthesis of 6-isoamyl and 6-naphthethyl pyrimidines; **B**, synthesis of 2-isoamyl and 2-naphthethyl pyrimidines.



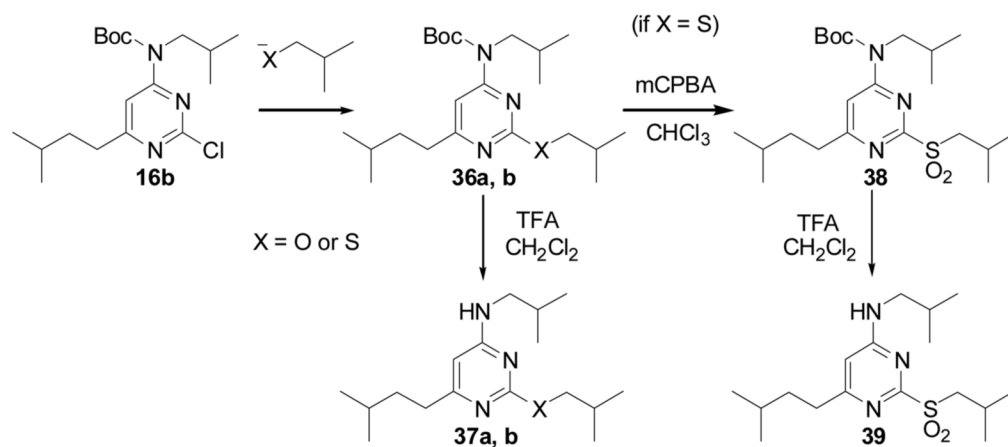
Scheme 3.
 Synthesis of 4,6-dialkyl-2-aminopyrimidines



Scheme 4.
 Synthesis of tri-heteroatom-substituted pyrimidines



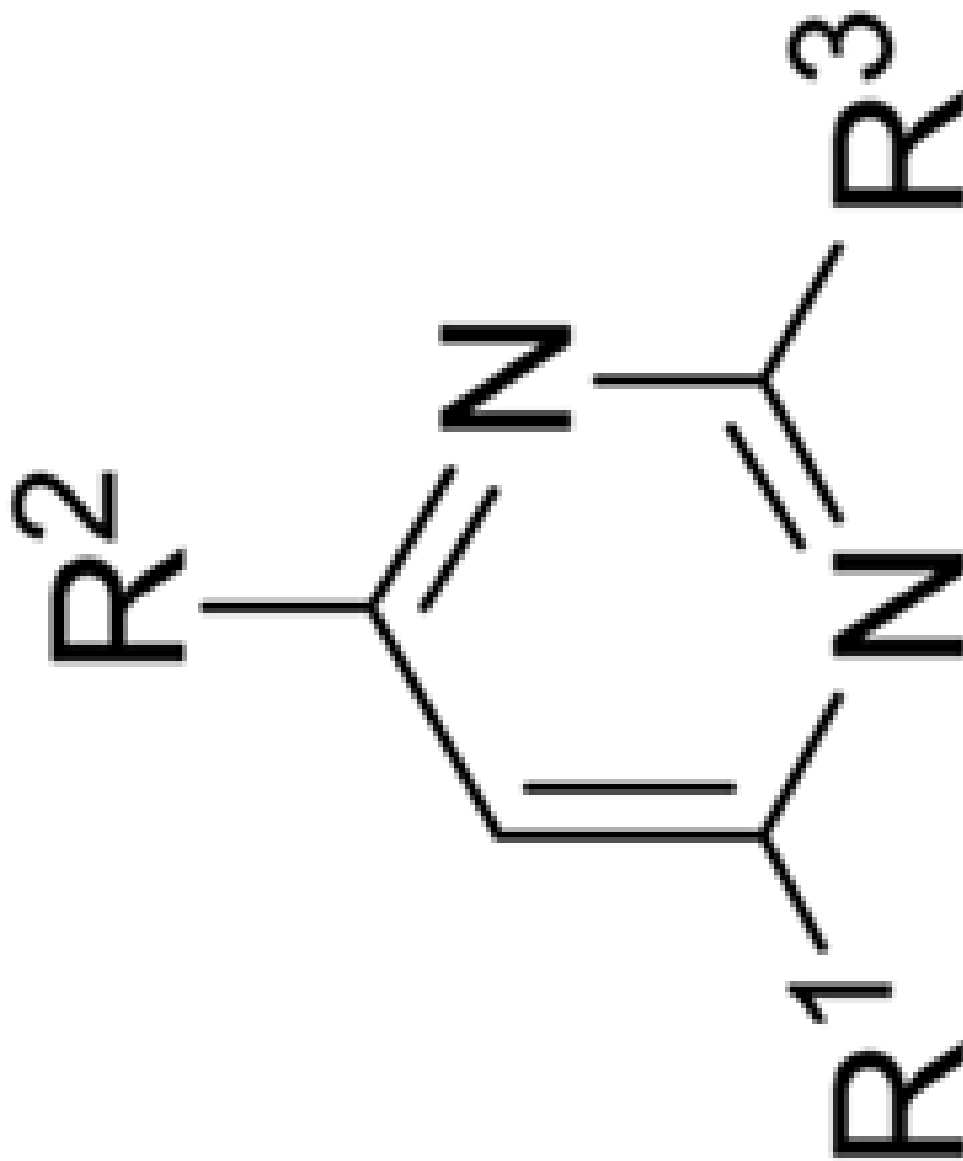
Scheme 5.
 Synthesis of *N*-methylated pyrimidines



Scheme 6.
Synthesis 2-alkoxy, 2-sulfanyl, and 2-sulfonylpyrimidines.

Table 1

Inhibitory activity of 6-alkyl-2,6-diaminopyrimidines on the ER α and ER β /coactivator interaction as measured in TR-FRET and luciferase reporter gene assays.



TR-FRET(μ M) Reporter Gene IC₅₀(μ M)

ER α

ER β

R³

R²

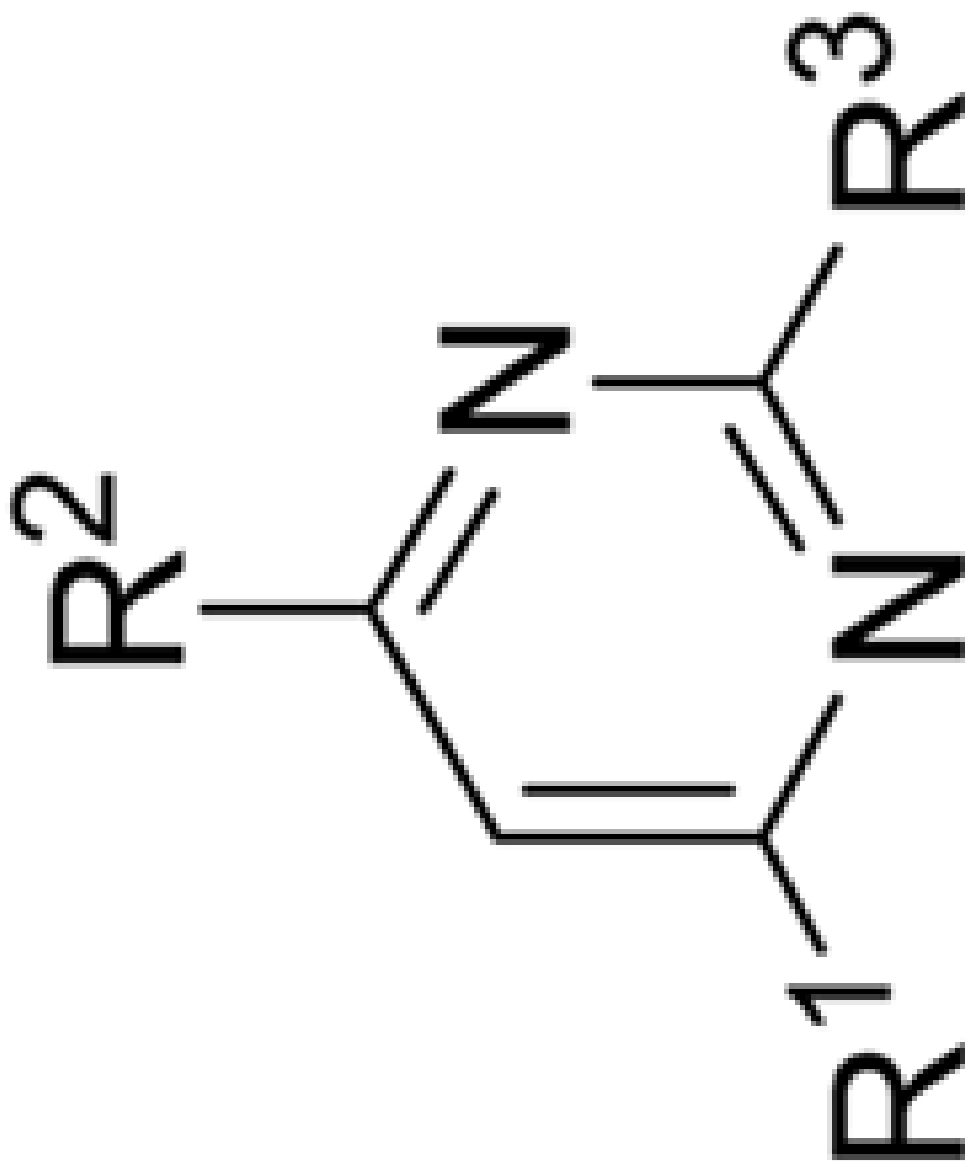
R¹

Cmpd #

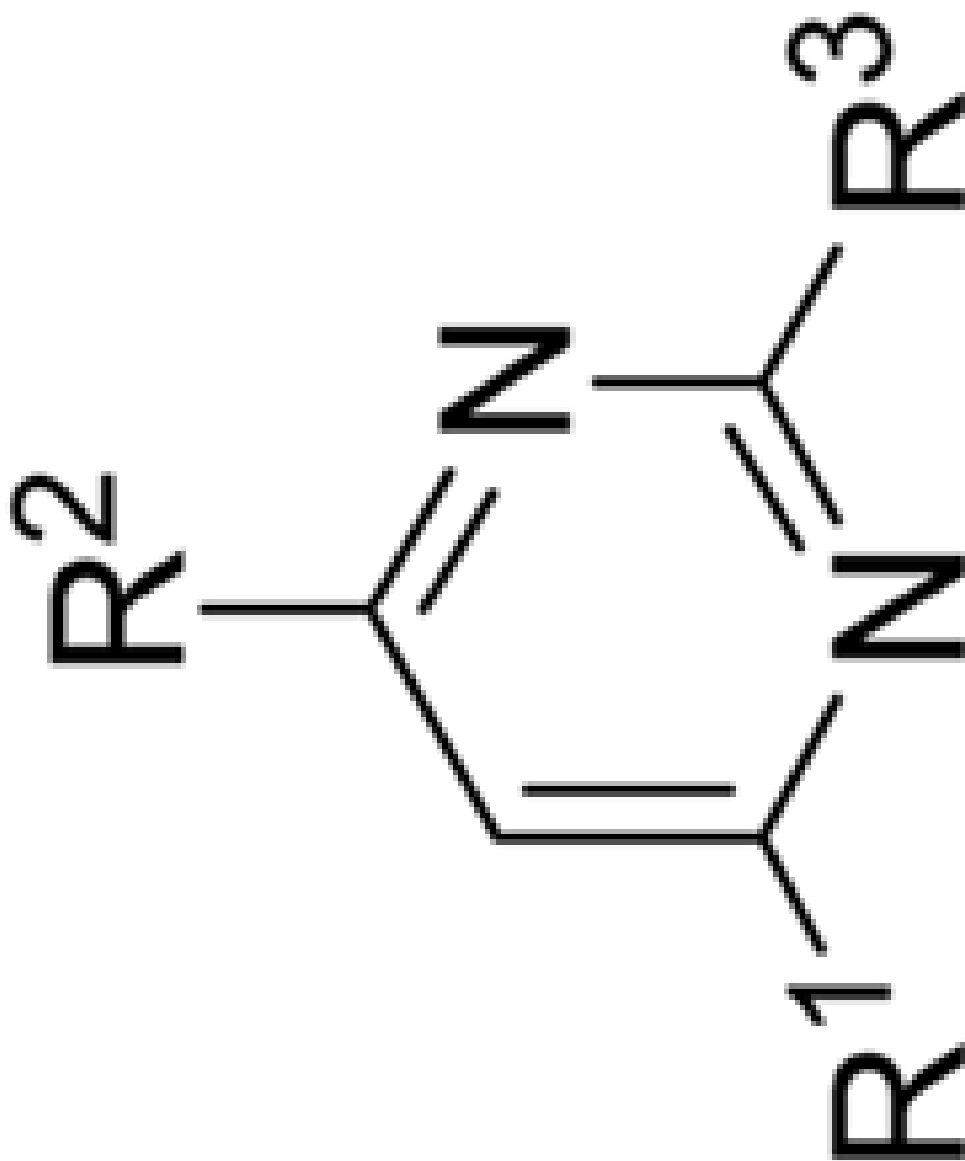
0.065 0.066

SRC-1 BoxII

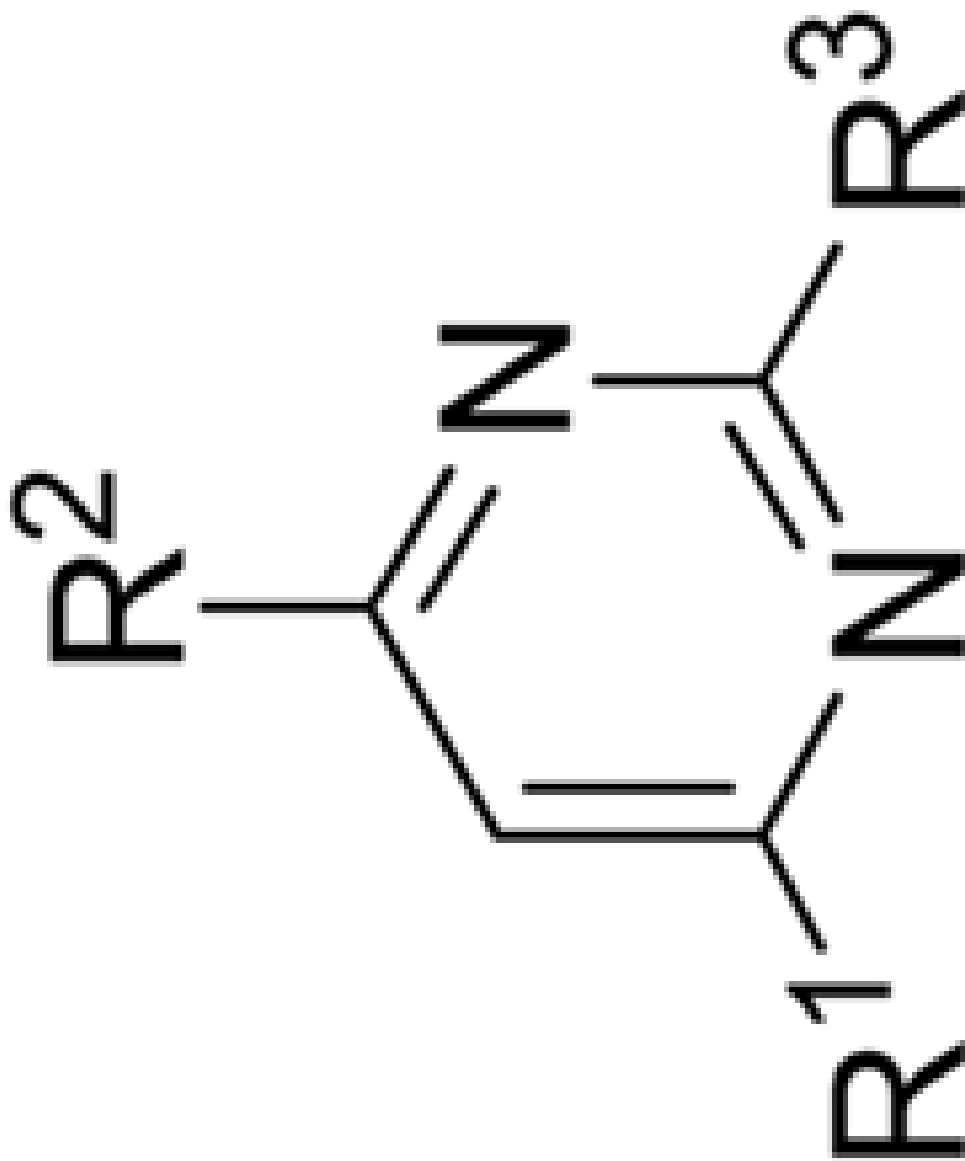
control



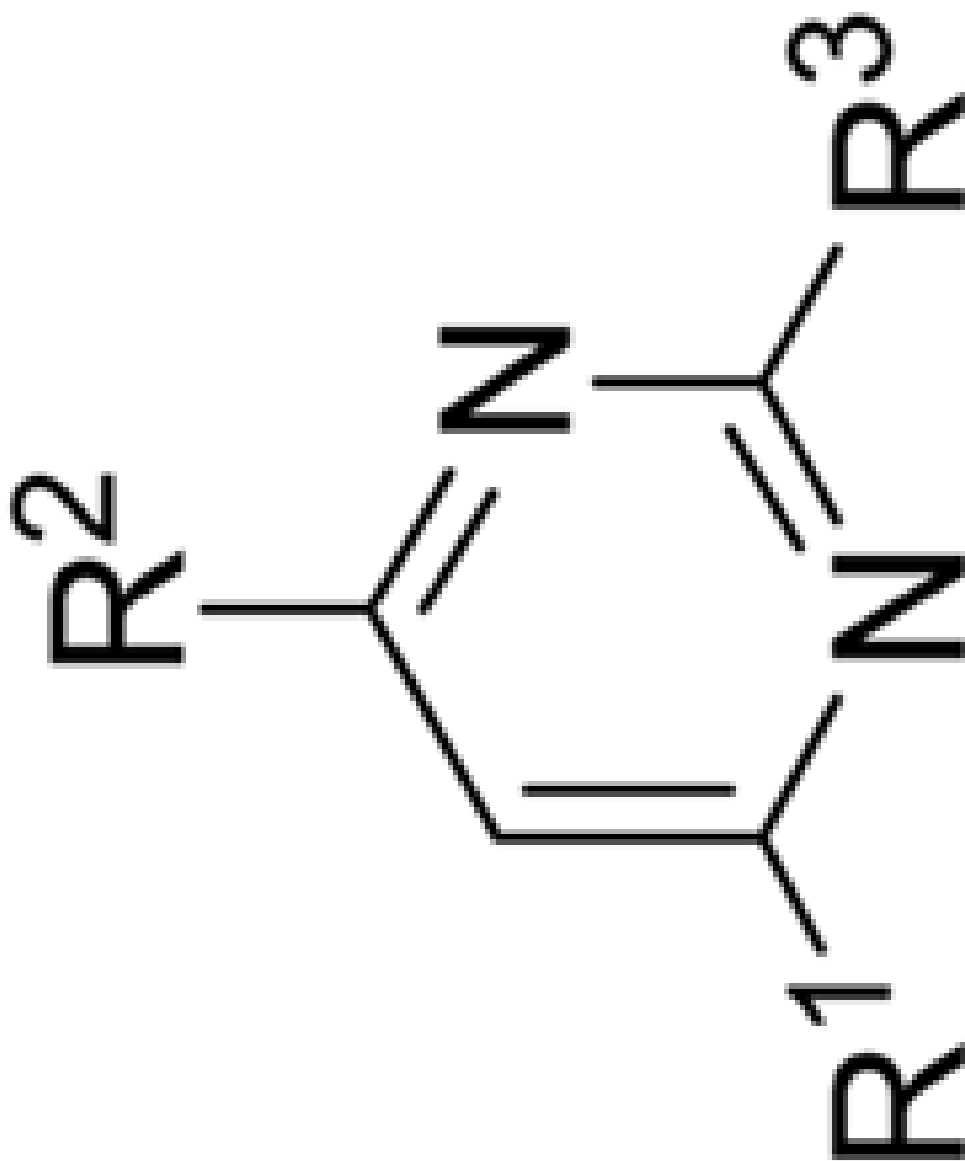
Cmpd #	R ¹	R ²	R ³	TR-FRET _(μM)			Reporter Gene IC ₅₀ (μM)
				ERα	ERβ	ERα	
2a	-styryl	-NHCH ₂ CH(CH ₃) ₂	-NHCH ₂ CH(CH ₃) ₂	7.5	242	6.9	
2b	-styryl	-NHCH ₂ Ph	-NHCH ₂ Ph	>1000	>1000	>1000	
3a	-CH ₂ CH ₂ Ph	-NHCH ₂ CH(CH ₃) ₂	-NHCH ₂ CH(CH ₃) ₂	5.8	>1000	2.1	



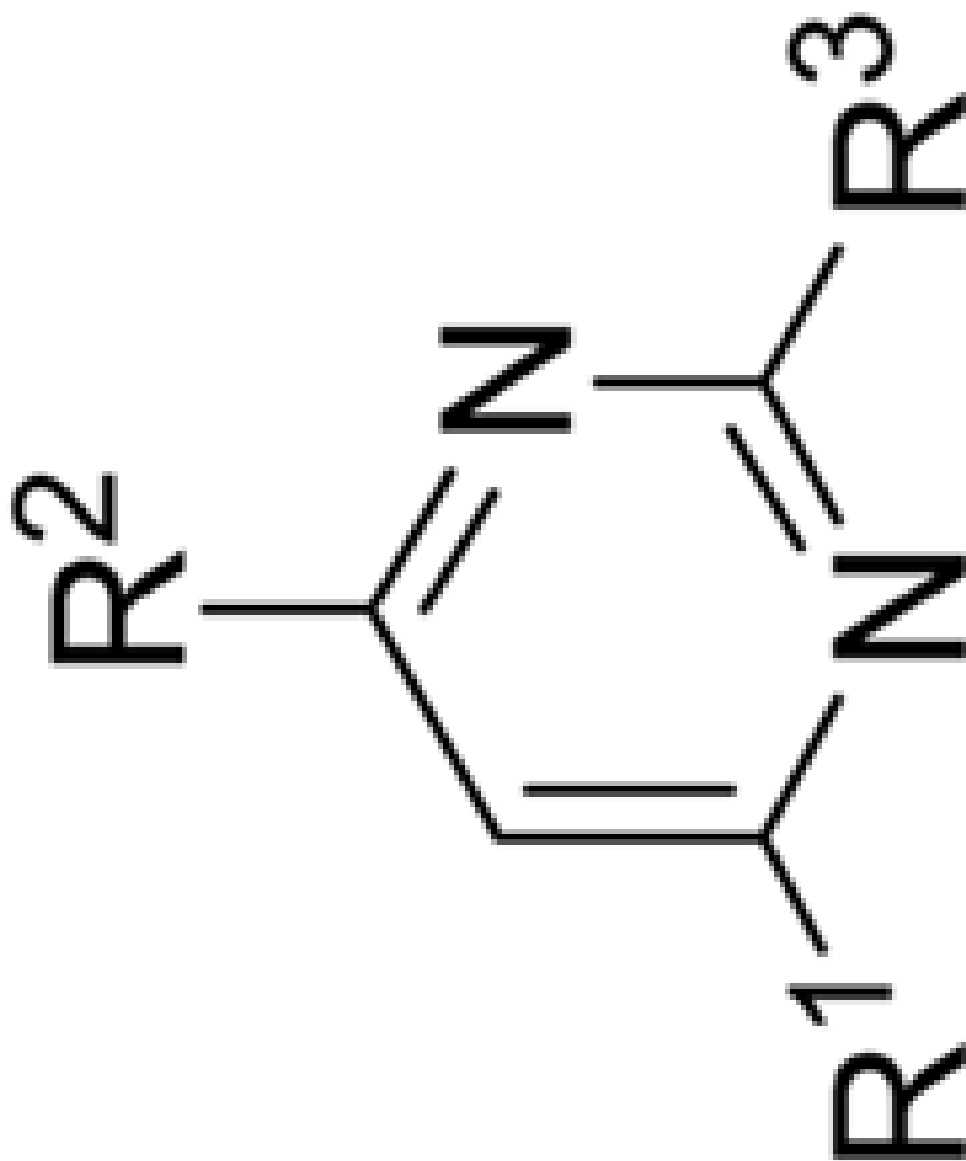
Cmpd #	R ¹	R ²	R ³	TR-FRET ¹ (μ M)			Reporter Gene IC ₅₀ (μ M)
				ER α	ER β	ER α	
3b	-CH ₂ CH ₂ Ph	-NHCH ₂ Ph	-NHCH ₂ Ph	>1000	>1000	>1000	>1000
8b	-styryl	-N(Boc)CH ₂ Ph	-NHCH ₂ CH(CH ₃) ₂	>1000	132	>1000	>1000
9a	-CH ₂ CH ₂ Ph	-N(Boc)CH ₂ CH(CH ₃) ₂	-NHCH ₂ Ph	>1000	>1000	>1000	>1000



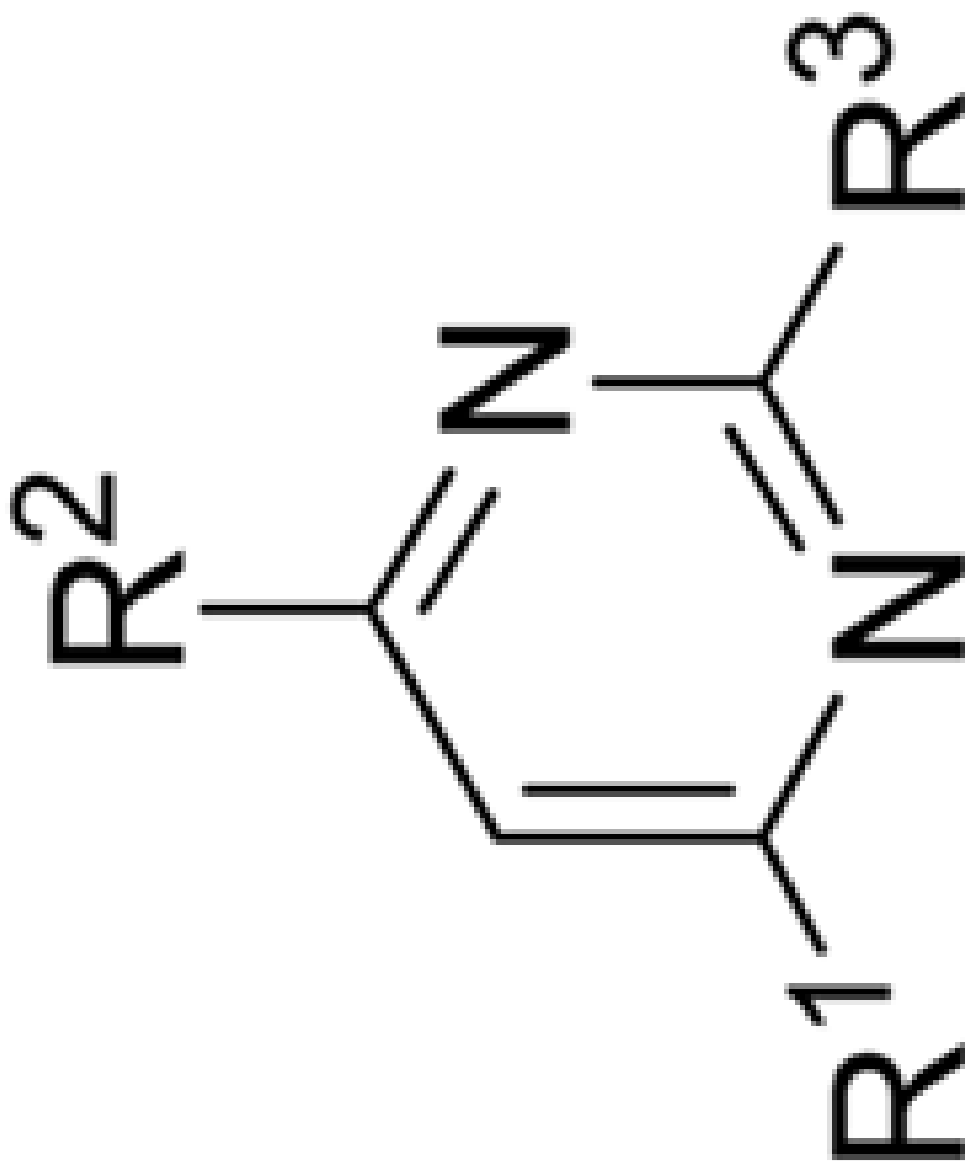
Cmpd #	R ¹	R ²	R ³	TR-FRET _(μM)			Reporter Gene IC ₅₀ (μM)
				ERα	ERβ	ERα	
9b	-CH ₂ CH ₂ Ph	-N(Boc)CH ₂ Ph	-NHCH ₂ CH(CH ₃) ₂	>1000	>1000	>1000	
10a	-styryl	-NHCH ₂ CH(CH ₃) ₂	-NHCH ₂ Ph	>1000	>1000	>1000	12
10b	-styryl	-NHCH ₂ CH(CH ₃) ₂	-NHCH ₂ -1-Nap	>1000	>1000	>1000	>1000



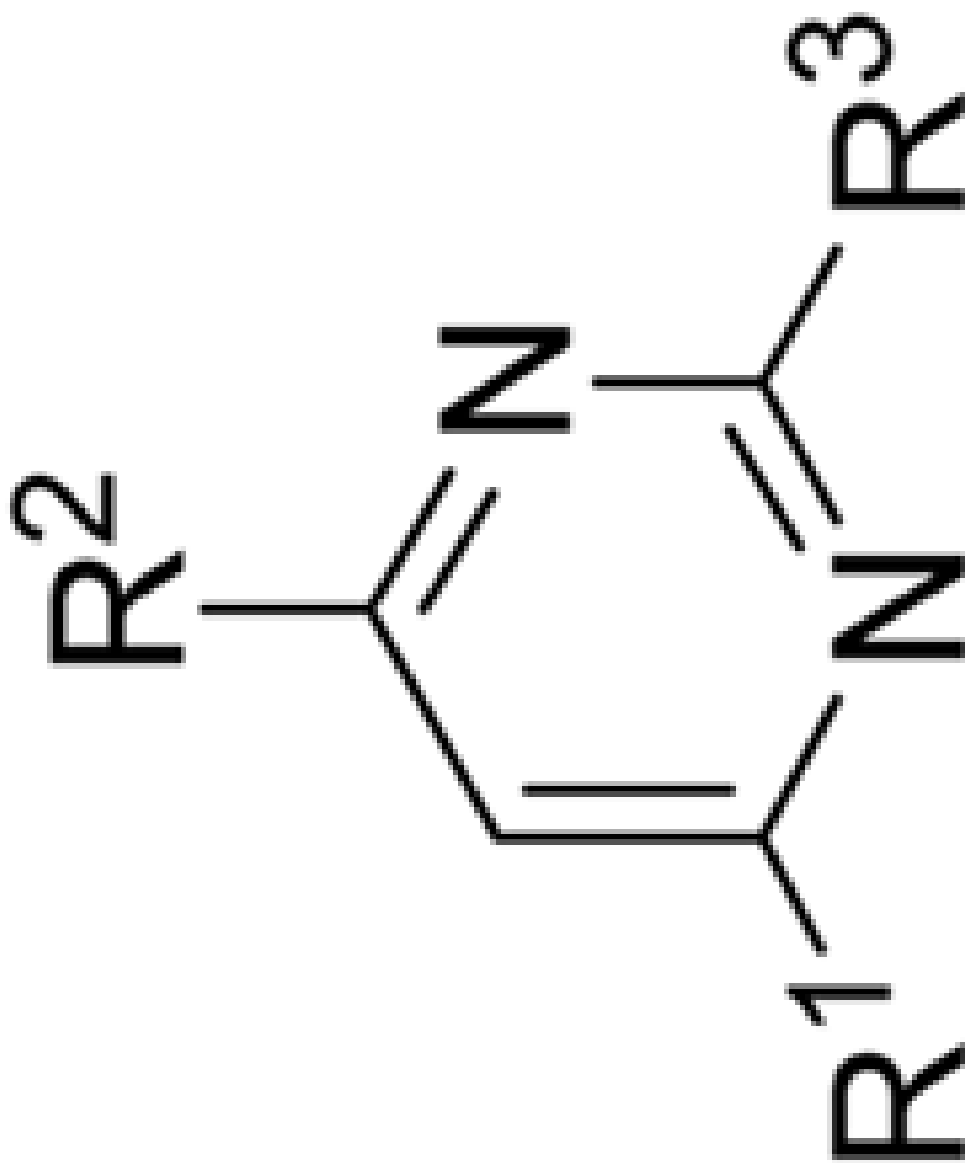
Cmpd #	R ¹	R ²	R ³	TR-FRET ¹ (μ M)			Reporter Gene IC ₅₀ (μ M)
				ER α	ER β	ER α	
10c	-styryl	-NHCH ₂ Ph	-NHCH ₂ CH(CH ₃) ₂	16	>1000	>1000	9.8
10d	-styryl	-NHCH ₂ Ph	-NHCH ₂ -1-Nap	>1000	>1000	>1000	
10g	-styryl	-NHCH ₂ -1-Nap	-NHCH ₂ -1-Nap	>1000	>1000	>1000	



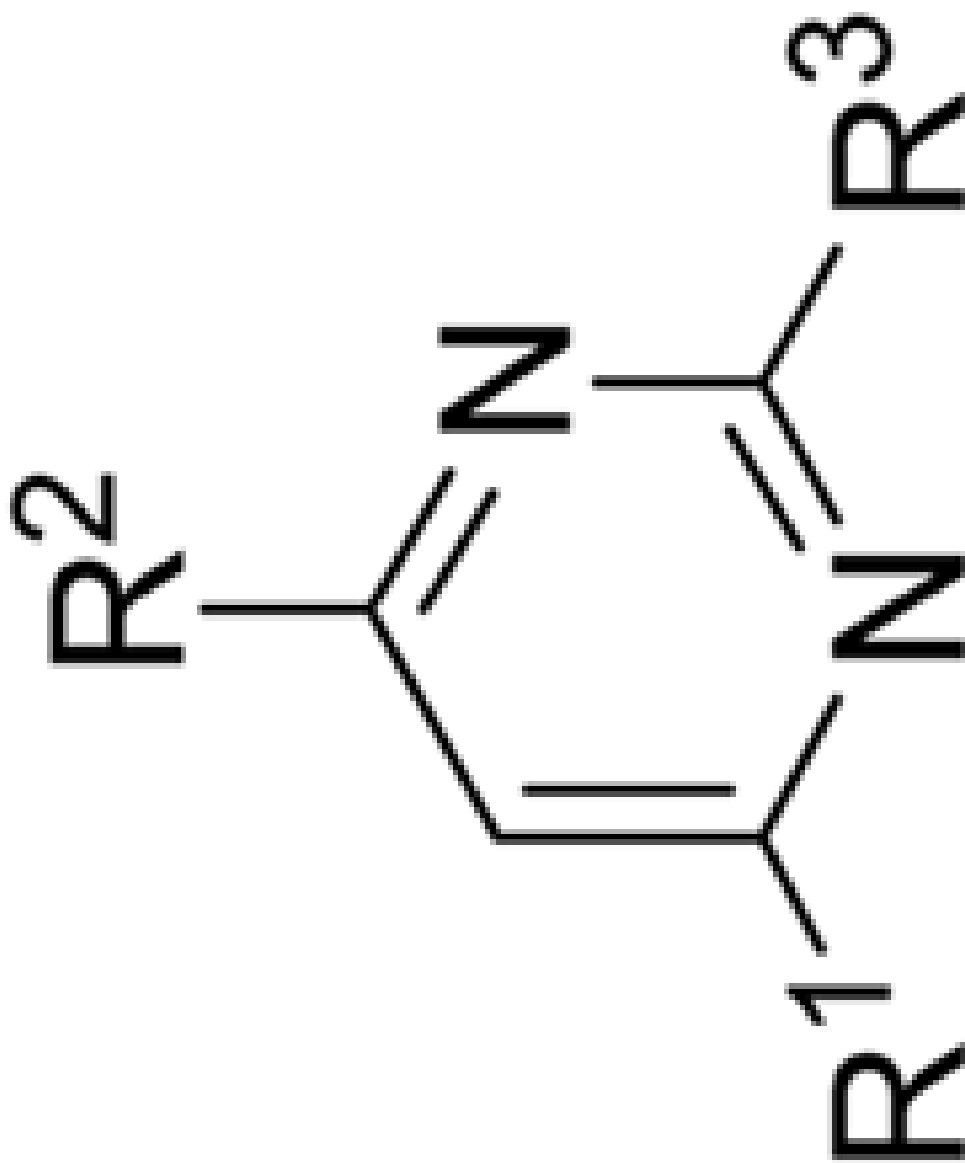
Cmpd #	R ¹	R ²	R ³	TR-FRET ¹ (μ M)			Reporter Gene IC ₅₀ (μ M)
				ER α	ER β	ER α	
11a	-CH ₂ CH ₂ Ph	-NHCH ₂ CH(CH ₃) ₂	-NHCH ₂ Ph	7.6	>1000	>1000	4.5
11b	-CH ₂ CH ₂ Ph	-NHCH ₂ CH(CH ₃) ₂	-NHCH ₂ -1-Nap	>1000	>1000	>1000	>1000
11c	-CH ₂ CH ₂ Ph	-NHCH ₂ Ph	-NHCH ₂ CH(CH ₃) ₂	1.7	>1000	>1000	1.9



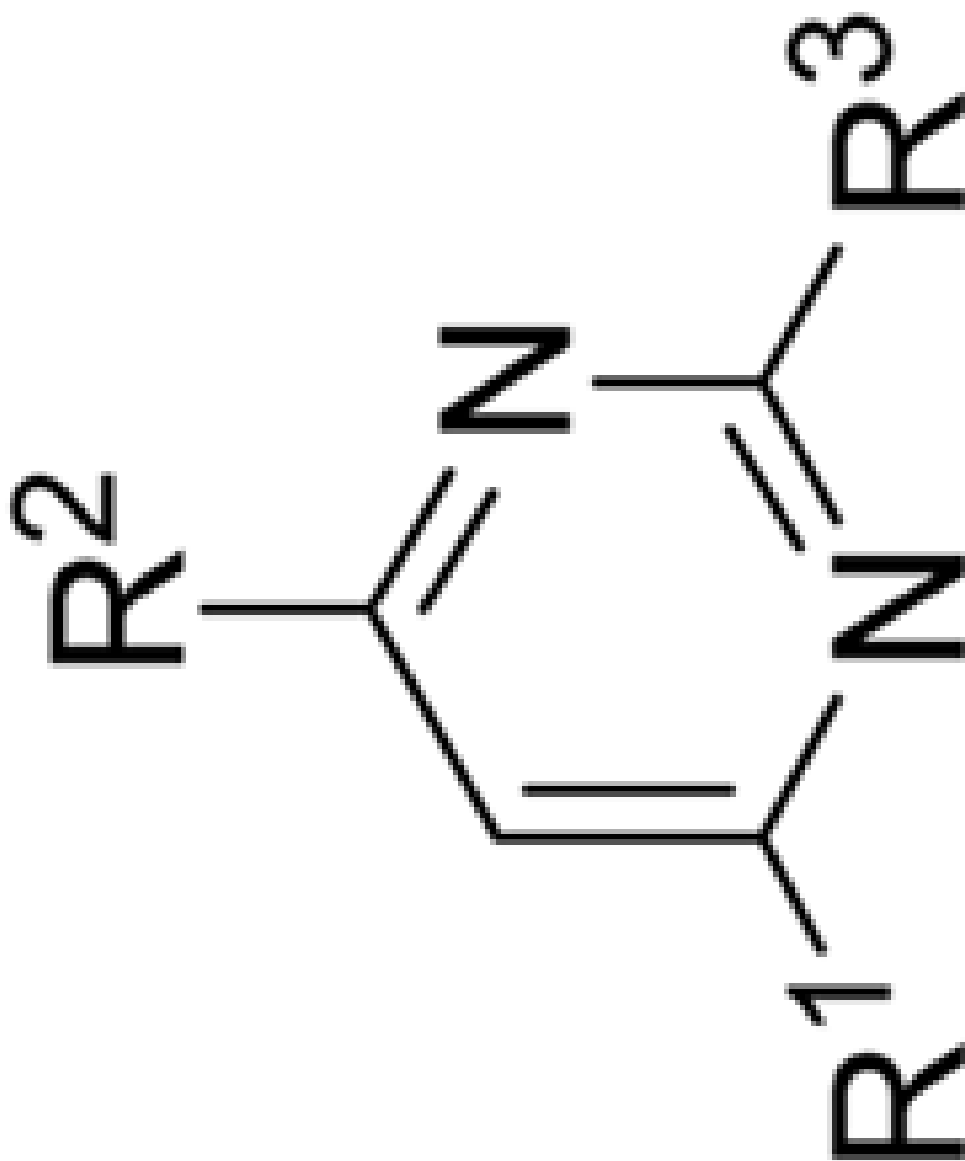
Cmpd #	R ¹	R ²	R ³	TR-FRET ¹ (μ M)			Reporter Gene IC ₅₀ (μ M)
				ER α	ER β	ER α	
11d	-CH ₂ CH ₂ Ph	-NHCH ₂ Ph	-NHCH ₂ -1-Nap	>1000	>1000	>1000	>1000
11f	-CH ₂ CH ₂ Ph	-NHCH ₂ -1-Nap	-NHCH ₂ Ph	>1000	>1000	>1000	>1000
11g	-CH ₂ CH ₂ Ph	-NHCH ₂ -1-Nap	-NHCH ₂ -1-Nap	>1000	>1000	>1000	>1000



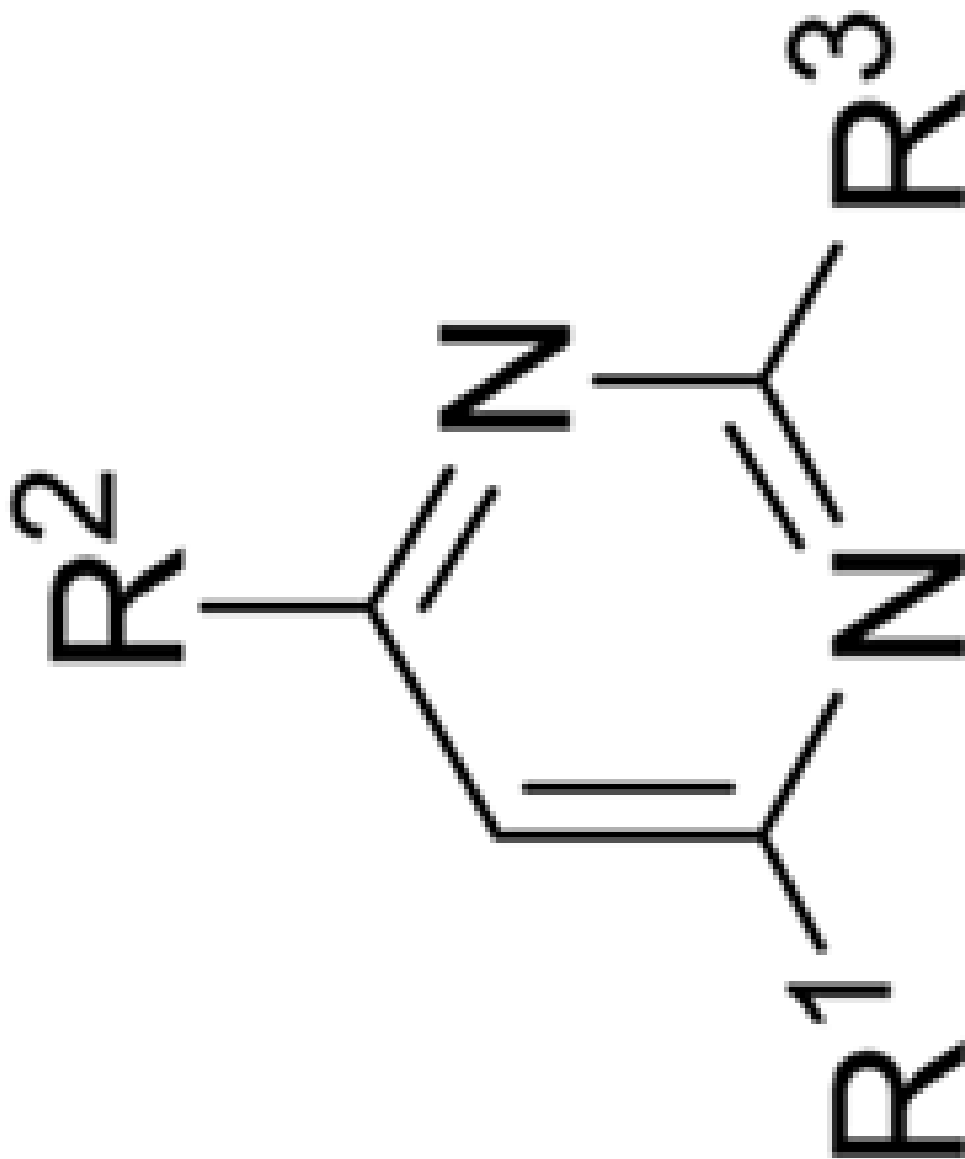
Cmpd #	R ¹	R ²	R ³	Reporter Gene IC ₅₀ (μM)		
				ERα	ERβ	ERα
13a	-CH ₂ (CH ₂) ₂ CH ₃	-NH(CH ₂) ₂ CH ₃	-NH(CH ₂) ₂ CH ₃	16	>1000	13
13b	-CH ₂ CH ₂ CH(CH ₃) ₂	-NHCH ₂ CH(CH ₃) ₂	-NHCH ₂ CH(CH ₃) ₂	2.8	>1000	3.1
13c	-CH ₂ CH ₂ CH(CH ₃) ₂	-NHCH ₂ Ph	-NHCH ₂ Ph	4.1	>1000	8.3



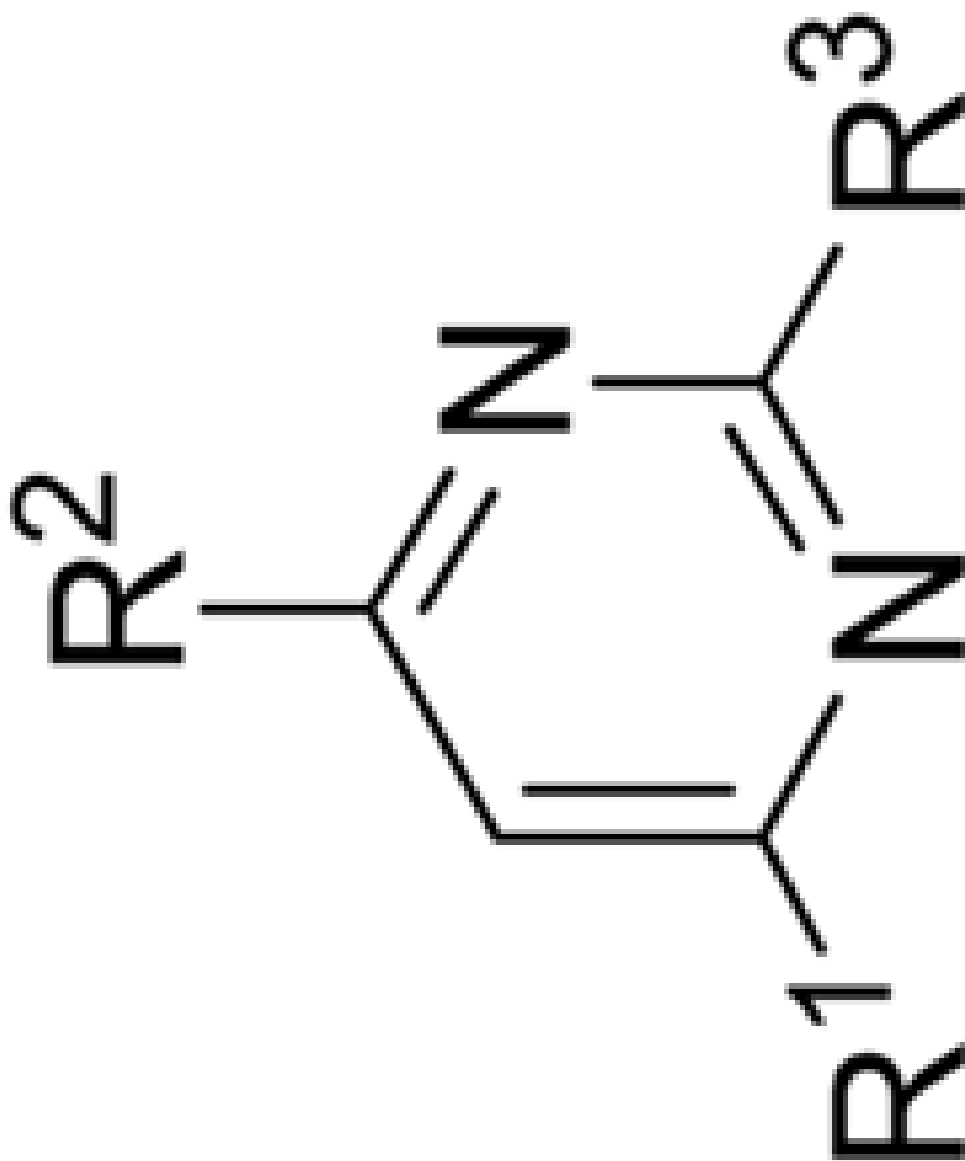
Cmpd #	R ¹	R ²	R ³	TR-FRET _(μM)			Reporter Gene IC ₅₀ (μM)
				ERα	ERβ	ERα	
13d	-CH ₂ CH ₂ CH(CH ₃) ₂	-NHCH ₂ -1-Nap	-NHCH ₂ -1-Nap	>1000	>1000	>1000	>1000
13i	-CH ₂ CH ₂ -1-Nap	-NHCH ₂ CH(CH ₃) ₂	-NHCH ₂ CH(CH ₃) ₂	2.5	>1000	>1000	2.1
13j	-CH ₂ CH ₂ -1-Nap	-NHCH ₂ Ph	-NHCH ₂ Ph	>1000	>1000	>1000	>1000



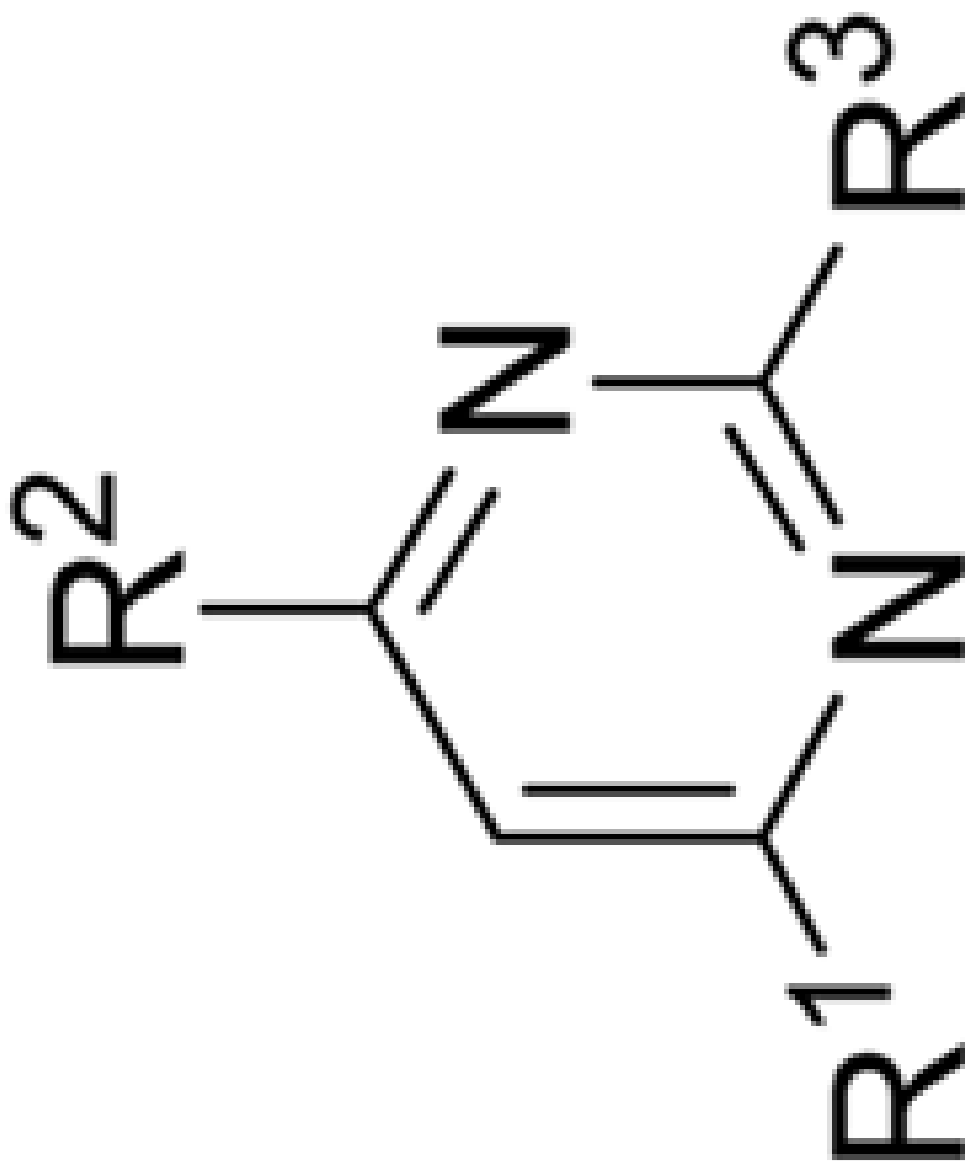
Cmpd #	R ¹	R ²	R ³	TR-FRET ¹ (μ M)			Reporter Gene IC ₅₀ (μ M)
				ER α	ER β	ER α	
13k	-CH ₂ CH ₂ -1-Nap	-NHCH ₂ -1-Nap	-NHCH ₂ -1-Nap	>1000	>1000	>1000	>1000
18a	-CH ₂ CH ₃	-NHCH ₂ CH(CH ₃) ₂	-NHCH ₂ CH(CH ₃) ₂	10	>1000	7.3	7.3
18b	-CH ₂ CH ₂ CH(CH ₃) ₂	-NHCH ₂ CH(CH ₃) ₂	-NHCH ₂ Ph	7.9	>1000	1.8	1.8



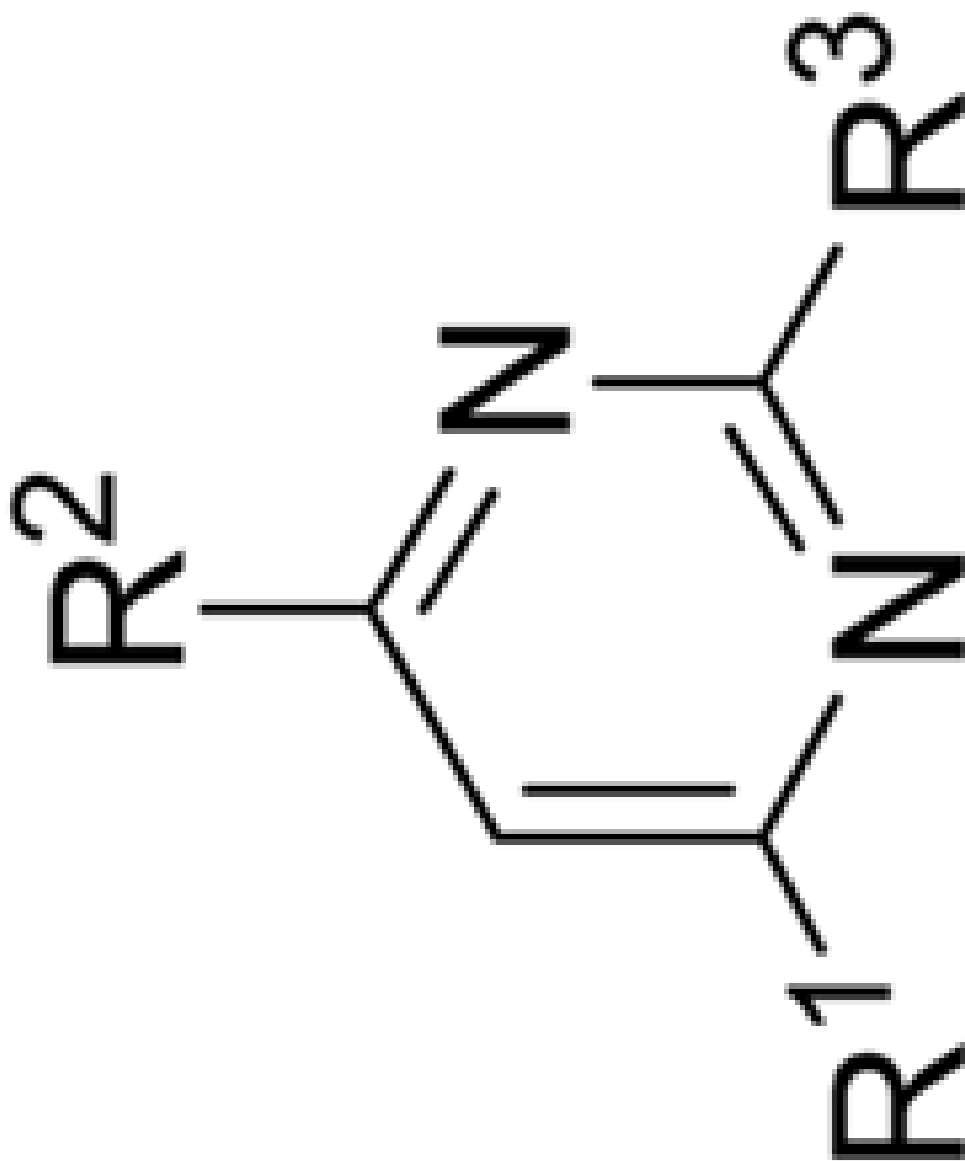
Cmpd #	R ¹	R ²	R ³	TR-FRET _(μM)			Reporter Gene IC ₅₀ (μM)
				ERα	ERβ	ERα	
18c	-CH ₂ CH ₂ CH(CH ₃) ₂	-NHCH ₂ CH(CH ₃) ₂	-NHCH ₂ -1-Nap	7.2	>1000	4.1	
18d	-CH ₂ CH ₂ CH(CH ₃) ₂	-NHCH ₂ Ph	-NHCH ₂ CH(CH ₃) ₂	5.8	>1000	5.8	
18e	-CH ₂ CH ₂ CH(CH ₃) ₂	-NHCH ₂ Ph	-NHCH ₂ -1-Nap	>1000	>1000	>1000	



Cmpd #	R ¹	R ²	R ³	TR-FRET ¹ (μ M)			Reporter Gene IC ₅₀ (μ M)
				ER α	ER β	ER α	
18f	-CH ₂ CH ₂ CH(CH ₃) ₂	-NHCH ₂ -1-Nap	-NHCH ₂ CH(CH ₃) ₂	2.4	>1000	>1000	6.7
18g	-CH ₂ CH ₂ CH(CH ₃) ₂	-NHCH ₂ -1-Nap	-NHCH ₂ Ph	>1000	>1000	>1000	>1000
18h	-CH ₂ CH ₂ -1-Nap	-NHCH ₂ CH(CH ₃) ₂	-NHCH ₂ Ph	>1000	>1000	>1000	>1000



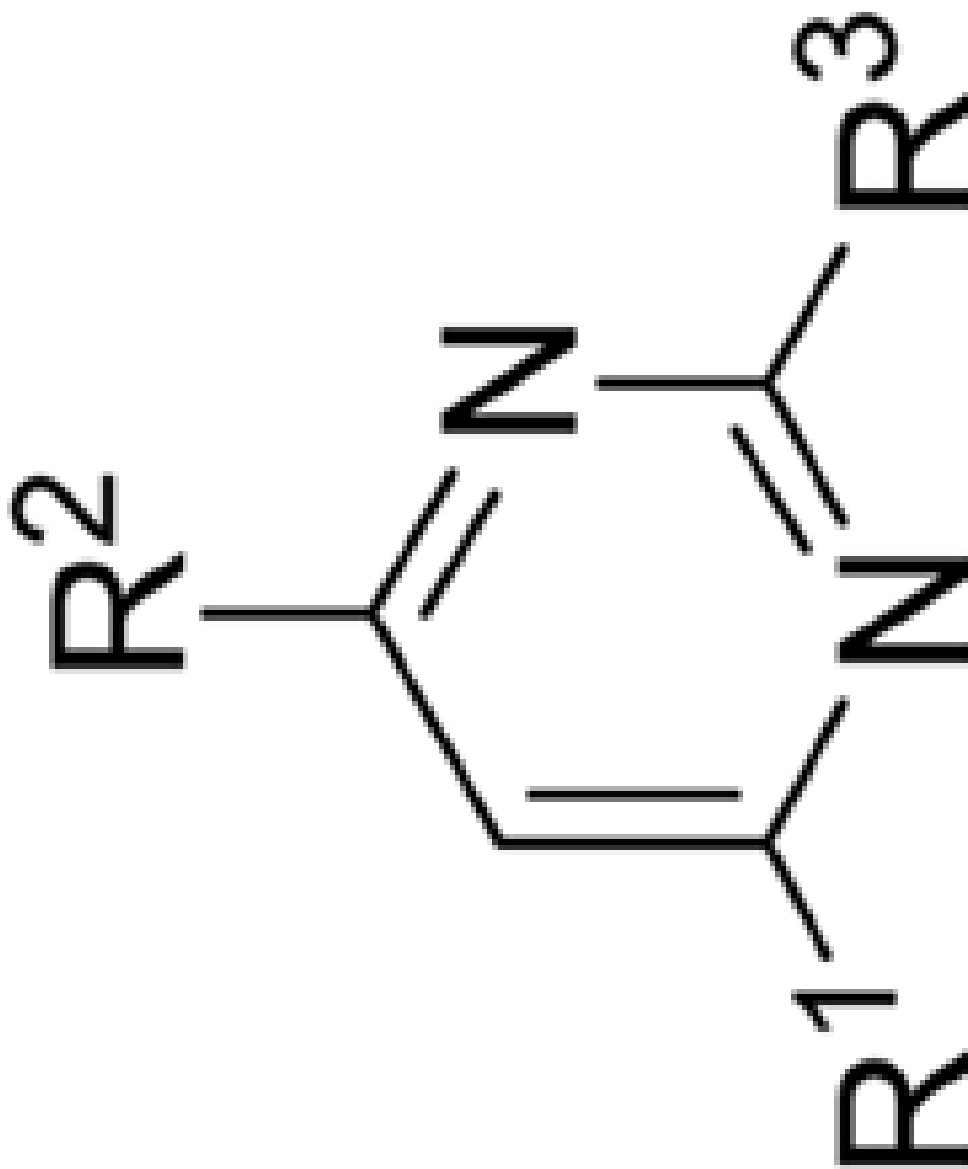
Cmpd #	R ¹	R ²	R ³	Reporter Gene IC ₅₀ (μM)		
				ERα	ERβ	ERα
18j	-CH ₂ CH ₂ -1-Nap	-NHCH ₂ Ph	-NHCH ₂ CH(CH ₃) ₂	>1000	>1000	>1000
18l	-CH ₂ CH ₂ -1-Nap	-NHCH ₂ -1-Nap	-NHCH ₂ CH(CH ₃) ₂	>1000	>1000	>1000
26	-NHCH ₂ CH(CH ₃) ₂	-Cl	-NHCH ₂ CH(CH ₃) ₂	>1000	>1000	>1000



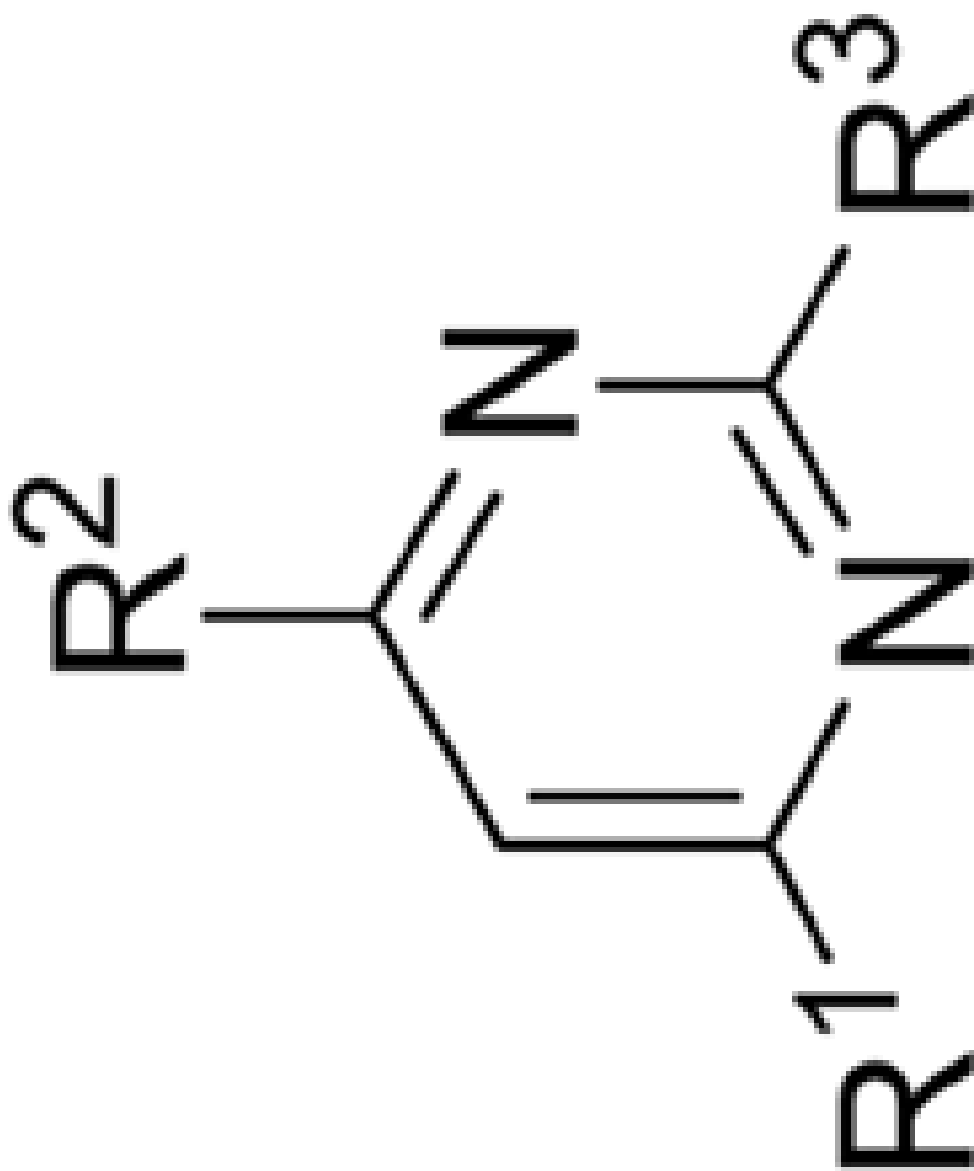
Cmpd #	R ¹	R ²	R ³	TR-FRET _(μM)			Reporter Gene IC ₅₀ (μM)
				ERα	ERβ	ERα	
27d	-NHCH ₂ CH(CH ₃) ₂	-H	-NHCH ₂ CH(CH ₃) ₂	>1000	>1000	>1000	

Table 2

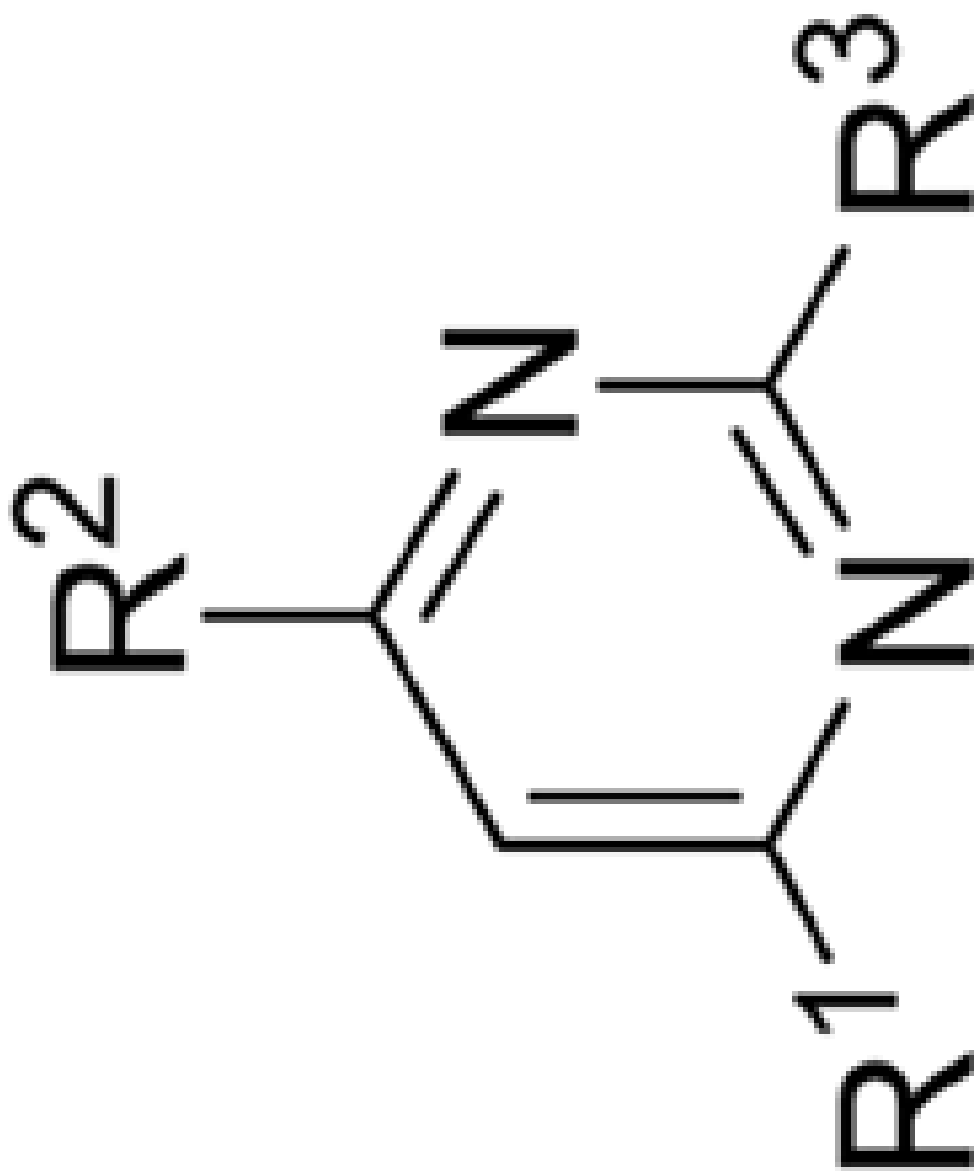
Inhibitory activity of various pyrimidines on the ER α and ER β /coactivator interaction as measured in TR-FRET and Luciferase reporter gene assays.



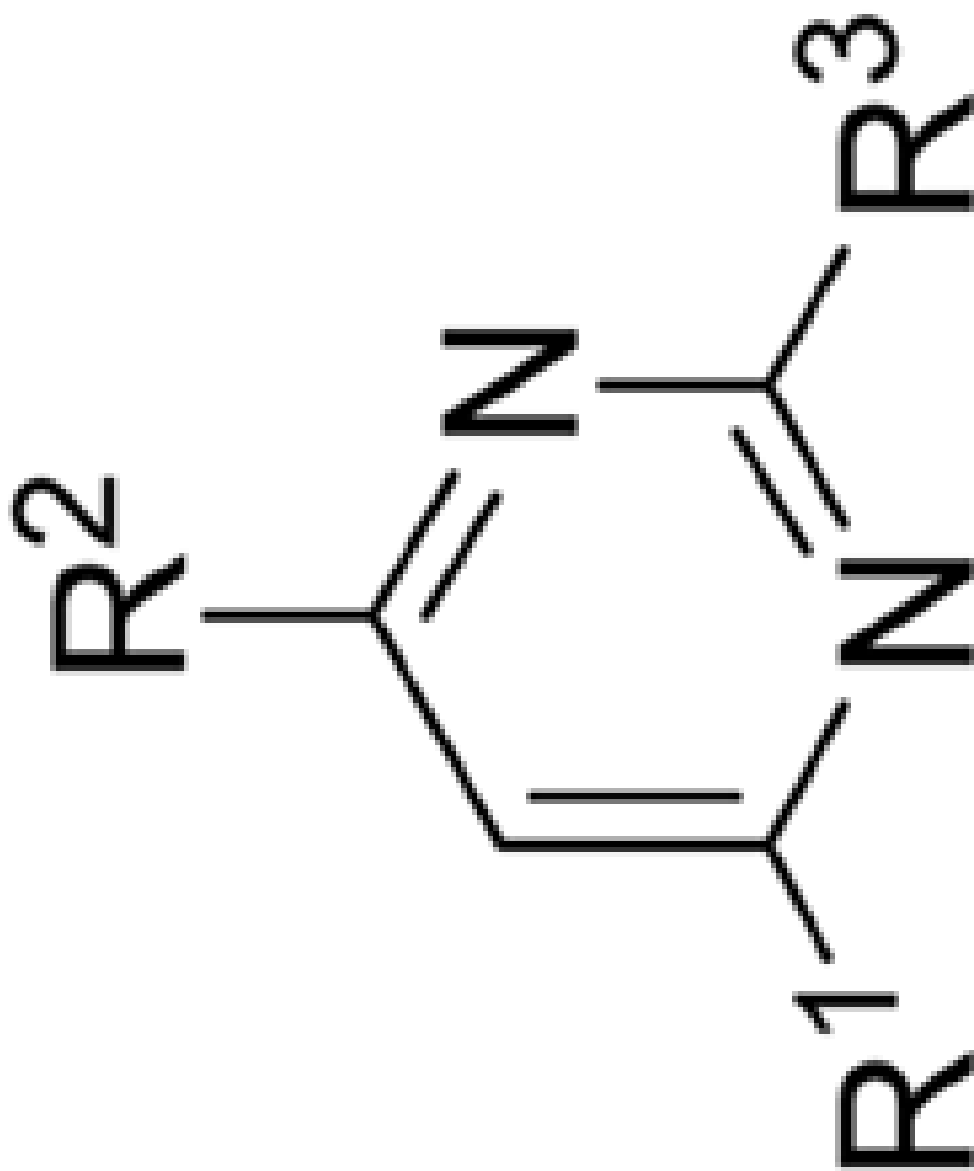
Cmpd #	R ¹	R ²	R ³	TR-FRET Ki (μM)		Reporter Gene IC ₅₀ (μM)	
				ER α	ER β	ER α	ER α
control				0.065	0.066		
			SRC-1 BoxII				



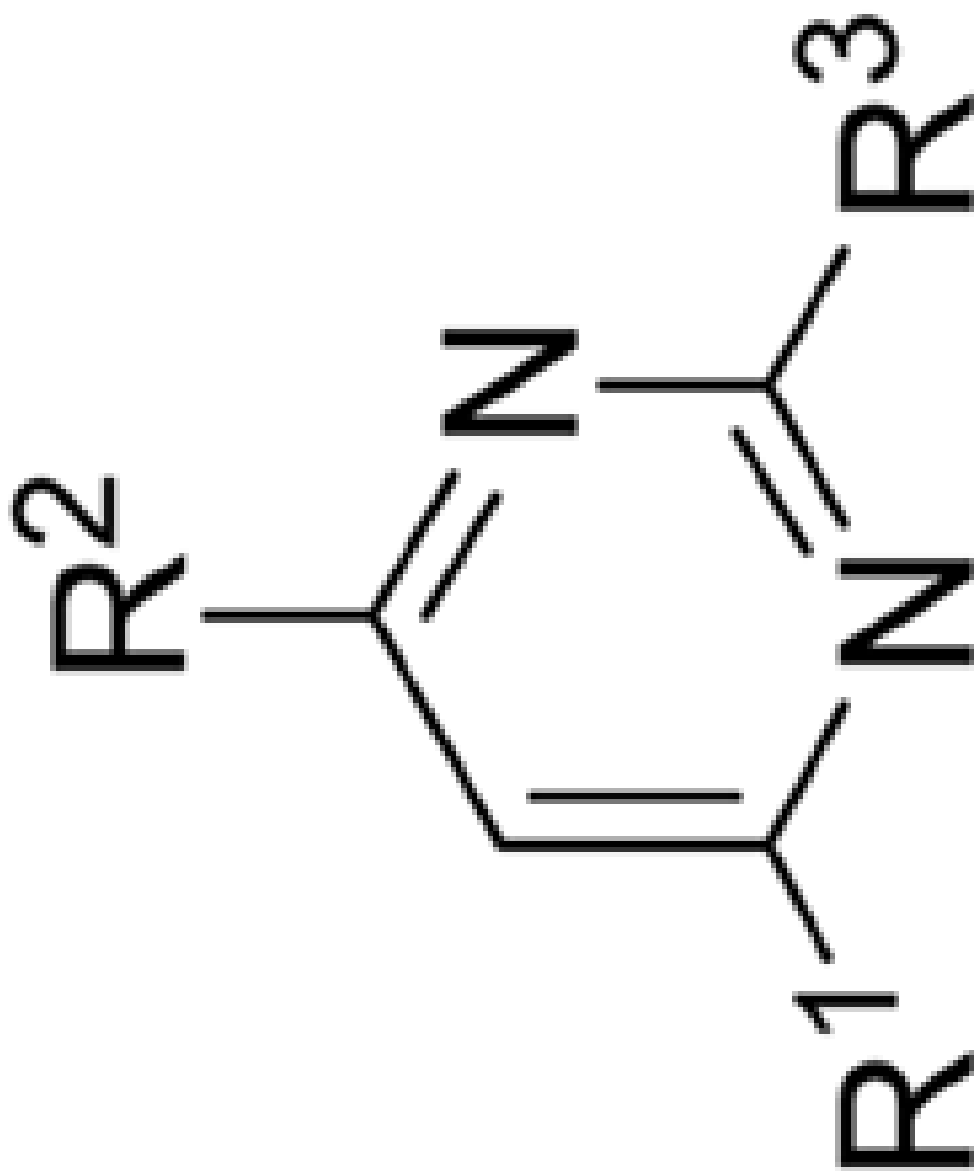
Cmpd #	R ¹	R ²	R ³	TR-FRET Ki (μM)			Reporter Gene IC ₅₀ (μM)
				ER α	ER β	ER α	ER α
3c	-CH ₂ CH ₂ Ph	-OCH ₂ CH(CH ₃) ₂	-OCH ₂ CH(CH ₃) ₂	>1000	>1000	>1000	>1000
5b	-CH ₂ CH ₂ Ph	-SCH ₂ CH(CH ₃) ₂	-SCH ₂ CH(CH ₃) ₂	>1000	>1000	>1000	>1000
6a	-CH ₂ CH ₂ Ph	-SO ₂ CH ₂ CH(CH ₃) ₂	-SO ₂ CH ₂ CH(CH ₃) ₂	>1000	>1000	>1000	>1000



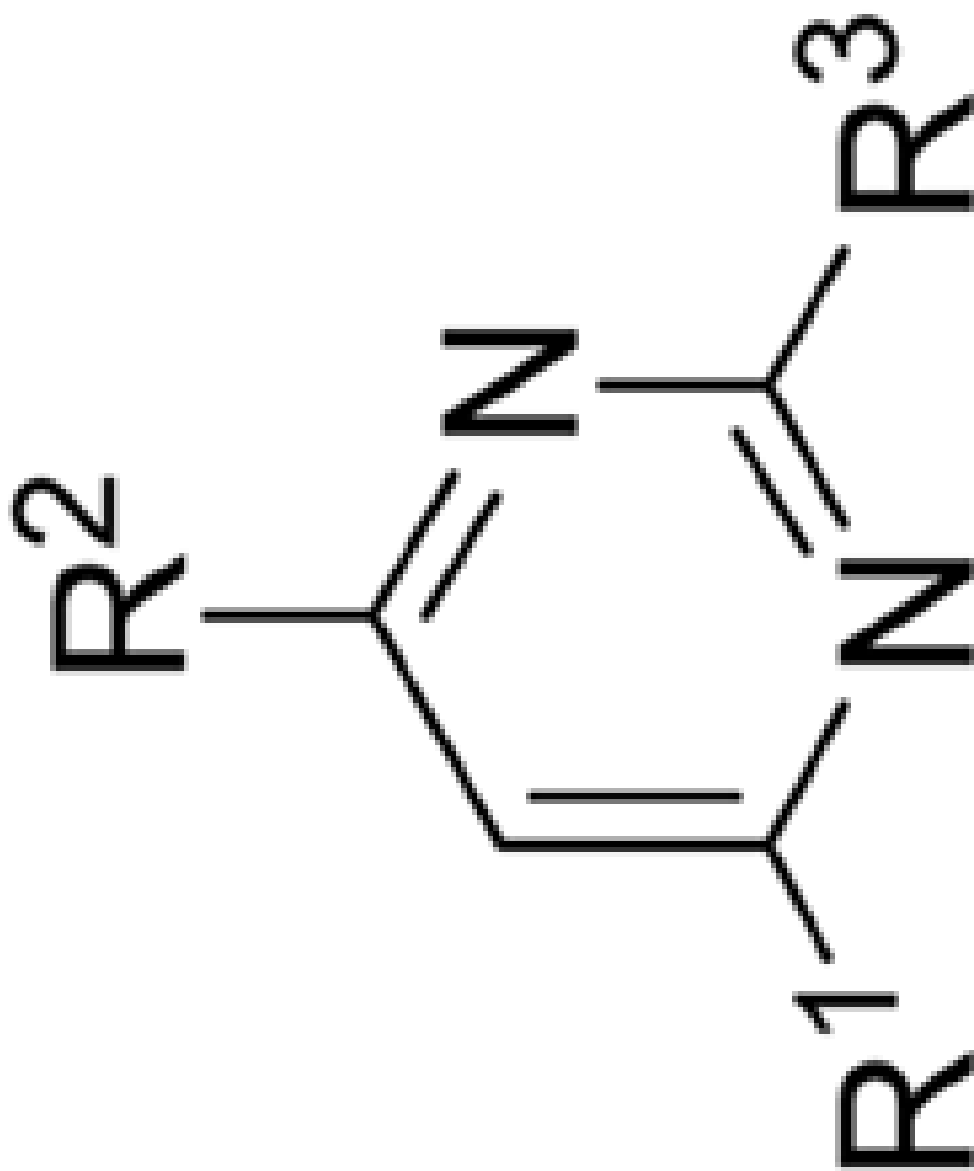
Cmpd #	R ¹	R ²	R ³	TR-FRET Ki (μM)		Reporter Gene IC ₅₀ (μM)
				ER α	ER β	ER α
13e	-CH ₂ CH ₂ CH(CH ₃) ₂	-OCH ₂ CH(CH ₃) ₂	-OCH ₂ CH(CH ₃) ₂	>1000	>1000	>1000
13g	-CH ₂ CH ₂ CH(CH ₃) ₂	-SCH ₂ CH(CH ₃) ₂	-SCH ₂ CH(CH ₃) ₂	>1000	>1000	>1000
14a	-CH ₂ CH ₂ CH(CH ₃) ₂	-SO ₂ CH ₂ CH(CH ₃) ₂	-SO ₂ CH ₂ CH(CH ₃) ₂	>1000	>1000	>1000



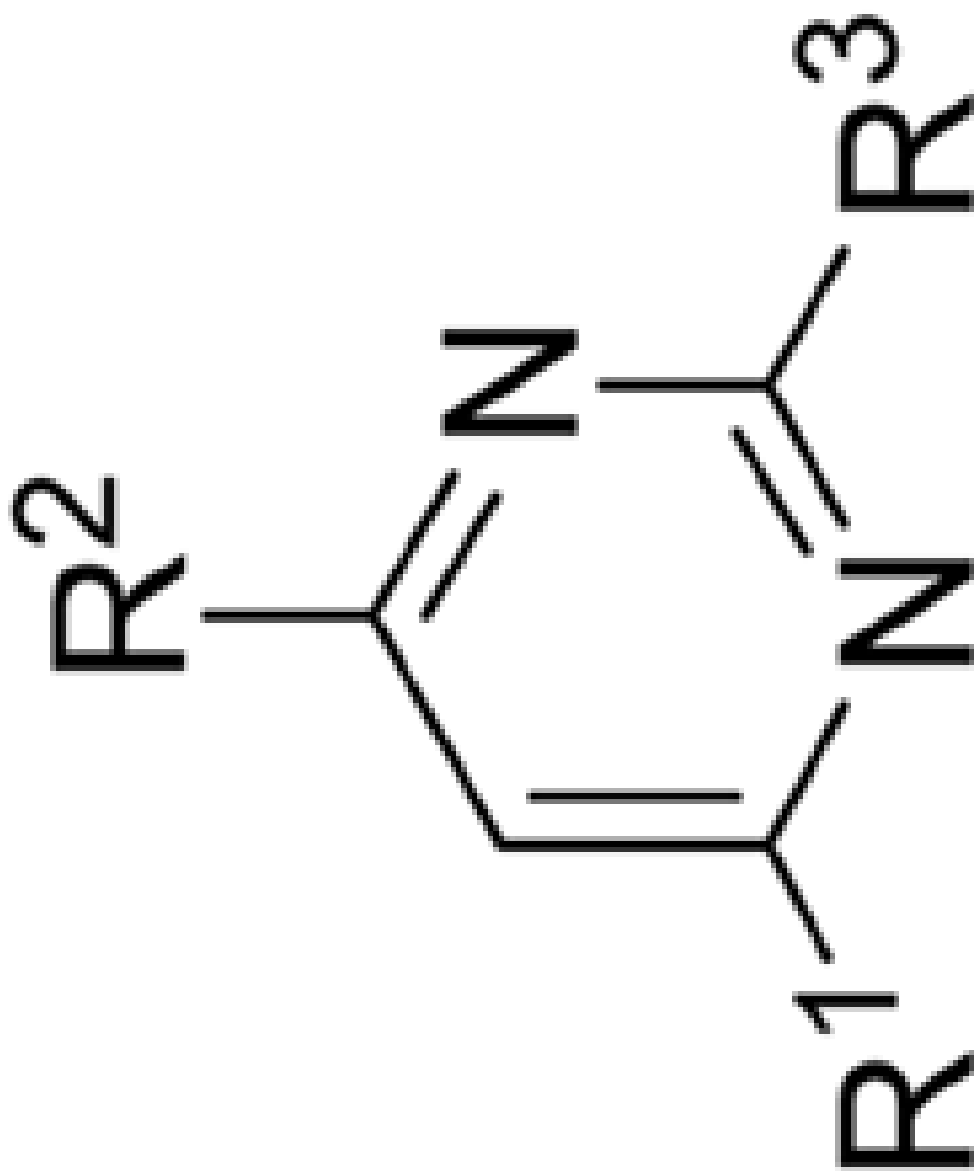
Cmpd #	R ¹	R ²	R ³	TR-FRET Ki (μM)		Reporter Gene IC ₅₀ (μM)
				ER α	ER β	ER α
21a	-NHCH ₂ CH(CH ₃) ₂	-NHCH ₂ CH(CH ₃) ₂	-CH ₂ CH ₂ CH(CH ₃) ₂	>1000	>1000	>1000
21d	-NHCH ₂ CH(CH ₃) ₂	-NHCH ₂ -1-Nap	-CH ₂ CH ₂ CH(CH ₃) ₂	>1000	>1000	>1000
23a	-CH ₂ CH ₂ CH(CH ₃) ₂	-CH ₂ CH ₂ CH(CH ₃) ₂	-NHCH ₂ CH(CH ₃) ₂	>1000	>1000	>1000



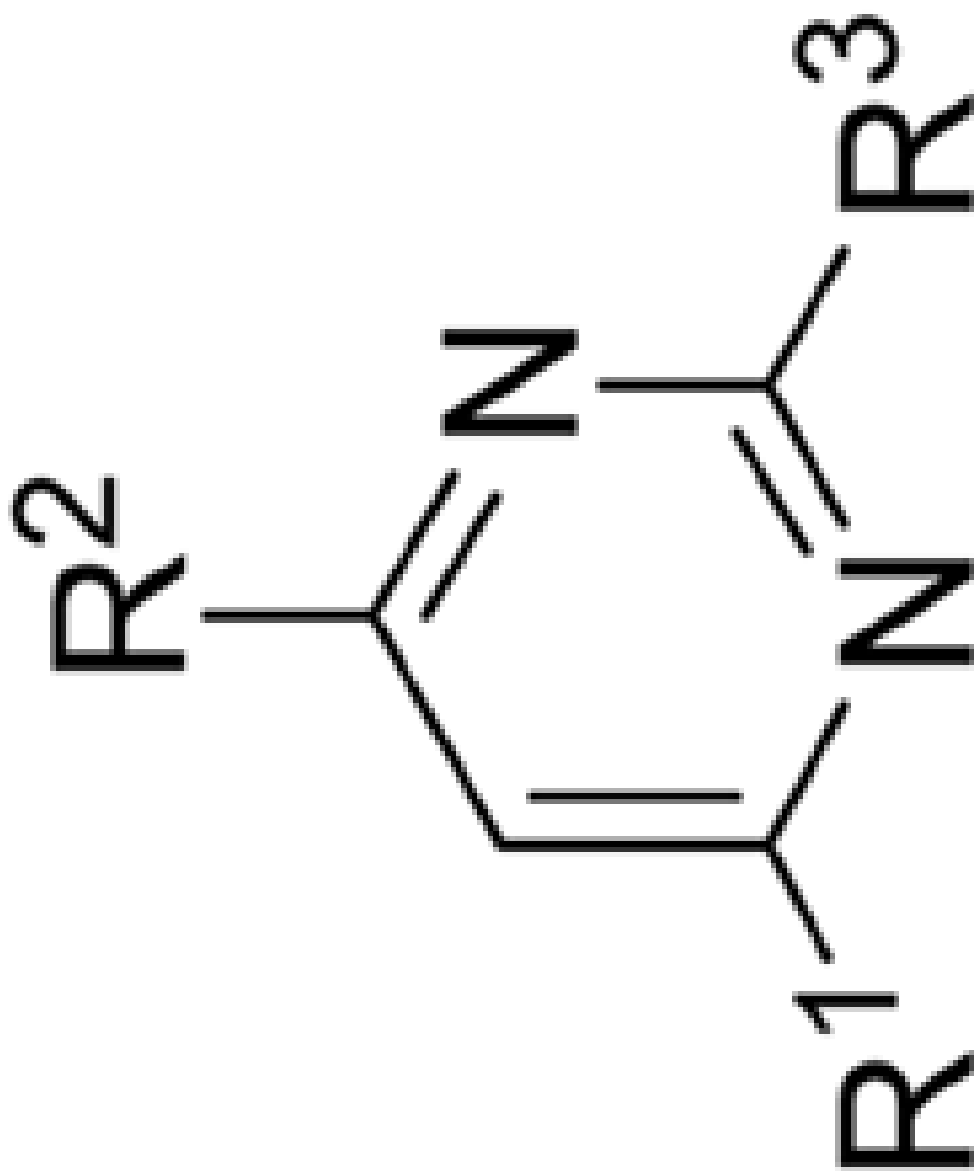
Cmpd #	R ¹	R ²	R ³	TR-FRET Ki (μM)			Reporter Gene IC ₅₀ (μM)
				ER α	ER β	ER α	
23b	-CH ₂ CH ₂ CH(CH ₃) ₂	-CH ₂ CH ₂ CH(CH ₃) ₂	-NHCH ₂ Ph	>1000	>1000	>1000	>1000
23c	-CH ₂ CH ₂ CH(CH ₃) ₂	-CH ₂ CH ₂ CH(CH ₃) ₂	-NHCH ₂ -1-Nap	>1000	>1000	>1000	>1000
24a	-CH ₂ CH ₂ Ph	-CH ₂ CH ₂ Ph	-NHCH ₂ CH(CH ₃) ₂	>1000	>1000	>1000	>1000



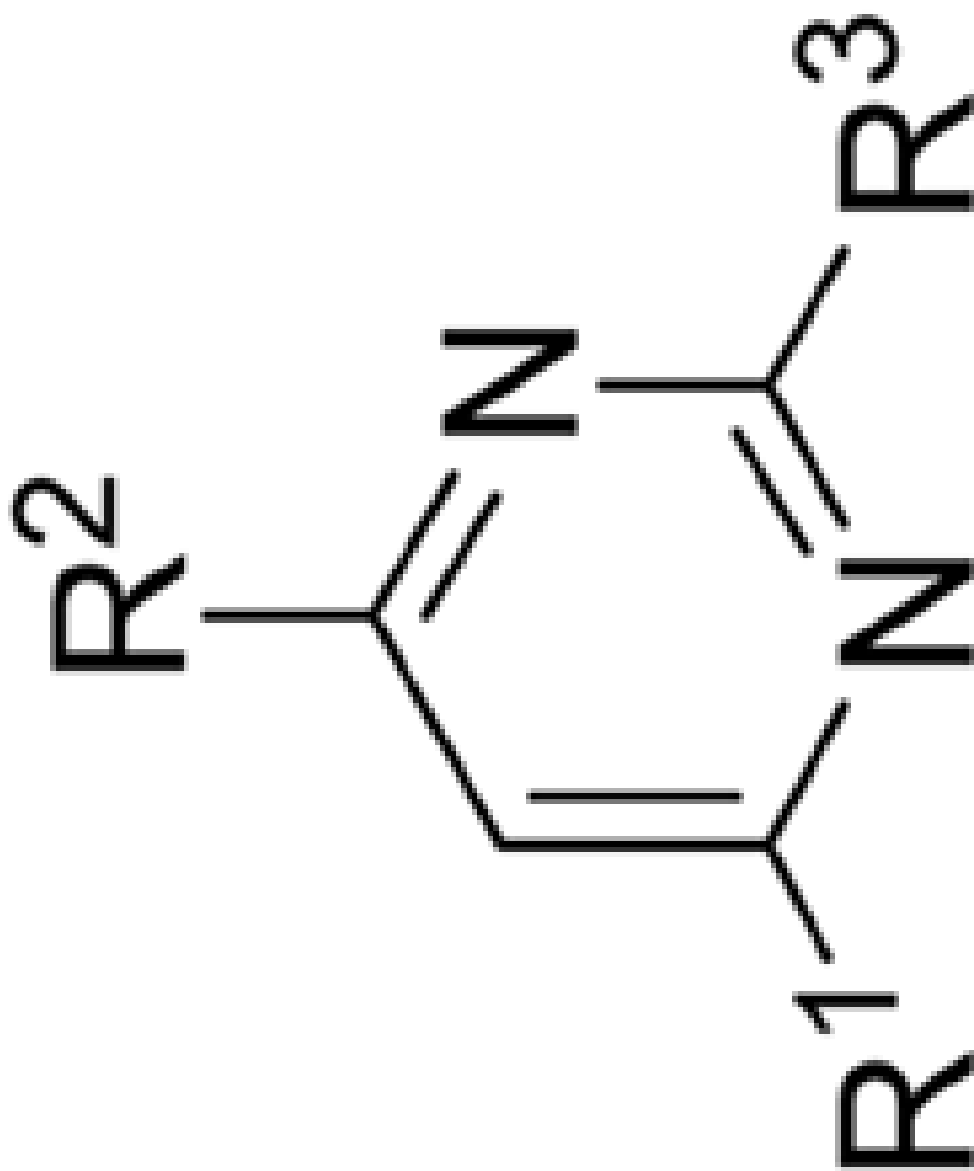
Cmpd #	R ¹	R ²	R ³	TR-FRET Ki (μM)		Reporter Gene IC ₅₀ (μM)
				ER α	ER β	ER α
25a	-NHCH ₂ CH(CH ₃) ₂	-NHCH ₂ CH(CH ₃) ₂	-NHCH ₂ CH(CH ₃) ₂	5.7	299	2.4
25c	-OCH ₂ CH(CH ₃) ₂	-OCH ₂ CH(CH ₃) ₂	-OCH ₂ CH(CH ₃) ₂	>1000	>1000	>1000
25e	-SCH ₂ CH(CH ₃) ₂	-SCH ₂ CH(CH ₃) ₂	-SCH ₂ CH(CH ₃) ₂	120	>1000	>1000



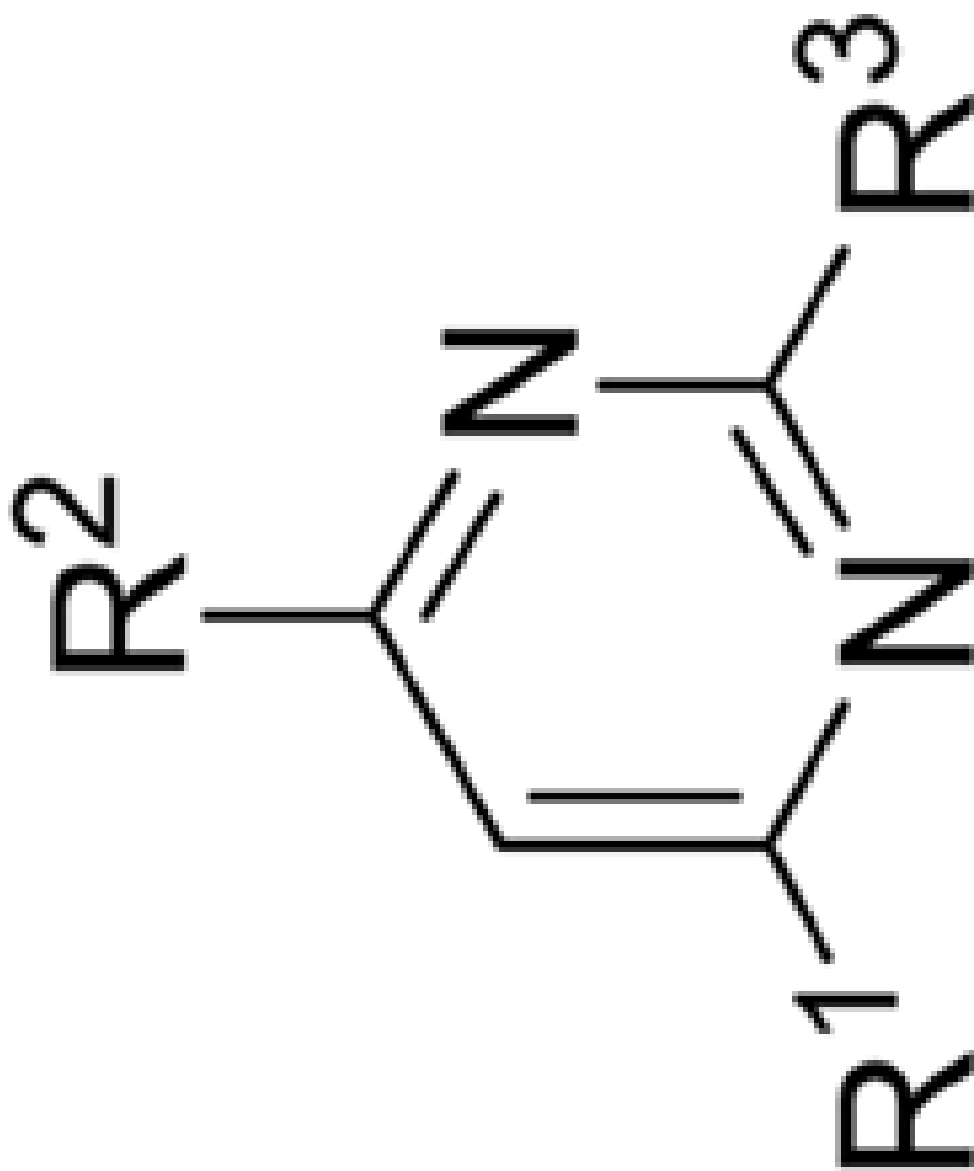
Cmpd #	R ¹	R ²	R ³	TR-FRET Ki (μM)		Reporter Gene IC ₅₀ (μM)
				ER α	ER β	
27a	-NHCH ₂ CH(CH ₃) ₂	-NHCH ₂ Ph	-NHCH ₂ CH(CH ₃) ₂	7.3	>1000	9.5
27b	-NHCH ₂ CH(CH ₃) ₂	-OCH ₂ CH(CH ₃) ₂	-NHCH ₂ CH(CH ₃) ₂	>1000	>1000	
27c	-NHCH ₂ CH(CH ₃) ₂	-SCH ₂ CH(CH ₃) ₂	-NHCH ₂ CH(CH ₃) ₂	>1000	>1000	



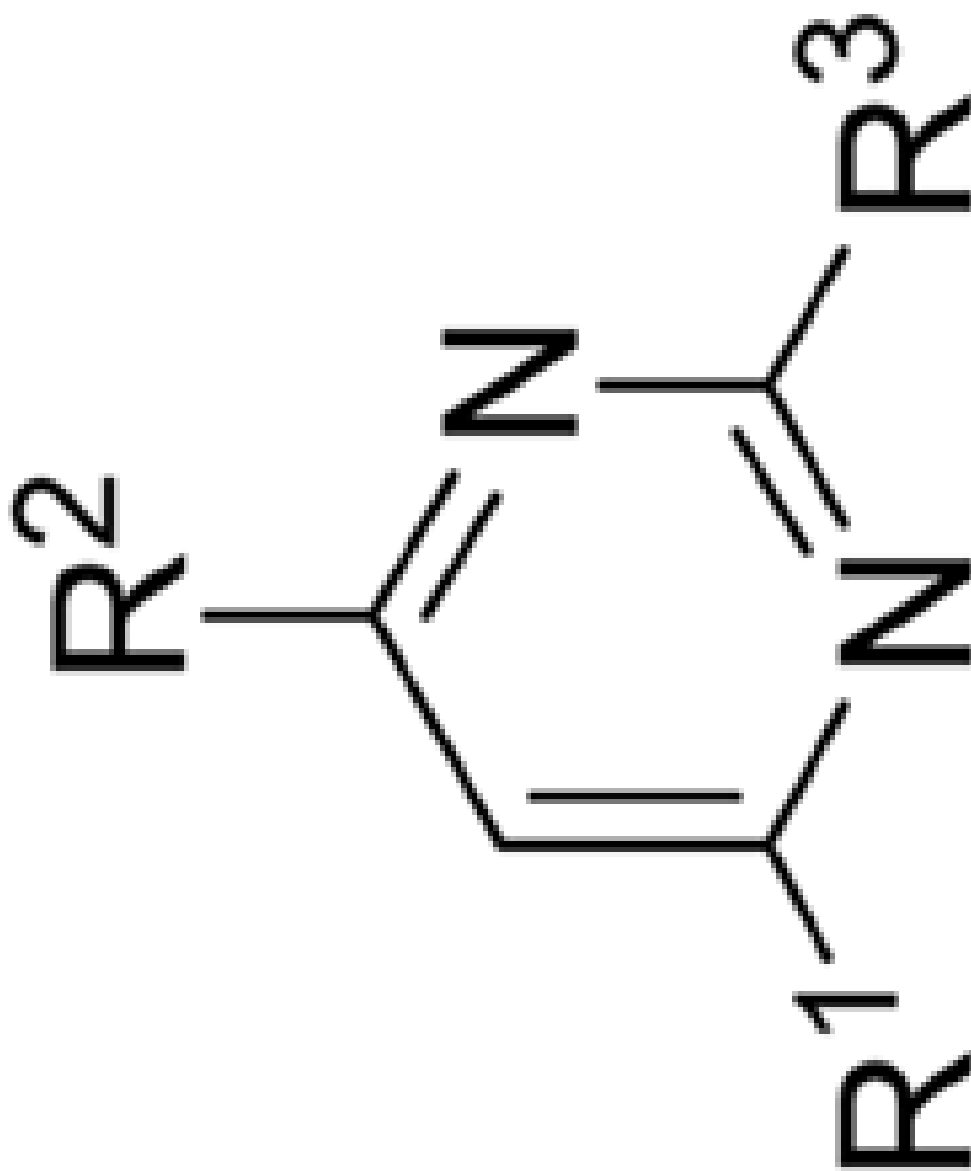
Cmpd #	R ¹	R ²	R ³	TR-FRET Ki (μM)		Reporter Gene IC ₅₀ (μM)
				ER α	ER β	ER α
28	-NHCH ₂ CH(CH ₃) ₂	-SO ₂ CH ₂ CH(CH ₃) ₂	-NHCH ₂ CH(CH ₃) ₂	>1000	>1000	>1000
29a	-CH ₂ CH ₂ CH(CH ₃) ₂	-N(CH ₃)CH ₂ CH(CH ₃) ₂	-N(CH ₃)CH ₂ CH(CH ₃) ₂	>1000	>1000	>1000
29c	-CH ₂ CH ₂ -1-Nap	-N(CH ₃)CH ₂ CH(CH ₃) ₂	-N(CH ₃)CH ₂ CH(CH ₃) ₂	>1000	>1000	>1000



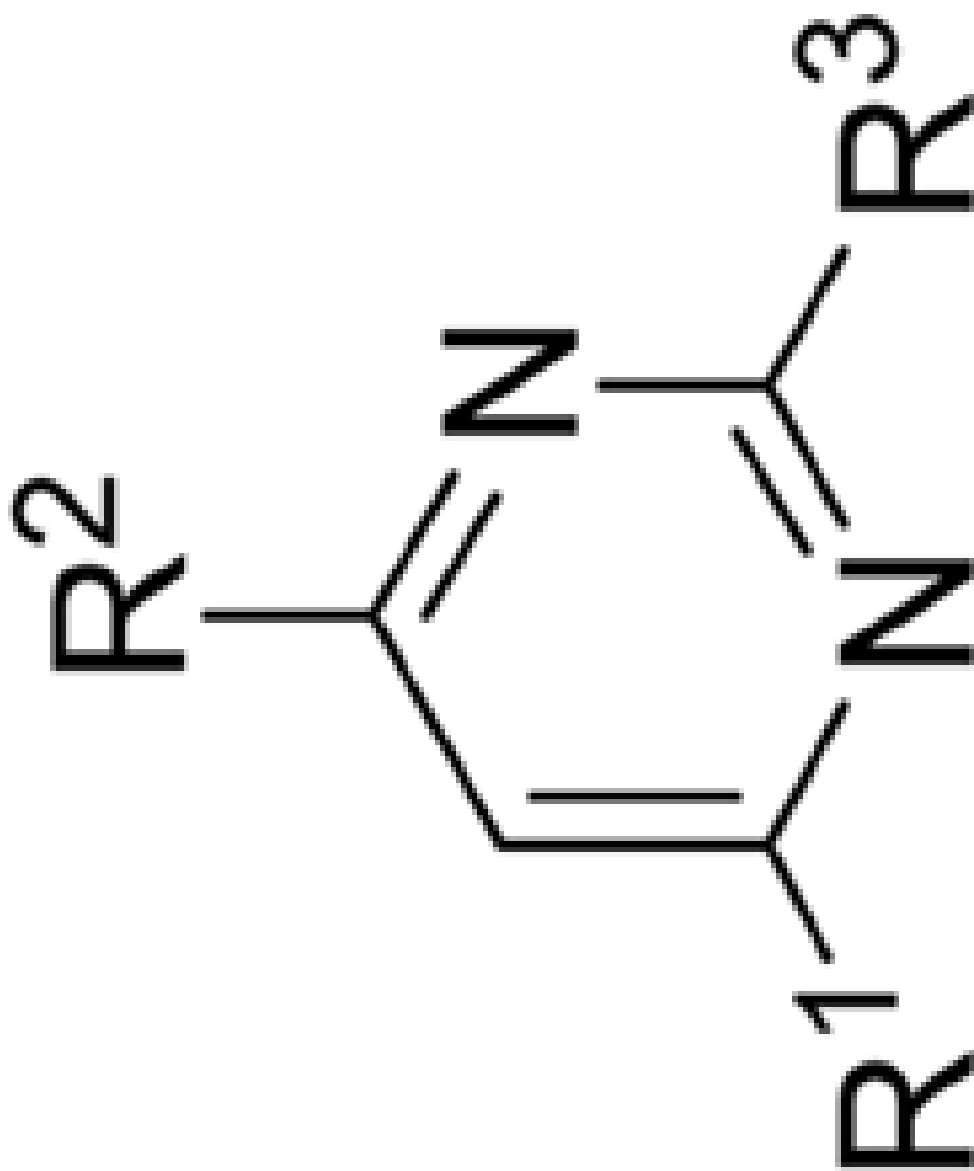
Cmpd #	R ¹	R ²	R ³	TR-FRET Ki (μM)		Reporter Gene IC ₅₀ (μM)
				ER α	ER β	ER α
30	-CH ₂ CH ₂ Ph	-N(CH ₃)CH ₂ CH(CH ₃) ₂	-N(CH ₃)CH ₂ CH(CH ₃) ₂	>1000	>1000	
31a	-CH ₂ CH ₂ CH(CH ₃) ₂	-NHCH ₂ CH(CH ₃) ₂	-N(CH ₃)CH ₂ CH(CH ₃) ₂	7.2	>1000	9.7
31c	-CH ₂ CH ₂ -1-Nap	-NHCH ₂ CH(CH ₃) ₂	-N(CH ₃)CH ₂ CH(CH ₃) ₂	>1000	>1000	



Cmpd #	R ¹	R ²	R ³	TR-FRET Ki (μM)		Reporter Gene IC ₅₀ (μM)
				ER α	ER β	ER α
32	-CH ₂ CH ₂ Ph	-NHCH ₂ CH(CH ₃) ₂	-N(CH ₃)CH ₂ CH(CH ₃) ₂	>1000	>1000	>1000
34a	-CH ₂ CH ₂ CH(CH ₃) ₂	-N(CH ₃)CH ₂ CH(CH ₃) ₂	-NHCH ₂ CH(CH ₃) ₂	>1000	>1000	>1000
34c	-CH ₂ CH ₂ -1-Nap	-N(CH ₃)CH ₂ CH(CH ₃) ₂	-NHCH ₂ CH(CH ₃) ₂	2.4	>1000	4.4



Cmpd #	R ¹	R ²	R ³	TR-FRET Ki (μM)		Reporter Gene IC ₅₀ (μM)
				ER α	ER β	
35	-CH ₂ CH ₂ Ph	-N(CH ₃)CH ₂ CH(CH ₃) ₂	-NHCH ₂ CH(CH ₃) ₂	8.4	>1000	5.5
37a	-CH ₂ CH ₂ CH(CH ₃) ₂	-NHCH ₂ CH(CH ₃) ₂	-OCH ₂ CH(CH ₃) ₂	>1000	>1000	6.9
37b	-CH ₂ CH ₂ CH(CH ₃) ₂	-NHCH ₂ CH(CH ₃) ₂	-SCH ₂ CH(CH ₃) ₂	>1000	>1000	>1000



Cmpd #	R ¹	R ²	R ³	TR-FRET Ki (μM)		Reporter Gene IC ₅₀ (μM)
				ER α	ER β	ER α
39	-CH ₂ CH ₂ CH(CH ₃) ₂	-NHCH ₂ CH(CH ₃) ₂	-SO ₂ CH ₂ CH(CH ₃) ₂	>1000	>1000	>1000